DESIGN AND ASSESSMENT OF VIBROTACTILE BIOFEEDBACK AND

INSTRUCTIONAL SYSTEMS FOR

BALANCE REHABILITATION APPLICATIONS

by

Beom Chan Lee

A dissertation submitted in partial fulfillment
of the requirements for the degree of
Doctor of Philosophy
(Mechanical Engineering)
in The University of Michigan
2012

Doctoral Committee:

    Assistant Professor Kathleen H. Sienko, Chair
    Associate Professor Brent Gillespie
    Associate Professor Bernard J. Martin
    Research Professor James A. Ashton-Miller

DEDICATION

To my family

ACKNOWLEDGEMENTS

I would like to express my appreciation and gratitude to a number of individuals who have contributed to the different phases of my work. First and foremost, I would like to express my deepest gratitude to Professor Kathleen H. Sienko for her gentle guidance and great inspiration during my doctoral studies at the University of Michigan. Kathleen, these three and half years have been an honor. I also would like to sincerely acknowledge the intellectual suggestions, helpful criticisms, and valuable supports made by my doctoral committee members, Professor James Ashton-Miller, Brent Gillespie, and Bernard Martin.

I have had the privilege to complete this thesis under support of highly dedicated and proficient researchers as co-authors for the publications, Bernard Martin, Jeonghee Kim, Kelli Bechly, Shu Chen, Vivek Vichare, and Wendy Carender. Especially, I would like to express my warmest gratitude to Bernard Martin for his continual guidance and encouragement, and so enabling me to extend my knowledge in the field of the human perception and motor behavior.

Sensory Augmentation and Rehabilitation Laboratory (SARL) is a fantastic laboratory that encourages the personal and intellectual growth. I would like especially like to call out to Amir Sabet, Ibrahim Mohedas, and Stephanie Haggerty as your camaraderie and intellectual input. To the former members of SARL: Dan Ursu, Dongwon Kim, Seunghun

TABLE OF CONTENTS

viii

LIST OF FIGURES

LIST OF TABLES

LIST OF APPENDICES

ABSTRACT

Balance rehabilitation exercises are designed to recover, retrain, or develop new sensorimotor strategies to facilitate functional mobility, decrease dizziness, and re-establish effective coordination. During typical clinical balance rehabilitation programs, a physical therapist demonstrates an exercise, provides physical guidance and verbal feedback regarding the patient's performance, and assesses short-term and long-term changes in the patient's capabilities. Sensory augmentation, a type of biofeedback, is a technique for supplementing or reinforcing native sensory inputs. In the context of balance-related applications, it provides users with additional information about body motion, usually with respect to the gravito-inertial environment. Multiple studies have demonstrated that biofeedback, regardless of the feedback modality (i.e., vibrotactile, electrotactile, auditory), decreases body sway during real-time use within a laboratory setting. However, in their current laboratory-based form, existing vibrotactile biofeedback devices are not appropriate for use in clinical and/or home-based rehabilitation settings due to the expense, size, and operating complexity of the instrumentation required.

This dissertation describes the design, development, and preliminary assessment of two technologies that support clinical and home-based balance rehabilitation training.

xviii

The first system provides vibrotactile-based instructional motion cues to a trainee based on the measured difference between the expert's and trainee's motions. The design of the vibrotactile display is supported by a study that characterizes the non-volitional postural responses to vibrotactile stimulation applied to the skin over the torso. This study shows that vibration applied individually by tactors over the internal oblique and erector spinae muscles induces a postural shift of the order of one degree oriented in the direction of the stimulation, while simultaneous activation of all tactors and activation of those over external oblique muscles do not produce significant postural effects. The directional aspect of vibration-induced postural shifts suggests that cutaneous information from the stimulated areas contributes to proprioception and to the spatial representation of the upper body. Furthermore, human performance is characterized both experimentally and theoretically when the expert–trainee error thresholds and nature of the control signal are varied. The results of these studies suggest that expert–subject cross-correlation values are maximized and average position errors and time delays are minimized when the controller uses a 0.5 error threshold and proportional plus derivative feedback control signal, and that subject performance decreases as motion speed and complexity increase.

The second system provides vibrotactile biofeedback of body motion using a cell phone. The system is capable of providing real-time vibrotactile cues that inform corrective trunk tilt responses. When feedback is available, both healthy subjects and those with vestibular involvement significantly reduce their anterior-posterior or medial-lateral root-mean-square body sway depending on the direction of feedback, have significantly smaller elliptical area fits to their sway trajectory, spend a significantly

greater mean percentage time within the no feedback zone, and show a significantly greater A/P or M/L mean power frequency.

CHAPTER 1: Introduction and Background

1.1. Balance and the vestibular system

The central nervous system (CNS) integrates sensory inputs from vestibular, proprioceptive, and visual sources in order to regulate upright postural control while walking or standing [1-4]. Among the aforementioned sensory inputs, the vestibular system, located in the inner ear, plays a crucial role in stabilizing vision and maintaining posture in space [5-6]. The vestibular system detects translational and rotational movements of the head and is composed of otolith organs and semicircular canals [5-7]. The saccule and utricle comprise the otolith organs and sense vertical and horizontal linear accelerations of the head, respectively [6]. The three semicircular canals (the lateral, anterior, and posterior semicircular canals) detect angular (rotational) acceleration of the head. The three semicircular canals are positioned approximately in three orthogonal planes [7]. Signals from the vestibular system are transmitted to the brain through sensory nerve fibers. When vestibular information degrades or fails to transmit entirely due to a vestibular dysfunction, one's ability to maintain balance is compromised [8].

1

Vestibular dysfunction can result from injury, disease, or aging. Typically, vestibular dysfunction is categorized as either central or peripheral in origin [9-10]. Abnormalities within the brain (e.g., cereberovascular disorders, migraines, central positional nystagmus, and neurodegenerative disorders) can cause central vestibular dysfunction [9-10]. Peripheral vestibular dysfunction can be caused by vestibular neuritis, benign paroxysmal positional vertigo, Ménière disease, ototoxicity, and abnormalities within the nerves of the inner ear [9]. Vestibular dysfunction can produce symptoms of dizziness, vertigo, or some form of balance deficit [9-13].

More than a third of Americans over the age of forty have vestibular dysfunction, with the number increasing by approximately 16 million each year [14]. Furthermore, at least two million Americans experience chronic impairment due to dizziness or a balance disorder, resulting in healthcare costs of over one billion dollars annually [15]. Balance disorders due to vestibular dysfunction increase the risk of falling, ultimately resulting in a lower quality of life [12, 16-18]. Although not solely resulting from vestibular deficits, each year non-fatal and fatal falls lead to medical costs of approximately 19 billion and 200 million dollars, respectively [19].

1.2. Balance rehabilitation

Clinical rehabilitation therapy provides patients with a set of customized, therapist-supervised exercises. The primary idea of balance rehabilitation therapy is to leverage the CNS's ability to reweight unimpaired sensory inputs in the event of sensory loss [20]. The exercises practiced in clinical balance rehabilitation programs are typically designed

to retain intact sensorimotor abilities and regain dysfunctional sensorimotor abilities, or to develop new sensorimotor strategies in order to facilitate functional mobility and restore a sense of balance [17, 21-22]. Therapy programs for balance rehabilitation usually incorporate sensory and motor enhancements as well as cognitive and psychological processes; they are proven to be more effective than muscular training alone for alleviating balance deficits [23-24].

Cawthorne [25] and Cooksey [26] are credited for developing a series of balance exercises in the 1940s known as the Cawthorne-Cooksey exercises. These exercises were developed to bolster the vestibular system and minimize dizziness; they are primarily composed of eye and head movements performed while sitting, standing, or various dynamic balance tasks [27]. This form of exercise was further developed to enhance visual stability (stabilizing the visual gaze) with head movements, visual function without head movements, and interactions between the visual and vestibular systems [28]. Multiple studies have shown that clinical balance rehabilitation exercises help improve the symptoms of patients with vestibular dysfunction, some patients even completely recover from their symptoms [29-34]. Patients are instructed to continue performing the balance exercises at home following the completion of their therapy program.

Due to the costs associated with physical therapy and the limited number of physical therapists [15, 35], some patients cannot participate in the ideal number of clinical balance training sessions. In such situation, patients are commonly prescribed home-based exercises. However, compliance decreases over time due to a lack of feedback while the exercise is being performed and after the exercise has been performed [36-38]. Furthermore, patients are often unable to recall the proper procedures for the exercises

[39-40]. This uncertainty often leads to further decreases in the number of repetitions performed, or even cessation of balance training altogether. Technology that augments traditional rehabilitation practice in a clinical setting or increases compliance in at-home-based exercise programs has the potential to provide both instructions for the intended rehabilitation exercises and real-time or delayed feedback about performance.

1.3. Sensory augmentation for balance-related applications

Sensory augmentation is a technique for supplementing or reinforcing compromised sensory information and typically consists of three parts: a sensor, a processor, and a display (typically a stimulator). The sensor measures the desired signal and relays the information to the processor, which then interprets the signal and activates the stimulator.

Non-invasive or wearable sensory augmentation systems, also known as biofeedback systems or sensory substitution systems, provide cues that typically require a volitional response, as opposed to an invasive system that might stimulate nerves directly.

In general, biofeedback seeks to help patients regain their sensorimotor abilities by providing visual, auditory, or tactile cues in real time. These cues can correspond to body limb kinematics, kinetics, or neuromuscular activity [41-43]. Biofeedback systems provide the user with information about an instantaneous error associated with the current physical task. Users are typically instructed to generate correctional responses based on the information about the error in their movement [44]. Although the underlying neurological mechanisms are unclear, Basmajian [45] suggested that new pathways might be developed in the brain as a result of using biofeedback. It is hypothesized that the

concurrent use of biofeedback during task performance will promote task learning [42-43], increase retention [46], and motivate users during the repetitive exercises [47-48], thereby leading them to enhanced sensorimotor function recovery [43, 49]. Furthermore, Wolf demonstrated that new sensory memory can be established by repeated biofeedback training, and thus help patients perform functional tasks, even without feedback [49].

In the context of balance-related applications, laboratory-based biofeedback systems have been shown to improve balance in a number of different populations, including healthy younger and older adults [50-52], individuals with vestibular loss [53-58], and individuals with stroke [59]. The most commonly used biofeedback modality and control signal for balance-related applications is visual biofeedback of the body's center of pressure (COP); forward and backward motion of the COP is continuously displayed as upward and downward motion of a virtual object (e.g., a cursor), and left and right COP motion is displayed as left and right motion of the virtual object. Visual biofeedback through the use of a virtual object can be accomplished using computer graphics projected onto monitors or head-mounted displays (HMD) in two dimensional virtual environments. Furthermore, virtual reality-based biofeedback systems have been shown to reduce body sway in both healthy subjects and individuals with vestibular deficits [60-62].

Recently, auditory tones have been used to represent body sway [55, 63-64]. Auditory biofeedback systems provide information about the body's center of mass (COM), as measured by accelerometers worn on a belt around the trunk, by varying the volume and frequency of the tones delivered to each ear. The use of auditory biofeedback systems has

been shown to reduce body sway in both healthy subjects and in individuals with vestibular loss while standing with their eyes closed [55, 64].

Compared to visual and auditory biofeedback displays, tactile inputs have several advantages. Tactile stimulation can be provided in a discreet manner while not interfering with important visual and auditory exteroceptive information. Human tactile sensation is achieved through the cutaneous system, which consists of mechanoreceptors embedded in the skin. Tactile displays used for balance-related applications can be subcategorized into two forms: electrotactile and vibrotactile.

Electrotactile biofeedback systems pass a small electric current through the skin to provide cues about head or whole body motion [54, 65-66]. Young healthy subjects exhibited reduced COP displacements when tongue-based electrotactile biofeedback was used during standing tasks on foam and firm surfaces [54, 65-66]. Although electrotactile biofeedback devices have been shown to improve postural stability, such systems can cause pain and fatigue in the skin and discomfort to the user.

1.4. Vibrotactile biofeedback technology for balance-related applications

Vibrotactile biofeedback technology for balance-related applications was inspired by aviation-based directional cuing systems developed by the Naval Aerospace Medical Research Laboratory. The Tactile Situation Awareness System (TSAS) [67-69] provides pilots with information about their aircraft's altitude and orientation through a vibrotactile display embedded in their flight suit [67-69]. The early balance-related vibrotactile biofeedback systems were developed to provide real-time information to patients with vestibular deficits about their body's motion in space. Subjects were

6

instructed to use the information provided by the vibrotactile display to generate postural corrections [70-72]. Subsequent laboratory-based studies have assessed the efficacy of vibrotactile biofeedback systems to improve balance performance during quiet [57-58, 73-75] and perturbed [56, 76-78] stance. Due to their increasingly successful results during quiet and perturbed stance, vibrotactile biofeedback displays have been further employed for use during locomotor activities [51, 79-82]. During gait-related tasks, vibrotactile biofeedback has been shown to reduce trunk sway, COM displacement, and/or medial-lateral (M/L) step width in young healthy subjects [51], older adult subjects [81-82], and subjects with vestibular loss [79-80]. However, Verhoeff et al. [82] and Wall et al. [81] have found a decrease in gait velocity when vibrotactile biofeedback was used during walking exercises.

The most common sensing instrument used in biofeedback systems is an inertial measurement unit (IMU). IMUs eliminate the need for an expensive external apparatus, such as a mechanical link, camera, or magnetic emitter, which are widely used in mechanical, optical, and electromagnetic tracking systems. The IMU provides a platform for real-time motion tracking in unconstrained environments [75, 83-85]. In general, the IMU is composed of rate gyroscopes, accelerometers, and magnetometers.

Several types of vibrotactile actuators are commercially available, the most common variations being inertial (a.k.a. inertial shakers), linear, and rotational actuators [86-87]. The Tactaid VBW32 tactor (Audiological Engineering Corporation, USA) is an inertial transducer, which consists of a rigid case surrounding a mass suspended on a spring [86]; both the mass and the case vibrate when an alternating electromagnetic force is generated. The C-2 tactor (Engineering Acoustics Inc., USA) is a voice-coil-type linear actuator that

incorporates a moving contactor lightly preloaded against the skin [86]. When an electrical signal is applied, the contactor oscillates perpendicular to the skin, while the surrounding skin area is shielded with a passive housing. Tactaid and C-2 tactors both generate a vibration in a plane normal to the surface of the skin. The coin-style tactor is a rotary electromechanical actuator that includes a semi-circular cylindrical weight, which is mounted onto the motor's shaft, and varies its rotational speed based on the amount of DC voltage that is run through it. Unlike the Tactaid VBW32 and C-2 tactor, the coin-style tactor generates a rotational vibration in a plane parallel to the skin. In the balance-related application domain, laboratory-based vibrotactile biofeedback systems widely employ Tactaid and C-2 tactors [52, 56, 58, 70, 75, 88-92]. Recently, however, coin-style tactors have also become widely used due to their small size, low weight, and low cost when compared to the both Tactaid VBW32 and C-2 tactors [93-98].

Currently the most preferred vibrotactile display arrangement and location for upright stance applications is an array of tactors distributed along a belt placed around the torso [56, 70, 75-76, 99-102]. Previous studies have demonstrated that the torso is moderately sensitive to vibration, and thus might be a suitable location for providing directional cues. Cholewiak et al. [103] suggested that tactile localization was most precise when eight separated tactors are placed equidistantly around the torso. In addition, van Erp [104] conducted a study regarding the spatial accuracy of vibrations around the torso and found that the spatial resolution of the torso area is roughly less than 3.0 cm. In most torso-based vibrotactile biofeedback studies, forward, backward, left and right body sway are displayed on their respective sides of the torso.

Directional cues through vibrotactile biofeedback devices can be either attractive or repulsive. When users are instructed to move toward the vibration, the vibration is considered an attractive cue. Alternatively, when users are instructed to move away from the vibration, it is termed a repulsive cue. The most common torso-based vibrotactile biofeedback systems provide directional information about body tilt with repulsive cues. This paradigm was also used by Wall et al. [70] for the first vibrotactile feedback balance device. However, the responses of the natural posture to the vibration around the torso remain unknown. Hence, studies on the effect of vibration on postural responses are necessary in order to determine whether one cuing strategy has any advantages over the other.

Vibrotactile biofeedback balance training systems have recently become commercially available outside the U.S. [105-106]. The BalanceFreedom™ [105] measures angular deviations and angular velocities of the trunk, as well as provides auditory, vibrotactile, and visual cues through a headband. The VertiGuard® RT [106] is a vibrotactile feedback system that measures body sway and provides vibrotactile cues to the trunk where the intensity and location of the vibration is directly proportional to and indicative of the magnitude and direction of the body sway.

1.5. Dissertation aims

There are three main goals of this dissertation: 1) to characterize non-volitional human postural behavioral responses to torso-based vibrotactile stimulation (i.e., in the absence of instruction); 2) to design, develop, model, and experimentally evaluate a system for

conveying motion instructions to a trainee based on the error between an expert and trainee for potential clinical and home-based balance rehabilitation training applications; and 3) to design, develop, and assess a cell phone based vibrotactile biofeedback system that could be used for home-based balance rehabilitation applications.

Aim 1: It is known that the vibration of several skeletal muscles can lead to an illusion of movement by driving proprioceptive afferents or modifying reflex responses. Hence, the first study seeks to investigate the effects of torso vibrotactile stimulation on standing posture as a function of the location of stimulus application and the strength of the vibrotactile stimulation. The primary goal of this study is to determine whether vibrotactile stimulation induces a directional postural shift in the absence of instructions.

> **H1$_1$:** If torso tactile information contributes to kinesthesia, vibration will induce a repeatable and measurable directional shift in posture.
>
> **H1$_2$:** If vibrotactile stimulation induces a postural shift, the amount of postural shift will be dependent on the strength of the stimulation.

Aim 2: The goal of this study is to design, develop, and initially assess a wearable, wireless IMU-based expert-trainee motion error detection and vibrotactile instructional cuing technology, which would enable an expert (i.e., physical therapist) to map his/her movements to a trainee (i.e., patient). This study will investigate the effects of changing the expert-trainee error thresholds (0.5°, 1.0°, and 1.5°), and the effects of varying the nature of the control signal (proportional, proportional plus derivative) during anterior-posterior (A/P) trunk movements (using pre-specified target trajectories representing

ideal expert movements and only two actuators) in pilot experiments with young, healthy subjects. Mathematical modeling will be performed using a simple inverted pendulum to gain insight into the effects of the control signal on performance. In addition, the effects of speed and complexity of the expert pattern will be evaluated. Finally the effects of attractive versus repulsive vibrotactile instructional cues will be evaluated when the speed and complexity of the expert pattern are varied. The primary outcome measures include: a cross-correlation value ranging between 0 and 1, with 1 indicating perfectly matched motion; a time delay, with a positive delay indicating a time lag between the expert and trainee motion; and average position error.

$H2_1$: Performance for replicating a pre-specified A/P trunk movement will be improved with the addition of velocity information to the position information when compared to performance with only position information.

$H2_2$: Performance while replicating a pre-specified A/P trunk movement will improve if the smallest error threshold is employed.

$H2_3$: Increasing motion speed and complexity will lead to decreased performance for replicating a pre-specified A/P trunk movement.

$H2_4$: Attractive instruction will produce better performance than repulsive instruction.

Aim 3: The goal of this research is to demonstrate proof-of-concept for a cell phone based balance training system that could eventually be used at home to augment balance rehabilitation exercises. This study quantitatively assesses the effectiveness of the proposed system among young healthy subjects and subjects with vestibular involvement.

11

The subjects' performance will be characterized by both time and frequency domain metrics that include RMS sway, elliptical area fits to their sway trajectory, percentage of time spent in the dead zone, and mean power frequency.

H3$_1$: The cell phone based vibrotactile feedback system will improve balance performance during a subset of standing balance rehabilitation exercises among young healthy subjects and subjects with vestibular involvement.

1.6. Overview of dissertation structure

Chapter 2, *Directional postural responses induced by vibrotactile stimulations applied to the torso*, describes the motor and perceptual effects on standing posture of vibrotactile stimulation when applied to various locations around the torso in the absence of instructions. The results reveal involuntary compensatory postural shifts in the direction of vibration when vibrotactile stimulation is applied over the internal oblique and erector spinae muscles. Postural responses show that tactile information at the level of the iliac crest contributes to a spatial representation of the upper body and a postural shift toward the stimulation provides an understanding that is critical to the design of torso-based vibrotactile displays. These results may have clinical implications, since vibrotactile stimulation can be used to indicate the direction in which an individual affected by a balance disorder should move in order to maintain a stable standing posture. To date, vibrotactile stimulation has been used to indicate the direction of the body's postural tilt with instructions to "move away from the vibration," analogous to an aversion response. This instruction seems incompatible with the natural tendency (postural shift in the

direction of the stimulation) revealed here. Thus, the use of vibrotactile biofeedback should be carefully considered, and instruction of reactive/corrective movements should be made compatible with the unconstrained response to stimulation in order to properly facilitate postural adjustments.

Chapter 3, *A wearable device for real-time motion error detection and vibrotactile instructional cuing*, describes the design, development, and assessment of a wearable IMU-based expert-trainee motion error detection and vibrotactile instructional cuing technology platform. Specifically, this chapter: 1) describes the hardware and software components of the device, 2) quantitatively assesses the device's effectiveness in a young healthy pilot subject population during a simple trunk bend exercise, 3) determines the optimal control signals and movement error thresholds for vibrotactile instructional cuing, 4) examines the effect of speed and complexity on performance, and 5) evaluates the effects of attractive versus repulsive vibrotactile instructional cuing. From the results, subjects performed best when using a 0.5 degree error threshold and a control signal comprising proportional plus half derivative information. Furthermore, cross-correlation values are maximized and average position errors are minimized when the movements are performed slowly and the motion patterns being replicated are simple. Finally, results show that repulsive cues may be effective when subjects perform motion replication tasks for short-term applications.

Chapter 4, *Modeling and simulation of the Mobile Instrument for Motion Instruction and Correction (MIMIC)*, presents a simple model based on the work of Goodworth et al.

(2009). Simulations are performed to examine the effects of the controller gains on performance. The simulation findings are found to be in agreement with the experimental results reported in Chapter 3.

Chapter 5, *Cell phone based balance trainer*, describes the technology and reports on a proof-of-concept study that quantitatively assesses the effectiveness of the cell phone based balance aid in improving postural stability during a standard balance exercise. Up until now, commercial and laboratory-based vibrotactile sensory augmentation platforms have been composed of costly and bulky high fidelity inertial measurement units and computational processors. This chapter describes the design and development of a cell phone based system that provides vibrotactile cues to inform postural corrections, and offers advantages in terms of cost, size, weight, functionality, flexibility, and accessibility. The long-term goal of this work is to develop an effective system that can be used at home to assist patients with therapist-assigned balance exercises, or in an environment where access to balance therapy is limited (e.g., rural regions in the developing world, where health care access is difficult but cell phone networks are increasingly prevalent).

Chapter 6, *Discussion*, summarizes the major conclusions, contributions, and limitations of this research.

Chapter 7, *Future work*, provides recommendations for additional studies and technological development to be completed in this field to facilitate the transition of

vibrotactile instructional and feedback systems from a research/laboratory setting into the clinic and/or home.

References

[1]   H. J. Allum, "Organization of stabilizing reflex responses in tibialis anterior muscles following ankle flexion perturbations of standing man.," *Brain Research,* vol. 264, no. 2, pp. 297-201, Apr. 1983.

[2]   B. L. Day, S. C. A., L. Bartolomei, M. A. Pastor, and I. N. Lyon, "Human body-segment tilts induced by galvanic stimulation: a vestibularly driven balance protection mechanism," *Journal of Physiology,* vol. 500, no. 3, pp. 661-672, May. 1997.

[3]   R. J. Peterka, "Sensorimotor Integration in human postural control," *Journal of Neurophysiology,* vol. 88, no. 3, pp. 1097-1118, Sep. 2002.

[4]   D. N. Lee and J. R. Lishman, "Visual proprioceptive control of stance," *Journal of Human Movement Studies,* vol. 1, no. 2, pp. 87-95, Jun. 1975.

[5]   S. M. Highstein, *The Vestibular System*, 1st ed.: Springer Verlag, 2004.

[6]   D. E. Angelaki and K. E. Cullen, "Vestibular System: The Many Facets of a Multimodal Sense," *Annual Review of Neuroscience,* vol. 31, pp. 125-150, Jul. 2008.

[7]   C. C. Della Santina, V. Potyagaylo, A. A. Migliaccio, L. B. Minor, and J. P. Carey, "Orientation of human semicircular canals measured by three-dimensional

multiplanar CT reconstruction," *Journal of the Association for Research in Otolaryngology,* vol. 6, no. 3, pp. 191-206, Sep. 2005.

[8]   C. G. Horlings, U. M. Kueng, F. Honegger, B. R. Bloem, N. Van Alfen, and B. G. Van Engelen, "Identifying deficits in balance control following vestibular or lower leg proprioceptive loss using posturographic analysis of stance tasks," *Clinical Neurophysiology,* vol. 119, no. 10, pp. 2338-2346, Oct. 2008.

[9]   M. Alrwaily and S. L. Whitney, "Vestibular rehabilitation of older adults with dizziness," *Otolaryngologic clinics of North America,* vol. 44, no. 2, pp. 473-496, Apr. 2011.

[10]   M. Dieterich, "Central vestibular disorders," *Journal of Neurology,* vol. 254, no. 5, pp. 559-568, May. 2007.

[11]   R. W. Baloh, K. M. Jacobson, K. Beykirch, and V. Honrubia, "Static and dynamic posturography in patients with vestibular and cerebellar lesions," *Archives of Neurology,* vol. 55, no. 5, pp. 649-654, May. 1998.

[12]   S. J. Herdman, P. Blatt, M. C. Schubert, and R. J. Tusa, "Falls in patients with vestibular deficits," *American Journal of Otolaryngology* vol. 21, no. 6, pp. 847-851, Nov. 2000.

[13]   F. B. Horak, L. M. Nashner, and H. C. Diener, "Postural strategies associated with somatosensory and vestibular loss," *Experimental Brain Research,* vol. 82, no. 1, pp. 167-177, 1990.

[14]   Y. Agrawal, J. P. Carey, C. C. Della Santina, M. C. Schubert, and L. B. Minor, "Disorders of balance and vestibular function in US adults," *Archives of Internal Medicine,* vol. 169, no. 10, pp. 938-944, May. 2009.

[15]   "National Strategic Research Plan: Language and Language Impairments, Balance and Balance Disorders, Voice and Voice Disorders," in *National Institutes of Health*.

[16]   D. Avers and C. Lindsey, "What You Need to Know about Balance and Falls; a Physical Therapist's Perspective," in *American Physical Therapy Association patient education brochures*, ed, 1998.

[17]   E. E. Hansson, N. O. Mansson, K. A. Ringsberg, and A. Hakansson, "Falls among dizzy patients in primary healthcare: An intervention study with control group," *International Journal of Rehabilitation Research,* vol. 31, no. 1, pp. 51-57, Mar. 2008.

[18]   M. E. Tinetti, M. Speechley, and S. F. Ginter, "Risk factors for falls among elderly persons living in the community," *New England Journal of Medicine,* vol. 319, no. 26, pp. 1701-1007, Dec. 1988.

[19]   J. A. Stevens, P. S. Corso, E. A. Finkelstein, and T. R. Mille, "The costs of fatal and non-fatal falls among older adults," *Injury Prevention,* vol. 12, no. 5, pp. 290-295, Oct. 2006.

[20]   S. J. Herdman, *Vestibular Rehabilitation*, 2nd ed. vol. 102. Philadelphia: F.A. Davis Company. 597, 2000.

[21]   J. Y. Jung, J. S. Kim, P. S. Chung, S. H. Woo, and C. K. Rhee, "Effect of vestibular rehabilitation on dizziness in the elderly," *American Journal of Otolaryngology,* vol. 20, no. 5, pp. 295-299, Feb. 2009.

[22]   M. Pavlou, A. Shumway-Cook, F. Horak, L. Yardley, and A. Bronstein, "Rehabilitation of balance disorders in the patient with vestibular pathology," vol.

Clinical disorders of balance and gait, A. Bronstein, Brandt, Thomas, Woollacott, Marjorie H. and Nutt, JG. 1996, Ed., ed New York. : Oxford University Press, Inc., 2004, pp. 211-235.

[23]   B. A. Alsalaheen, A. Mucha, L. O. Morris, S. L. Whitney, J. M. Furman, C. E. Camiolo-Reddy, M. W. Collins, M. R. Lovell, and P. J. Sparto, "Vestibular rehabilitation for dizziness and balance disorders after concussion," *Journal of Neurologic Physical Therapy,* vol. 34, no. 2, pp. 87-93, Jun. 2010.

[24]   T. C. Hain. 2010, *Vestibular Rehabilitation Therapy (VRT).*
Available: http://www.dizziness-and-balance.com/treatment/rehab.html#general

[25]   T. Cawthorne, "Vestibular Injuries," *Proc. Royal Society of Medicine,* vol. 39, no. 5, pp. 270-273, Mar. 1946.

[26]   F. S. Cooksey, "Rehabilitation in Vestibular Injuries," *Proc. Royal Society of Medicine,* vol. 39, no. 5, pp. 273-278, Mar. 1946.

[27]   J. L. Cowand, D. M. Wrisley, M. Walker, B. Strasnick, and J. T. Jacobson, "Efficacy of vestibular rehabilitation," *Otolaryngology - Head and Neck Surgery,* vol. 118, no. 1, pp. 49-54, Jan. 1998.

[28]   D. Zee, *Treatment of vertigo*. Philadelphia: BC Decker, 1985.

[29]   A. U. Alahakone and S. M. N. A. Senanayake, "A Real-Time System With Assistive Feedback for Postural Control in Rehabilitation," *IEEE/ASME Transactions on Mechatronics,* vol. 15, no. 2, pp. 226-233, Apr. 2010.

[30]   H. Cohen, "Vestibular rehabilitation reduces functional disability," *Otolaryngology Head and Neck Surgery,* vol. 107, no. 5, pp. 638-43, Nov. 1992.

[31]   F. B. Horak, C. Jones-Rycewicz, F. O. Black, and A. Shumway-Cook, "Effects of vestibular rehabilitation on dizziness and imbalance," *Otolaryngology - Head and Neck Surgery* vol. 106, no. 2, pp. 175-180, Feb. 1992.

[32]   R. J. Keim, M. Cook, and D. Martini, "Balance rehabilitation therapy," *Laryngoscope,* vol. 102, no. 11, pp. 1302-1307, Nov. 1992.

[33]   S. A. Telian, N. T. Shepard, M. Smith-Wheelock, and M. Hoberg, "Bilateral vestibular paresis: diagnosis and treatment," *Otolaryngology Head and Neck Surgery,* vol. 104, no. 1, pp. 67-71, Jan. 1991.

[34]   S. A. Telian, N. T. Shepard, M. Smith-Wheelock, and J. L. Kemink, "Habituation therapy for chronic vestibular dysfunction: preliminary results," *Otolaryngology Head and Neck Surgery,* vol. 103, no. 1, pp. 89-95, Jul. 1990.

[35]   BureauofLaborStatistics. *Occupational Outlook Handbook-Physical Therapists (2010-11 ed.).* Available: http://www.bls.gov/oco/ocos080.htm

[36]   C. L. Kao, L. K. Chen, C. M. Chern, L. C. Hsu, C. C. Chen, and S. J. Hwang, "Rehabilitation outcome in home-based versus supervised exercise programs for chronically dizzy patients," *Archives of Gerontology and Geriatrics,* Nov/Dec. 2009.

[37]   E. M. Sluijs, G. J. Kok, and J. van der Zee, "Correlates of exercise compliance in physical therapy," *Physical Therapy,* vol. 73, no. 11, pp. 771-782; discussion 783-786, Nov. 1993.

[38]   R. Forkan, B. Pumper, N. Smyth, H. Wirkkala, M. A. Ciol, and A. Shumway-Cook, "Exercise adherence following physical therapy intervention in older adults with impaired balance," *Physical Therapy,* vol. 86, no. 3, pp. 401-410, Mar. 2006.

[39]   R. P. Kessels, "Patients' memory for medical information," *Journal of the Royal Society of Medicine,* vol. 96, no. 5, pp. 219-222, May. 2003.

[40]   E. Sluijs, S. van Dulmen, L. van Dijk, D. Ridder, R. Heerdink, and J. Bensing, "Patient adherence to medical treatment: a meta-review," Netherlands Institute of Health Services Research, Utrecht, 2006.

[41]   A. U. Alahakone and S. M. N. A. Senanayake, "Vibrotactile feedback systems: Current trends in rehabilitation, sports and information display," in *IEEE/ASME International Conference on Advanced Intelligent Mechatronics*, 2009, pp. 1148 - 1153.

[42]   C. K. Fernando and J. V. Basmajian, "Biofeedback in physical medicine and rehabilitation," *Biofeedback and self-regulation* vol. 16, no. 3, pp. 435-455, Sep. 1978.

[43]   H. Huang, S. L. Wolf, and J. He, "Recent developments in biofeedback for neuromotor rehabilitation," *Journal of Neuroengineering and Rehabilitation,* vol. 3, no. 1, pp. 11-22, Sep. 2006.

[44]   R. A. Magill, *Motor learning and control: Concepts and applications*, 7th ed. New York: McGraw-Hill, 2003.

[45]   J. V. Basmajian, *Biofeedback : principles and practice for clinicians*, 3rd ed. Baltimore: Williams & Wilkins, 1989.

[46]   D. E. Thorpe and J. Valvano, "The effects of knowledge of performance and cognitive strategies on motor skill learning in children with cerebral palsy," *Pediatric Physical Therapy,* vol. 14, no. 1, pp. 2-15, Oct. 2002.

[47]   J. A. Adams, "Historical review and appraisal of research on the learning, retention, and transfer of human motor skills," *Psychological Bulletin,* vol. 101, no. 1, pp. 41-74, Jan. 1987.

[48]   J. J. Annesi, "Effects of computer feedback on adherence to exercise," *Perceptual and Motor Skills,* vol. 87, no. 2, pp. 723-730, Oct. 1998.

[49]   S. L. Wolf, "Electromyographic biofeedback applications to stroke patients. A critical review," *Physical Therapy,* vol. 63, no. 9, pp. 1448-1459, Sep. 1983.

[50]   L. L. Verhoeff, C. G. Horlings, L. J. Janssen, S. A. Bridenbaugh, and J. H. Allum, "Effects of biofeedback on trunk sway during dual tasking in the healthy young and elderly," *Gait and Posture,* vol. 30, no. 1, pp. 76-81, Jul 2009.

[51]   L. J. Janssen, L. L. Verhoeff, C. G. Horlings, and J. H. Allum, "Directional effects of biofeedback on trunk sway during gait tasks in healthy young subjects," *Gait & Posture,* vol. 29, no. 4, pp. 575-581, Jun. 2009.

[52]   D. Ursu, L. T. Jiang, and K. H. Sienko, "Effect of vibrotactile trunk tilt feedback on postural stability in older adults," in *Proc. Annual American Society of Biomechanics Meeting*, Pennsylvania, PA, USA, Aug., 2009.

[53]   M. Dozza, L. Chiari, B. Chan, L. Rocchi, F. B. Horak, and A. Cappello, "Influence of a portable audio-biofeedback device on structural properties of postural sway," *Journal of Neuroengineering and Rehabilitation,* vol. 31, pp. 2-13, May. 2005.

[54]   N. Vuillerme, O. Chenu, J. Demongeot, and Y. Payan, "Controlling posture using a plantar pressure-based, tongue-placed tactile biofeedback system," *Experimental Brain Research,* vol. 179, no. 3, pp. 409-414, Nov. 2007.

[55] M. Dozza, L. Chiari, and F. B. Horak, "Audio-biofeedback improves balance in patients with bilateral vestibular loss," *Archives of physical medicine and rehabilitation,* vol. 86, no. 7, pp. 1401-1403, Jul. 2005.

[56] K. H. Sienko, M. D. Balkwill, L. I. Oddsson, and C. Wall, "Effects of multi-directional vibrotactile feedback on vestibular-deficient postural performance during continuous multi-directional support surface perturbations," *Journal of Vestibular Research,* vol. 18, no. 5-6, pp. 273-285, Jan. 2008.

[57] C. Wall and E. Kentala, "Control of sway using vibrotactile feedback of body tilt in patients with moderate and severe postural control deficits," *Journal of Vestibular Research,* vol. 15, no. 5-6, pp. 313-325, Apr. 2005.

[58] E. Kentala, J. Vivas, and C. Wall, "Reduction of postural sway by use of a vibrotactile balance prosthesis prototype in subjects with vestibular deficits," *The Annals of otology, rhinology, and laryngology,* vol. 112, no. 5, pp. 404-409, May. 2003.

[59] C. Walker, B. J. Brouwer, and E. G. Culham, "Use of visual feedback in retraining balance following acute stroke," *Physical Therapy,* vol. 80, no. 9, pp. 886-895, Sep. 2000.

[60] D. Fitzgerald, N. Trakarnratanakul, L. Dunne, B. Smyth, and B. Caulfield, "Development and user evaluation of a virtual rehabilitation system for wobble board balance training," in *Annual International Conference of the IEEE Engineering in Medicine and Biology Society*, Vancouver, BC, Canada, Aug., 2008, pp. 4194 - 4198

[61]   N. G. Kim, C. K. Yoo, and J. J. Im, "A new rehabilitation training system for postural balance control using virtual reality technology," *IEEE Transactions on Rehabilitation Engineering* vol. 7, no. 4, pp. 482-485, Dec. 1999.

[62]   L. I. Oddsson, R. Karlsson, J. Konrad, S. Ince, S. R. Williams, and E. Zemkova, "A rehabilitation tool for functional balance using altered gravity and virtual reality," *Journal of Neuroengineering and Rehabilitation,* vol. 4, pp. 25-27, May. 2007

[63]   L. Chiari, M. Dozza, A. Cappello, F. B. Horak, V. Macellari, and D. Giansanti, "Audio-biofeedback for balance improvement: an accelerometry-based system," *IEEE Transactions on Biomedical Engineering,* vol. 52, no. 12, pp. 2108-2111, Dec. 2005.

[64]   M. Dozza, F. B. Horak, and L. Chiari, "Auditory biofeedback substitutes for loss of sensory information in maintaining stance," *Experimental Brain Research,* vol. 178, no. 1, pp. 37-48, Sep. 2007.

[65]   N. Vuillerme, N. Pinsault, O. Chenu, M. Boisgontier, J. Demongeot, and Y. Payan, "How a plantar pressure-based, tongue-placed tactile biofeedback modifies postural control mechanisms during quiet standing," *Experimental Brain Research,* vol. 181, no. 4, pp. 547-554, Sep. 2007.

[66]   N. Vuillerme, N. Pinsault, O. Chenu, J. Demongeot, Y. Payan, and Y. Danilov, "Sensory supplementation system based on electrotactile tongue biofeedback of head position for balance control," *Neuroscience letters,* vol. 431, no. 3, pp. 206-210, Sep. 2008.

[67] B. J. McGrath, N. Suri, R. Carff, A. K. Raj, and A. H. Rupert, "The Role of Intelligent Software in Spatial Awareness Displays," in *Proceedings for 3rd Annual Symposium and Exhibition on Situational Awareness in the Tactical Air Environment*, Piney Point, MD, USA, Jun., 1998, pp. 2-3.

[68] A. H. Rupert, A. Mateczun, and F. E. Guedry, "Maintaining Spatial Orientation Awareness," in *Proceedings of the AGARD Symposium on Situational Awareness. Spatial Awareness in Aerospace Operations*, Copenhagen, Denmark, Oct. 1989, 1990, pp. 1-4.

[69] A. H. Rupert. TSAS Tactile Situation Awareness System [Online]. Available: www.namrl.navy.mil/TSAS/TSASINT2.PPT

[70] C. Wall, M. S. Weinberg, P. B. Schmidt, and D. E. Krebs, "Balance prosthesis based on micromechanical sensors using vibrotactile feedback of tilt," *IEEE Transactions on Biomedical Engineering,* vol. 48, no. 10, pp. 1153-1161, Oct. 2001.

[71] P. B. Schmidt, C. Wall, D. Krebs, and M. S. Weinberg, "An evaluation of a single-axis balance prosthesis prototype with normal subjects," in *Mid-Winter Meeting Association for Research in Otolaryngology*, Tampa Bay, FL, USA, Feb., 1999.

[72] P. P. Kadkade, B. J. Benda, P. B. Schmidt, M. D. Balkwill, and C. Wall, "Optimizing vibrotactile cues for application to a balance prosthesis," in *Mid-Winter Meeting Association for Research in Otolaryngology*, Tampa Bay, FL, USA, Feb. 1999, 1999.

[73] B. C. Lee, K. Bechly, and K. H. Sienko, "Cell phone based vibrotactile feedback system for home-based vestibular rehabilitation balance training," *Journal of Vestibular Research,* vol. 20, no. 3-4, pp. 234-235, Jan. 2010.

[74] C. Wall, L. E. Oddsson, F. B. Horak, D. W. Wrisley, and M. Dozza, "Applications of vibrotactile display of body tilt for rehabilitation," in *Conf. Proc. 26th IEEE Ann. Int. Conf. Engineering in Medicine and Biology Society (EMBS' 04)*, San Francisco, CA, USA, 2004, pp. 4763-4765.

[75] M. S. Weinberg, C. Wall, J. Robertsson, E. O'Neil, K. Sienko, and R. Fields, "Tilt determination in MEMS inertial vestibular prosthesis," *Journal of Biomedical Engineering,* vol. 128, no. 6, pp. 943-956, Dec. 2006.

[76] K. H. Sienko, V. V. Vichare, M. D. Balkwill, and C. I. I. I. Wall, "Assessment of vibrotactile feedback on postural stability during pseudorandom multidirectional platform motion," *IEEE Transactions on Biomedical Engineering,* vol. 57, no. 4, pp. 944-952, Apr. 2010.

[77] V. V. Vichare, C. Wall, M. D. Balkwill, and M. D. Sienko, "Assessing the effect of vibrotactile feedback during continuous multidirectional platform motion: a frequency domain approach," in *Conf Proc IEEE Engineering in Medicine and Biology Society*, Minneapolis, MN, USA, Sep., 2009, pp. 6910-6913.

[78] D. A. Winter, *A.B.C.(Anatomy, Biomechanics, and Control) of balance during standing and walking*. Waterloo: University of Waterloo, 1995.

[79] M. Dozza, C. Wall, 3rd, R. J. Peterka, L. Chiara, and F. B. Horak, "Effects of practicing tandem gait with and without vibrotactile biofeedback in subjects with

unilateral vestibular loss," *Journal of Vestibular Research,* vol. 17, no. 4, pp. 195-204, Jan. 2007.

[80]   F. B. Horak, M. Dozza, R. Peterka, L. Chiari, and C. Wall, 3rd, "Vibrotactile biofeedback improves tandem gait in patients with unilateral vestibular loss," *Annals of the New York Academy of Sciences,* vol. 1164, pp. 279-281, May. 2009.

[81]   C. Wall, 3rd, D. M. Wrisley, and K. D. Statler, "Vibrotactile tilt feedback improves dynamic gait index: a fall risk indicator in older adults," *Gait and Posture,* vol. 30, no. 1, pp. 16-21, Jul. 2009.

[82]   L. Verhoeff, G. C. Horlings, J. F. Janssen, A. Bridenbaugh, and H. J. Allum, "Effects of biofeedback on trunk sway during dual tasking in the healthy young and elderly," *Gait & Posture,* vol. 30, no. 1, pp. 76-81, Jul. 2009.

[83]   E. R. Bachmann, Y. Xiaoping, D. McKinney, R. B. McGhee, and M. J. Zyda, "Design and implementation of MARG sensors for 3-DOF orientation measurement of rigid bodies," in *Conf. Proc. IEEE Int. Conf. Robotics and Automation (ICRA' 03),* Taipei, Taiwan, Sep., 2003, pp. 1171-1178.

[84]   Z. Rong and Z. Zhaoying, "A real-time articulated human motion tracking using tri-axis inertial/magnetic sensors package," *IEEE Transactions on Neural Systems and Rehabilitation Engineering,* vol. 12, no. 2, pp. 295-302, Jun. 2004.

[85]   A. M. Sabatini, C. Martelloni, S. Scapellato, and F. Cavallo, "Assessment of walking features from foot inertial sensing," *IEEE Transactions on Biomedical Engineering,* vol. 52, no. 3, pp. 486-494, Mar. 2005.

[86]   R. W. Cholewiak and M. Wollowitz, "The design of vibrotactile transducers," in *Tactile Aids for the Hearing Impaired, I. Summers, ed, Whurr Publishers Ltd*, London, UK, Oct., 1992, pp. 57-82.

[87]   B. J. Mortimer, G. A. Zets, and R. W. Cholewiak, "Vibrotactile transduction and transducers," *Journal of the Acoustical Society of America,* vol. 121, no. 5 Pt1, pp. 2970-1977, May. 2007.

[88]   C. Wall, L. E. Oddsson, F. B. Horak, D. W. Wrisley, and M. Dozza, "Applications of vibrotactile display of body tilt for rehabilitation," in *Engineering in Medicine and Biology Society, 2004. IEMBS '04. 26th Annual International Conference of the IEEE*, 2004, pp. 4763-4765.

[89]   C. I. I. I. Wall and M. S. Weinberg, "Balance prostheses for postural control," *Engineering in Medicine and Biology Magazine, IEEE,* vol. 22, no. 2, pp. 84-90, 2003.

[90]   R. J. Peterka, C. I. I. I. Wall, and E. Kentala, "Determining the effectiveness of a vibrotactile balance prosthesis," *Journal of Vestibular Research,* vol. 16, no. 1-2, pp. 45-65, Jan. 2006.

[91]   J. A. Goebel, B. C. Sinks, B. E. Parker, Jr., N. T. Richardson, A. B. Olowin, and R. W. Cholewiak, "Effectiveness of head-mounted vibrotactile stimulation in subjects with bilateral vestibular loss: a phase 1 clinical trial," *Otol Neurotol,* vol. 30, no. 2, pp. 210-216, Feb. 2009.

[92]   A. A. Priplata, B. L. Patritti, J. B. Niemi, R. Hughes, D. C. Gravelle, L. A. Lipsitz, A. Veves, J. Stein, P. Bonato, and J. J. Collins, "Noise-enhanced balance control

in patients with diabetes and patients with stroke," *Ann Neurol,* vol. 59, no. 1, pp. 4-12, Jan. 2006.

[93] R. W. Lindeman, Y. Yanagida, K. Hosaka, and S. Abe, "The TactaPack: A Wireless Sensor/Actuator Package for Physical Therapy Applications," in *Proc. IEEE Inter. Symp. Haptic Interfaces for Virtual Environment and Teleoperator Systems*, Arlington, VA, USA, Mar., 2006, pp. 337-341.

[94] P. Kapur, M. Jensen, L. J. Buxbaum, S. A. Jax, and K. J. Kuchenbecker, "Spatially distributed tactile feedback for kinesthetic motion guidance," in *IEEE Haptics Symposium*, Waltham, MA, USA, Mar., 2010, pp. 519-526.

[95] P. Kapur, S. Premakumar, S. A. Jax, L. J. Buxbaum, A. M. Dawson, and K. J. Kuchenbecker, "Vibrotactile feedback system for intuitive upper-limb rehabilitation," in *Conf. Proc. World Haptics 2009 - Third Joint EuroHaptics conf. and IEEE Inter. Symp. Haptic Interfaces for Virtual Environment and Teleoperator Systems*, Salt Lake City, UT, USA, Mar., 2009, pp. 621-622.

[96] J. Lieberman and C. Breazeal, "Development of a wearable vibrotactile feedback suit for accelerated human motor learning," in *Conf. Proc. IEEE Int. Conf. Robotics and Automation (ICRA' 09)*, Kobe, Japan, Oct., 2007, pp. 4001-4006.

[97] G. Shuxiang, S. Gang, and S. Zhibin, "Development of a Self-assisted Rehabilitation System for the Upper Limbs Based on Virtual Reality," in *Conf. Proc. IEEE Int. Conf. Mechatronics and Automation (ICMA'07)*, Harbin, China, Aug., 2007, pp. 1452-1457.

[98] J. van der Linden, E. Schoonderwaldt, and J. Bird, "Towards a real-time system for teaching novices correct violin bowing technique," in *Haptic Audio visual*

Environments and Games, 2009. HAVE 2009. IEEE International Workshop on, Lecco, Italy, 2009, pp. 81-86.

[99]   A. D. Goodworth, C. Wall, and R. J. Peterka, "Influence of Feedback Parameters on Performance of a Vibrotactile Balance Prosthesis," *IEEE Transactions on Neural Systems and Rehabilitation Engineering,* vol. 17, no. 4, pp. 397-408, Aug. 2009.

[100] S. Haggerty, L. T. Jiang, A. Galecki, and K. H. Sienko, "Effects of vibrotactile feedback on response time and postural stability in older adults," *Gait & Posture,* 2012 (In press).

[101] C. Wall, "Application of vibrotactile feedback of body motion to improve rehabilitation in individuals with imbalance," *Journal of Neurologic Physical Therapy,* vol. 34, no. 2, pp. 98-104, Jun. 2010.

[102] C. Wall and E. Kentala, "Effect of displacement, velocity, and combined vibrotactile tilt feedback on postural control of vestibulopathic subjects," *Journal of Vestibular Research,* vol. 20, no. 1, pp. 61-69, Jan. 2010.

[103] R. W. Cholewiak, C. J. Brill, and A. Schwab, "Vibrotactile localization on the abdomen: Effects of place and space," *Perception and Psychophysics,* vol. 66, no. 6, pp. 970-987, Aug. 2004.

[104] J. B. F. van Erp, "Tactile Navigation Display," in *First International Workshop on Haptic Human-Computer Interaction*, Glasgow, UK, Aug/Sept., 2001, pp. 165-173.

[105] BalanceFreedom™. 2008, *Balance International Innovations*.

Available: http://www.b2i.info

[106] VertiGuard®RT. 2008, *VestiCure*.

Available: http://www.vesticure.com/index.php?id=9&L=1

CHAPTER 2: Directional Postural Responses Induced by Vibrotactile Stimulations Applied to the Torso

2.1. Abstract

Torso-based vibrotactile feedback has been shown to significantly reduce postural sway in balance-compromised adults during quiet standing and in response to perturbations. The purpose of this study was to characterize the non-volitional postural responses to torso-based vibrotactile stimulation as a function of stimulation location for two types of vibrating actuators (tactors). Eleven young healthy adults (20 – 29 years old), naïve to the purpose of the experiment, were asked to maintain an upright erect posture with their eyes closed. Two types of tactors, Tactaid (electromagnetic inertial transducer) and C-2 (voice-coil-type linear transducer), were placed over the left and right external oblique, internal oblique, and erector spinae muscles, in a horizontal plane corresponding approximately to the L4/L5 level. Each tactor of the same type was randomly activated four times for each torso location at a frequency of 250 Hz for a period of 5 s. Regardless of the tactor type, vibration applied over the internal oblique and erector spinae muscles induced a postural shift in the direction of the stimulation. For these four locations, the

root-mean-square (RMS) of the sway was significantly greater during vibration than immediately before or after stimulation. Vibration-induced postural shifts and increases in RMS sway were greater for the C-2 than Tactaid tactors. Simultaneous activation of all tactors or those over the external oblique muscles did not produce significant directional postural shifts or increases in sway, regardless of the tactor type. The directional shifts of posture suggest that these non-volitional responses should be considered to improve the use of torso-based vibrotactile sensory augmentation display designed for clinical balance applications.

2.2. Motivation and objective

To date, the most preferred vibrotactile display arrangement and location for upright stance applications has been an array of vibrating actuators (tactors) distributed along a belt placed around the torso, co-located with an inertial motion sensing system that measures body angular and linear accelerations [1-7]. Directional cues may be assigned to correspond to attractive or repulsive responses. Attractive cues, for which individuals are instructed to move in the direction of the vibration, have previously been used to provide turning guidance during walking [8], driving [9], and flying [10] tasks and to provide pilots with information about the aircraft attitude with respect to gravity [10]. Repulsive cues, for which individuals are instructed to move in the direction opposite to the vibration, were used by Wall et al. (2001) in the first vibrotactile feedback balance device based on the notion that such vibrations may provoke an aversion/avoidance response similar to bumping into an obstacle [5]. Subsequent studies have employed a

32

similar scheme. However the postural adjustment is simply considered as a volitional response to a warning signal, which may not be congruent with possible kinesthetic information from the stimulated tactile receptors. Although cutaneous stretch receptors from joint areas (e.g., finger, elbow, knee, ankle) are known to provide kinesthetic information [11-16] and contribute to spatial coding of joint movements for multi-articular joints such as the ankle [11], the contribution of these receptors around the torso to a spatial representation of the upper body and postural control is unknown.

For vibrotactile-based balance-related applications, arrays of commercially available C-2 tactors are commonly used to provide vibrotactile instructional cues [6, 17-19]. This tactor type generates a linear displacement of the mobile element in the direction perpendicular to the surface in contact with the skin. Another frequently used stimulator called the Tactaid tactor [5, 7, 20-21], is an inertial vibrator with a moving mass (a magnet) on a spring that vibrates in a plane normal to the surface of the skin. However, the effects of tactor type on postural responses to vibrotactile torso stimulations are also unknown. It is hypothesized that if the number of tactile receptors recruited as well as the resulting tactile afferent flow differ between each type of stimulation, then the strength of vibration-induced directional postural shifts/posture alterations will differ.

Hence, the present study investigates the motor and perceptual effects on standing posture of vibrotactile stimulations applied to various locations around the torso in the absence of instructions. Furthermore, this study investigates the influence of tactor type on the direction and/or magnitude of postural responses. Based on the hypothesis, a primary goal of the study was to determine how the cutaneous information is integrated, or in other words, whether vibrotactile stimulation induces directional

adjustments/responses away from or toward the stimulation. Postural responses show that tactile information at the level of the iliac crest contributes to a spatial representation of the upper body and their direction toward the stimulation provides understanding that is critical to the design of torso-based vibrotactile displays for clinical applications.

2.3. Methods

2.3.1. Subjects

Two sets of subjects participated in this study. The first group included five young healthy adults (5 males, 1 females, mean age 25.4±3.5 yrs), and the second group included six young healthy adults (3 males, 3 females, mean age 20.8±0.9 yrs). Both subject groups were naïve to the purpose of the experiments. Exclusion criteria included any central neurological dysfunction (e.g., stroke, myelopathy, or vertigo), functionally significant musculoskeletal dysfunction, neurological disease (e.g., cerebral vascular accident or Parkinson's disease), use of a walking aid (e.g., cane or crutch), or a body mass index greater than 30 kg/m^2. All subjects were instructed to refrain from taking medications that may cause drowsiness or dizziness within 48 hours of the experimental session. In addition, all subjects were asked not to consume alcoholic beverages within 24 hours of the experimental session. Informed consent was obtained from each subject prior to the start of the experimental procedures. The study, which conformed to the Helsinki Declaration, was approved by the University of Michigan Institutional Review Board.

2.3.2. Instrumentation

The components of the experimental apparatus, comprising a commercial six degrees-of-freedom inertial measurement unit (IMU; Xsens Technologies, NL), six C-2 or six Tactaid tactors, and an elastic belt, are illustrated in Figure 2.3.1. The IMU was attached to the back of the torso at approximately the L3 vertebra level, as shown in Figure 2.3.1(a). The IMU signals, which indicate upper body angular displacements, velocities, and accelerations in the anterior-posterior (A/P) and medio-lateral (M/L) directions, were sampled at a rate of 100Hz in the main processor (Figure 2.3.1(b)). Manufacturer specifications for the IMU indicate a static accuracy better than $0.5°$ and an angular resolution of $0.05°$. The tactor driving circuit is a hardware interface that generated sinusoidal signals to drive the tactors (Figure 2.3.1(c)).

The Tactaid and C-2 tactors illustrated in Figure 2.3.2, were used to generate vibrotactile stimulations. The Tactaid VBW32 tactor (Audiological Engineering Corporation, USA) is an electromagnetic inertial actuator, weighing 6 grams and measuring 2.5 cm x 1.9 cm x 1.1 cm. This tactor is composed of a coil, magnet, and flat spring inside a sealed rigid case [22-24], shown in Figure 2.3.2(a). Thus, the user experiences the vibration through the rigid case. The C-2 tactor (Engineering Acoustics Inc., USA) is a voice-coil-type linear actuator that incorporates a moving contactor lightly preloaded against the skin [22-24]. The C-2 tactor measures 3 cm in diameter by 0.8 cm in depth. The contactor diameter measures 0.8 cm and oscillates perpendicular to the skin, while the surrounding skin area is shielded with a passive housing. Thus, the user only feels the vibration through the contactor. The contact areas of the Tactaid and

C-2 tactors are 3.74 cm^2 (square-shaped area) and 6.15 cm^2 (circular-shaped area), respectively. Manufacturer specifications state that the transient response times for the Tactaid VBW32 and C-2 tactor are 5 ms and 33 ms, respectively. The Tactaid VBW32 tactor costs approximately $80 US while a single C-2 Tactor costs over $200 US.
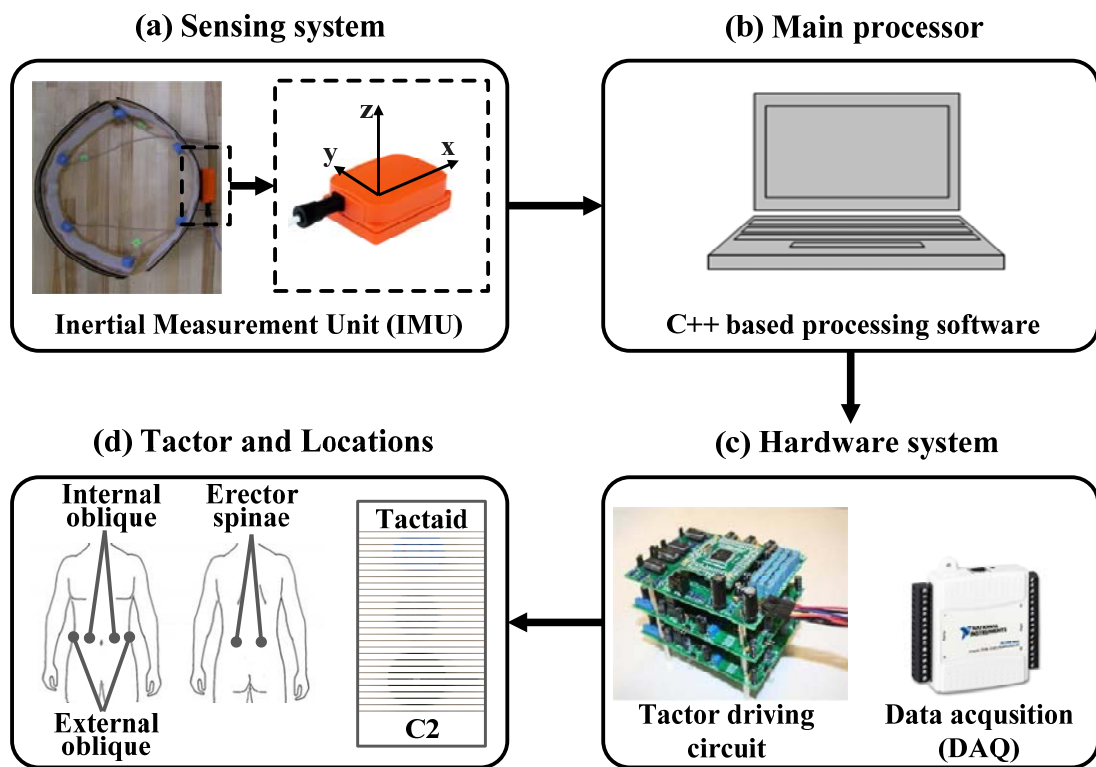
Figure 2.3.1. Experimental apparatus.
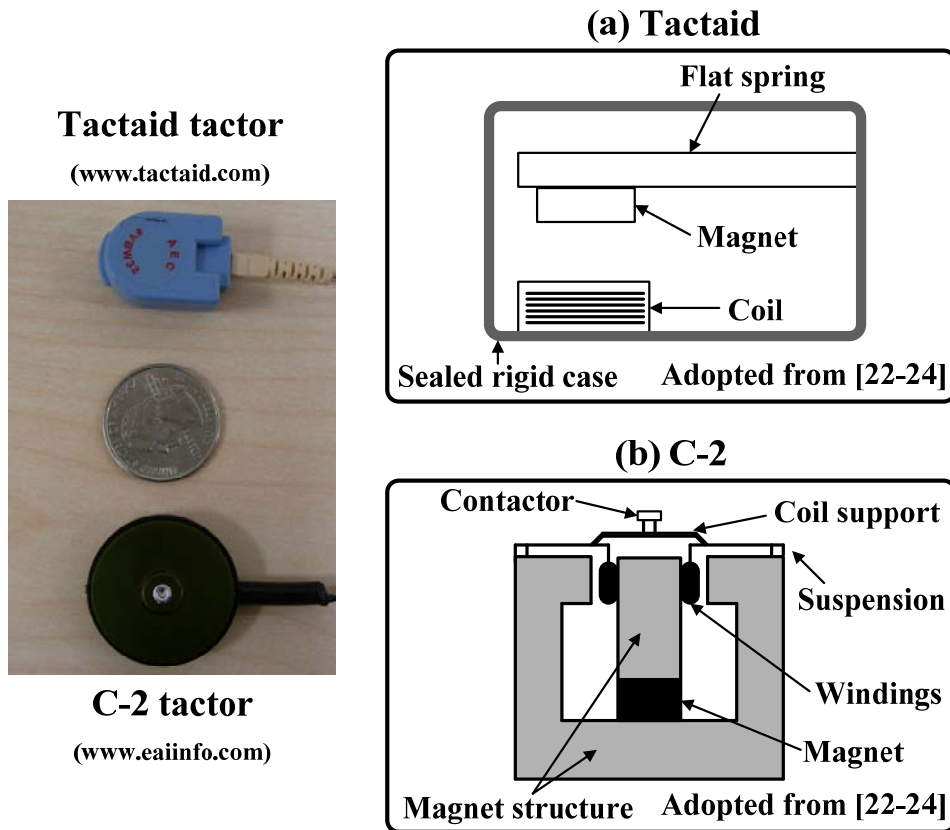
Figure 2.3.2. Tactor characteristics (a) Tactaid VBW32 tactor, (b) C-2 tactor.

The IMU and the tactors were attached with Velcro to an elastic belt worn around the torso. Figure 2.3.1(d) shows the location of tactor applications. Six tactors of the same type (i.e., either Tactaid or C-2) were placed on the skin over the left and right internal oblique, external oblique, and erector spinae muscles approximately at the level of the iliac crest, which corresponds to the L4/L5 vertebrae level. It was assumed that all tactors were equally pressurized by the elastic belt around the torso. Tactors were driven by a 250 Hz sinusoidal signal through a customized control circuit in order to keep the stimulation within the one-to-one frequency response of fast-adapting cutaneous receptors [25-26] and avoid the response of muscle spindles [27-28].

In order to compare the relative vibration amplitudes of the two types of tactors, a measurement apparatus composed of a Polytec OFV-3001 Laser Doppler Vibrometer (Plytec Inc., USA), a simulated skin substrate, and an adhesive were constructed. A Laser Doppler Vibrometer (LDV) is an instrument capable of making non-contact measurements of surface vibrations based on laser interferometry. Each type of tactor (C-2 and Tactaid) was placed on the simulated skin substrate with adhesive and the beam of the laser was focused on the center of the tactors. The voltage, which is proportional to the instantaneous vibration of tactors, was recorded at a rate of the 250 kHz for an extended period of time. The resolution of output voltage was selected as 1 mm/s/V. Measured voltage signals were integrated over extended periods of time in order to compute the vibrational displacement of each tactor type [29].

2.3.3. Experimental protocol

Subjects were asked to stand on a firm surface with their arms held at their sides and their feet hip-width apart with a 15° lateral rotation angle. Foam ear plugs and ear muffs were provided to subjects in order to eliminate environmental noise as well as noise due to tactor activation.

The experimental trial comprised of consecutive pre-, per-, and post-vibration measurement periods and either only one or all of the tactors were activated during the per-vibration period. Only one or all tactors were activated during the vibration period, henceforth referred to as "single location" and "all locations", respectively. Two groups of subjects participated in this study. Both sets of subjects used both types of tactors,

changing the tactor type after completing the series of trials. The initial tactor type was randomly assigned to each subject. For the first group of subjects (n=5), the stimulation included an initial period of 15 s with no vibrotactile stimulation, followed by 5 s of stimulation by one of the tactors, followed by 15 s with no stimulation. Trial sessions were repeated four times (i.e., a total of 28 trials). For the second group of subjects (n=6) the stimulation period was increased from 5 s to 15 s and the number of trial sessions was reduced from four to two, which corresponded to a total of 14 trials. For both experimental protocols, subjects were given a 15-second rest period after each trial. Both sets of subjects were instructed to maintain an upright stance (e.g., behaving as inverted pendulums) while closing their eyes and keeping their arms at their sides. No information was provided to subjects regarding tactor types, tactor locations, or the duration of vibration signals.

Subjects were given a short comparative Likert scale survey (strongly disagree (1), disagree (2), neither disagree nor agree (3), agree (4), and strongly agree (5)) after completing all of the trials performed with a given tactor type, in order to assess the perceived strength of vibrotactile stimulations as a function of location and the perceived postural changes induced by these vibrations. The survey statements were: Q1) The duration of each vibrotactile stimulus appeared to be the same, Q2) The vibrotactile stimulation affected my body sway, Q3) I experienced tilt or movement illusions during stimulation, and Q4) I continued to feel as though I was being stimulated even after the tactors were deactivated. Furthermore, we asked each participant the following questions: Q5) Which tactor (type) had more intensive vibrations during the experiment?

2.3.4. Data analysis

MATLAB (The Math Works, Natick, MA) was used to process the postural sway signals captured by the IMU. For data analysis, the "pre-vibration" and "post-vibration" periods were defined as the 5 s preceding and following the vibrotactile stimulation (per-vibration period), respectively. Three data analysis metrics were defined to quantify the postural responses to the vibrotactile stimulation: postural shift vector (indicating magnitude and direction of postural shift), root-mean-square (RMS), and power spectral density (PSD).

As illustrated in Figure 2.3.3, a two-step process was used to determine postural changes in the magnitude and shift direction between the consecutive periods of analysis (pre-/per- and per-/post-vibration periods). First, 95% confidence interval ellipses were fit to the 2D postural trajectories for each period, as shown in Figure 2.3.3(a). The center of each ellipse was used to calculate two-axis postural shift vectors that quantified the magnitude and direction of postural changes. A pre-vibration postural shift vector was computed from the origin to the center of the pre-vibration ellipse, indicating pre-existing postural change (see Figure 2.3.3(b)). A per-vibration postural shift vector was computed from the center of the pre-vibration ellipse to the center of the per-vibration ellipse, indicating change in posture when vibrotactile stimulation was activated (see Figure 2.3.3(b)). A post-vibration postural shift vector was computed from the center of the per-vibration ellipse to the center of the post-vibration ellipse, indicating postural recovery when vibrotactile stimulation was deactivated (see Figure 2.3.3(b)). Then, the coordinates of the center of the pre-vibration ellipse were subtracted from the centers of the pre-, per-,

and post-vibration ellipses in order to shift the origin of the coordinate system to the

center of the pre-vibration ellipse (i.e., (A/P, M/L)=(0,0)), as shown in Figure. 2.3.4.
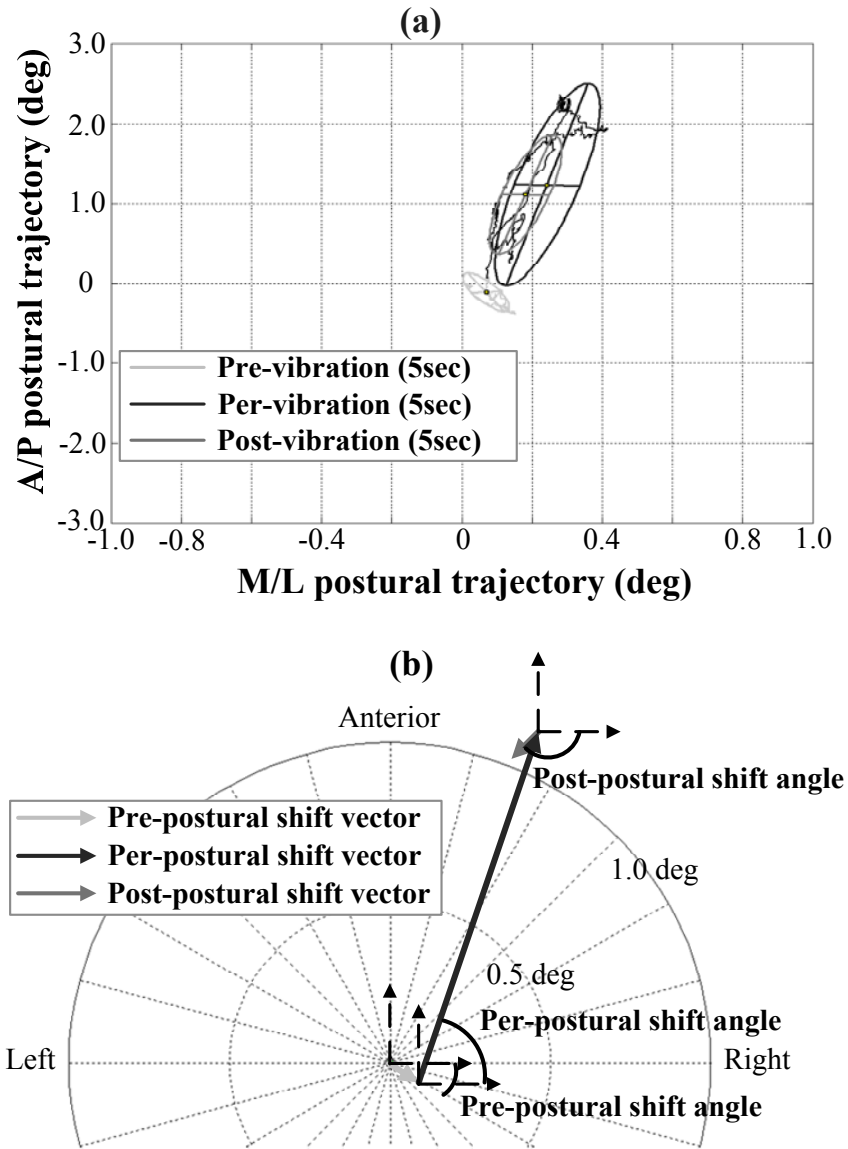
Figure 2.3.3. (a) Postural trajectories and elliptical fits (95% confidence interval) as a function of vibration period on the right internal oblique. Positive values defined as movement in the anterior and lateral (right) directions, respectively. (b) Calculation of two-axis postural shift vectors that quantified the magnitude and direction of postural changes. Light, dark, and intermediate grey lines represent pre-, per-, and post-vibration periods, respectively.
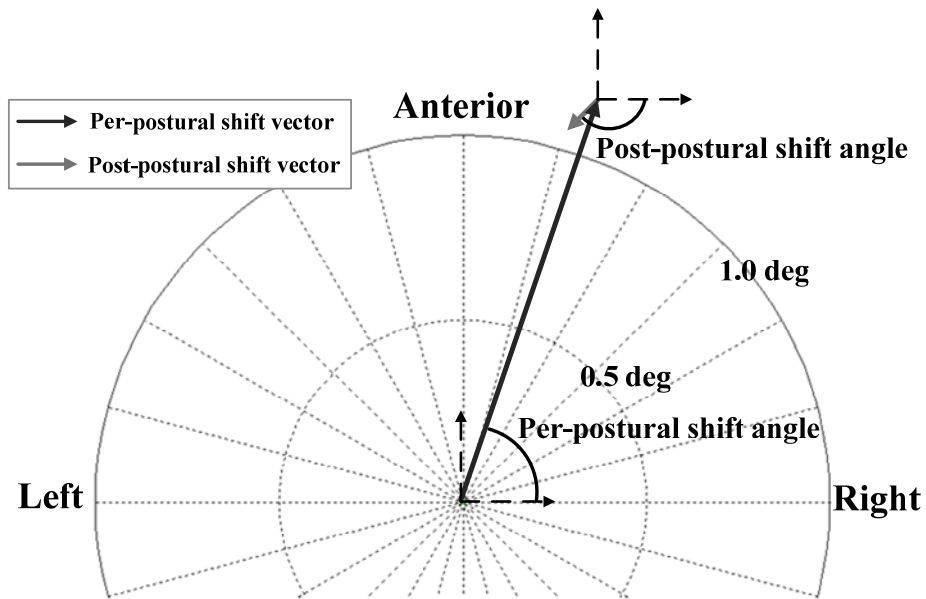
Figure 2.3.4. New coordination of two-axis postural shift vectors. Dark, and intermediate grey lines represent per-, and post-postural shift vectors, respectively.

Root-mean-square (RMS) and power spectral density (PSD) values of M/L and A/P angular displacements (sway) of the body posture as a function of pre-, per-, and post-vibration period were separately computed to evaluate the sway amplitude of body posture.

PSD analysis, which describes the distribution of power content across frequencies [30], was used to determine the spectral power and dominant frequency of the angular displacements of the body. PSD functions were computed using a discrete Fourier transform (DFT) to decompose the angular displacements of the body into sinusoidal components [30]. The DFT was applied to each 5 s period. The DFT was calculated at 20 frequencies ranging from f = 1/5= 0.2 Hz to f = 20/5 = 4.0 Hz. PSD magnitudes under 1.0 Hz were only considered for data analysis, since PSD magnitudes over 1.0 Hz were statistically not significant in the presence or absence of vibrotactile stimulation,

regardless of the tactor type or tactor location. Note that the computed average PSD magnitude beyond the 1.0 Hz range including the consecutive measurement periods (i.e., pre-, per-, and post-vibration periods) for all location conditions was approximately less than 13 deg^2/Hz, which is relatively small compared with the PSD magnitude of 390 deg^2/Hz for frequencies less than 1.0 Hz. A/P and M/L PSD magnitudes of the angular displacements of the body were computed for the pre-, per-, and post-vibration periods.

A three-way analysis of variance (ANOVA) was conducted to determine the main effects of tactor type (Tactaid and C2), location (six independent locations as well as the "all locations" condition), and period (pre-, per- and post-vibration) for each dependent variable (e.g., magnitude, direction, A/P RMS, M/L RMS, A/P PSD, and M/L PSD of postural sway). Hypotheses for the main effects of activated tactor location and measurement period as well as their interactions were tested using an F-test. One-way ANOVAs were also conducted on all dependent variables to further investigate the effects of vibrotactile stimulation and the activated tactor location. To determine which factors influenced the main and interaction effects, post-hoc tests (Tukey Honestly Significant Differences - HSD - for multiple comparisons) were conducted. The level of significance was set at $p<0.05$. To assure the assumptions of normality and constant variance of residual variance, dependent variables were transformed to a logarithmic scale.

2.4. Results

Representative results for a single subject are illustrated in Figure 2.4.1 (vibration applied to the skin over the left internal oblique muscle). The subject's posture shift is in

the direction of the tactile stimulation during the per-vibration period. A post effect, indicated by a shift in the direction opposite the vibration application direction, is also observed when the vibrotactile stimulation ceases.
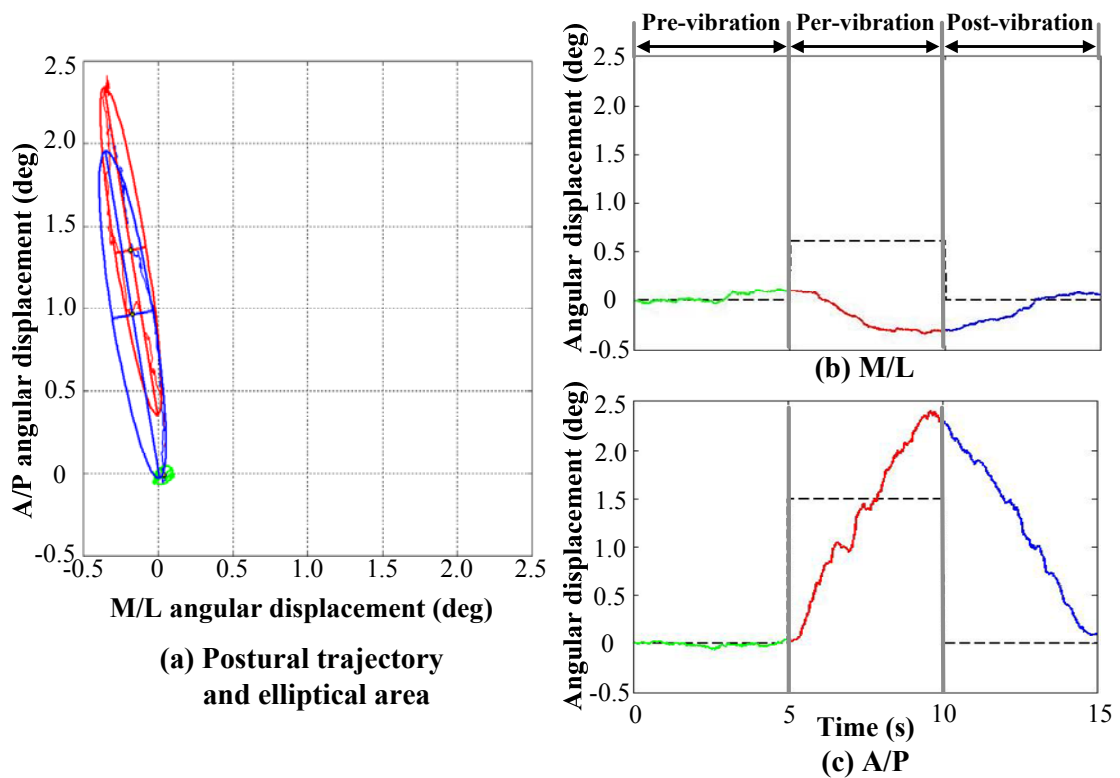
Figure 2.4.1. (a) Illustrative postural trajectories and 95% confidence interval elliptical fits for each vibration period when the tactor was placed over the left internal oblique. Positive values are defined as movement in the anterior and rightward directions, respectively. Green, red, and blue lines represent pre-, per-, and post-vibration periods, respectively. (b) Illustrative M/L postural trajectory. Positive values are defined as movement in the rightward direction. (c) Illustrative A/P postural trajectory. Positive values are defined as movement in the anterior direction.

2.4.1. Magnitudes of postural shift vectors

Figure 2.4.2 presents per- and post-vibration postural shift vectors (both normalized to show posture changes with respect to pre-existing tilt by subtracting the pre-vibration posture shift vector) as a function of the activated tactor location and the tactor type.

Table 2.4.1 reports the results of statistical analysis. Analysis of the magnitudes of postural shift vectors (i.e., during the per- and post-vibration periods) showed that the main effects of tactor type, location, and period, as well as the tactor type X location and the location X period interactions were significant. Post-hoc analysis showed that the magnitude of the postural shift vectors during the per-vibration period was significantly greater than that during the pre- and post-vibration periods for both types of tactors when vibration was applied over the internal oblique and erector spinae locations, regardless of the tactor type. For each tactor type, however, the relative magnitudes of the postural shift vectors during vibration were similar between the aforementioned four locations. However, changes in postural shift vectors were negligible when vibration was applied over the external obliques or at all locations, regardless of the tactor type.

Figure 2.4.3 shows the average magnitude of the postural shift vectors during vibration as a function of tactor location for both types of tactors. The magnitudes of the postural shift vectors were significantly greater with the C-2 than with Tactaid tactors when vibration was applied over the internal oblique and erector spinae locations. For these four locations, the average magnitude of the vibration-induced postural shift was on the order of $1.2°$ for C-2 tactors and $0.7°$ for Tactaid.
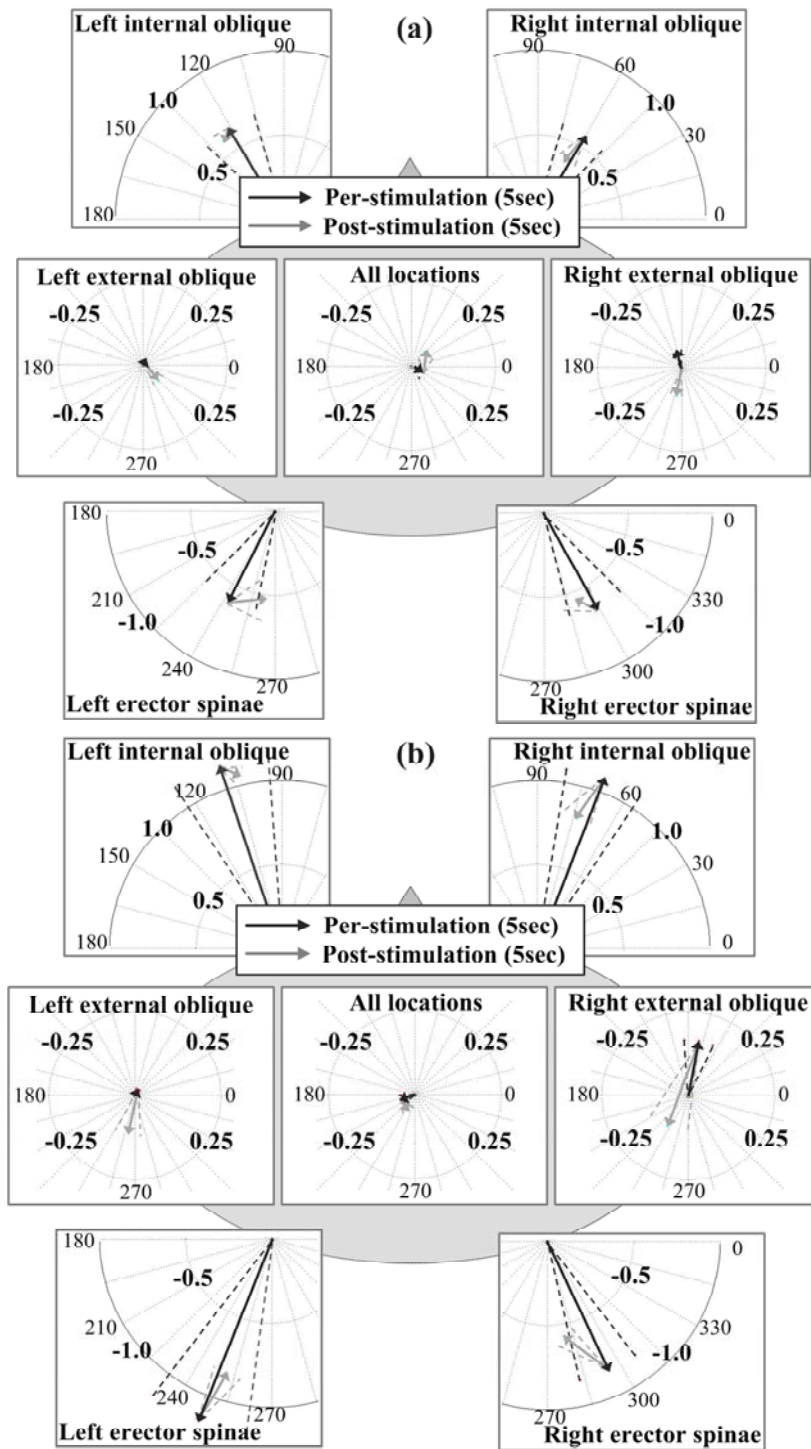
Figure 2.4.2. Average postural shift vectors during per- and post-vibration periods as a function of tactor location; (a) Tactaid and (b) C2. Black and light grey vectors indicate the magnitude and direction of vectors during the per- and post-vibration period, respectively. Dash vectors indicate standard error of the mean.

Table 2.4.1. Statistical analysis results of magnitude of postural shift vectors for tactor type (T), location (L), and period (P). *Statistical significance. RIO (Right Internal Oblique), REO (Right External Oblique), RES (Right Erector Spinae), LES (Left Erector Spinae), LEO (Left External Oblique), LES (Left Erector Spinae), and ALL (All locations).

Two-way ANOVA				
	Effects	DF	F Value	Pr>F
	T	1, 280	13.68	<0.0001 *
Main	L	6, 280	26.17	<0.0001 *
	P	1, 280	101.32	<0.0001 *
	T X L	6, 280	2.63	0.017 *
Interaction	T X P	1, 280	0.98	0.321
	L X P	6, 280	6.82	<0.0001 *
	T X L X P	6, 280	1.59	0.151

One-way ANOVA					
Tactor type	Location	Effects	DF	F Value	Pr>F
	RIO	P	1, 20	12.38	0.002 *
	REO	P	1, 20	1.57	0.224
	RES	P	1, 20	19.71	<0.0001 *
Tactaid	LES	P	1, 20	26.52	<0.0001 *
	LEO	P	1, 20	0.09	0.764
	LIO	P	1, 20	12.99	0.001 *
	ALL	P	1, 20	2.03	0.169
	RIO	P	1, 20	37.93	<0.0001 *
	REO	P	1, 20	0.15	0.707
	RES	P	1, 20	40.91	<0.0001 *
C2	LES	P	1, 20	61.00	<0.0001 *
	LEO	P	1, 20	1.67	0.211
	LIO	P	1, 20	37.11	<0.0001 *
	ALL	P	1, 20	0.03	0.859
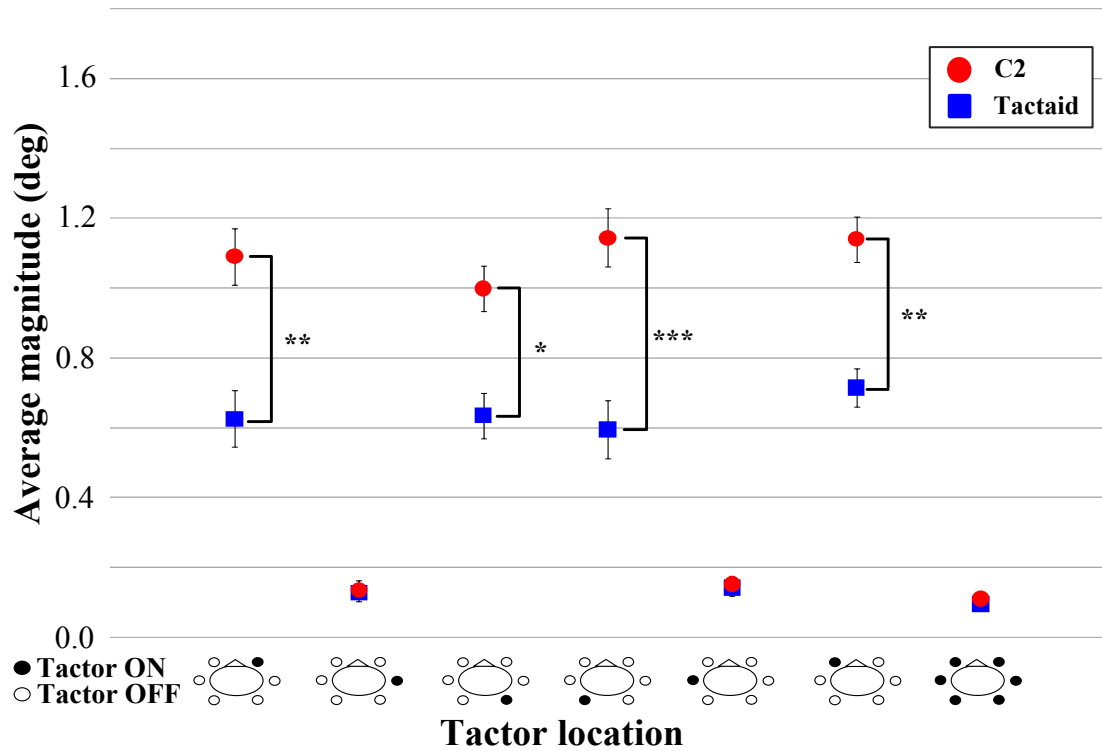
Figure 2.4.3. Average magnitude of the postural shift vector for the C-2 (●) and Tactaid (■) tactor during vibration periods as a function of tactor location. Error bars indicate standard error of the mean (*$p < 0.05$, **$p < 0.01$, ***$p<0.0001$). Bird's-eyeview drawings illustrate vibration locations.

Assuming postural corrections were primarily generated by rotation at the ankle joints (i.e., behavior corresponding to inverted pendulum control), this shift corresponds to a head displacement of 2.14 cm (Tactaid) and 3.68 cm (C-2) for a 50th percentile male and 1.99 cm (Tactaid) and 3.41 cm (C-2) for a 50th percentile female [31].

2.4.2. Directions of postural shift vectors

Analysis of the directional angle of postural shift vectors showed that the main effects of tactor type, location, and period, as well as the tactor type X location and the location X period interactions were significant (Table 2.4.2). Analysis of the directional angle of postural shift vectors during per- and post-vibration periods showed a significant main effect of the vibrotactile stimulation for right and left internal oblique as well as right and left erector spinae locations for both types of tactors. When vibration was applied over the right and left internal oblique locations, subjects exhibited a postural shift in the forward right and forward left directions, respectively. When vibration was applied over the erector spinae, the body posture shifted in the backward left and backward right directions, respectively. Upon cessation of the vibration, the body posture shifted in the direction opposite to the postural shift observed during vibration. Furthermore, both the magnitude and direction of the postural shift vectors were not significantly influenced when vibration was applied to all locations simultaneously or when it was applied over the external oblique muscles, regardless of the tactor type. These results are illustrated in Figure 2.4.2.

Table 2.4.2. Statistical analysis results of angle of postural shift vectors for tactor type (T), location (L), and period (P). *Statistical significance. RIO (Right Internal Oblique), REO (Right External Oblique), RES (Right Erector Spinae), LES (Left Erector Spinae), LEO (Left External Oblique), LES (Left Erector Spinae), and ALL (All locations).

		Two-way ANOVA			
		Effects	**DF**	**F Value**	**Pr>F**
		T	1, 280	15.14	<0.0001 *
Main		L	6, 280	31.12	<0.0001 *
		P	1, 280	112.02	<0.0001 *
		T X L	6, 280	3.24	0.010 *
Interaction		T X P	1, 280	0.74	0.390
		L X P	6, 280	8.26	<0.0001 *
		T X L X P	6, 280	0.76	0.604

		One-way ANOVA			
Tactor type	**Location**	**Effects**	**DF**	**F Value**	**Pr>F**
	RIO	P	1, 20	7.69	0.012 *
	REO	P	1, 20	2.87	0.106
	RES	P	1, 20	24.33	<0.0001 *
Tactaid	LES	P	1, 20	58.19	<0.0001 *
	LEO	P	1, 20	0.01	0.905
	LIO	P	1, 20	18.69	<0.0001 *
	ALL	P	1, 20	0.92	0.349
	RIO	P	1, 20	517.37	<0.0001 *
	REO	P	1, 20	1.50	0.235
	RES	P	1, 20	217.23	<0.0001 *
C2	LES	P	1, 20	5.75	0.026 *
	LEO	P	1, 20	0.79	0.383
	LIO	P	1, 20	16.99	0.001 *
	ALL	P	1, 20	0.01	0.956

2.4.3. Root mean square (RMS)

Average RMS values of the postural sway across the subjects in both M/L and A/P directions as a function of the tactor location with respect to pre-, per-, post-vibration period are illustrated in Figure 2.4.4.
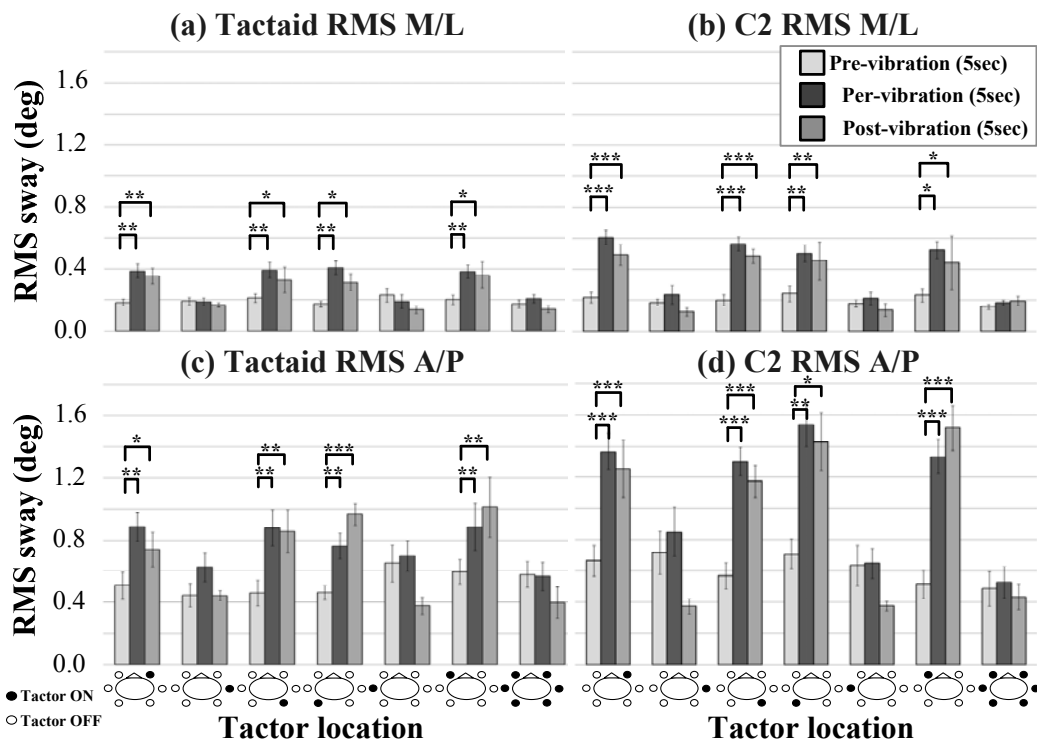
Figure 2.4.4. Average RMS sway as a function of tactor location. Light, dark, and intermediate grey bars represent pre-, per-, and post-vibration period, respectively. Error bars indicate standard error of the mean (*$p<0.05$; **$p<0.01$; ***$p<0.0001$). Bird's-eyeview drawings illustrate vibration locations.

The ANOVA applied to RMS sway indicated that the main effects of the tactor type, location, and period as well as the tactor type X location and the location X period interactions were significant in both the M/L and A/P directions, as shown in Table 2.4.3

(M/L RMS) and Table 2.4.4 (A/P RMS). Post-hoc analysis showed that the M/L and A/P RMS sway were significantly greater during the per- and post-vibration periods than during the pre-vibration period when vibration was applied over the internal oblique and erector spinae locations, regardless of the tactor type. For each tactor type, however, the M/L and A/P RMS sway during the per- and post-vibration periods were statistically equivalent between the aforementioned four locations. Regardless of the tactor type, this analysis also showed that the M/L and A/P RMS sway values during the pre-vibration period were not significantly different across the six single locations. Further, the M/L and A/P RMS sway values during the per-vibration period were similar for the left and right internal oblique and erector spinae locations for each tactor type. However, changes in the M/L and A/P RMS sway were negligible when vibration was applied over the external obliques or at all locations, regardless of the tactor type.

Figure 2.4.5 shows the comparison of the average RMS sway during the per-vibration period in terms of the tactor type. The C2 tactor M/L RMS sway value was significantly higher than the Tactaid tactor M/L RMS sway value for the right internal oblique ($F(1,20)=12.26$, $p=0.002$), right erector spinae ($F(1,20)=7.09$, $p=0.015$), and left internal oblique ($F(1,20)=6.12$, $p=0.031$) locations. In the case of the A/P RMS sway value, amplitudes were significantly higher for the C2 than for the Tactaid tactor when vibration was applied over the right internal oblique ($F(1,20)=11.75$, $p=0.003$) and left internal oblique ($F(1,20)=7.24$, $p=0.01$) as well as right erector spinae ($F(1,20)=8.55$, $p=0.008$) and left erector spinae ($F(1,20)=23.11$, $p<0.0001$) locations.
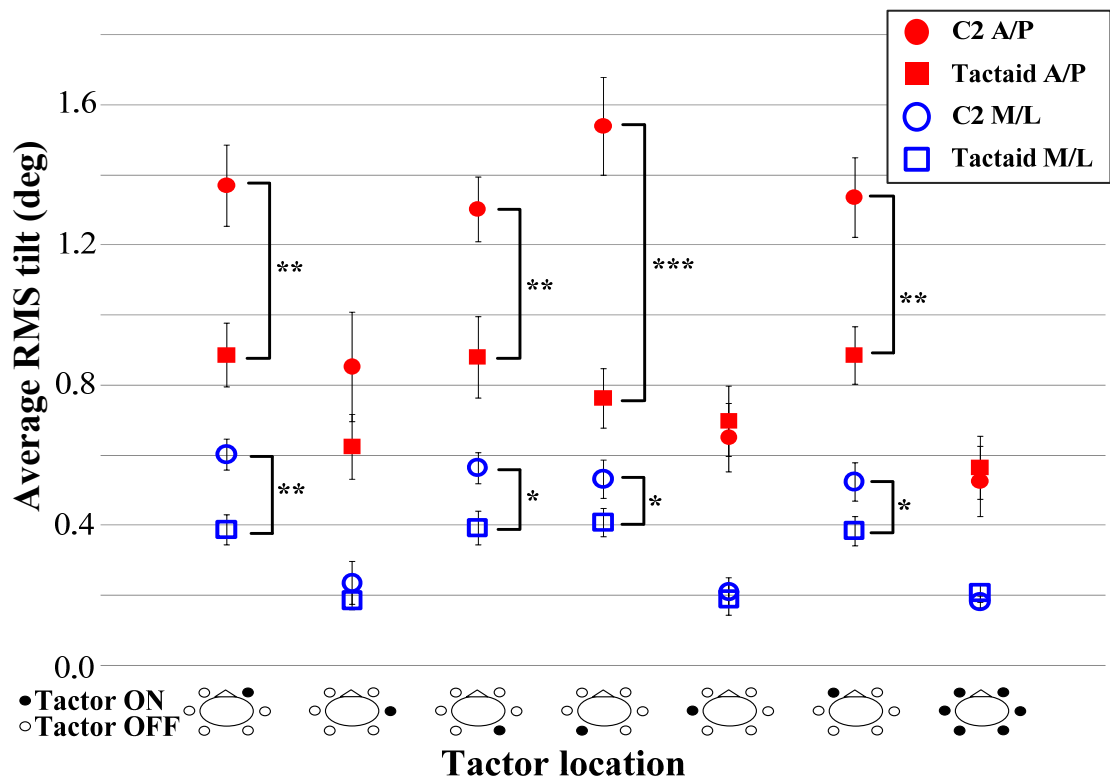
Figure 2.4.5. Average A/P and M/L RMS sway for the C-2 (●) and Tactaid (■) tactor during vibration periods as a function of tactor location. Red and blue symbols represent the A/P and M/L RMS sway, respectively. Error bars indicate standard error of the mean (*$p<0.05$; **$p<0.01$; ***$p<0.0001$). Bird's-eyeview drawings illustrate vibration locations.

Table 2.4.3. Statistical analysis results of the M/L RMS sway for tactor type (T), location (L), and period (P). *Statistical significance. RIO (Right Internal Oblique), REO (Right External Oblique), RES (Right Erector Spinae), LES (Left Erector Spinae), LEO (Left External Oblique), LES (Left Erector Spinae), and ALL (All locations).

	Two-way ANOVA			
	Effects	**DF**	**F Value**	**Pr>F**
	T	1, 420	10.87	0.001 *
Main	L	6, 420	60.63	<0.0001 *
	P	2, 420	55.806	<0.0001 *
	T X L	6, 420	2.41	0.026 *
Interaction	T X P	2, 420	0.74	0.480
	L X P	12, 420	4.99	<0.0001 *
	T X L X P	12, 420	0.298	0.990

		One-way ANOVA			
Tactor type	**Location**	**Effects**	**DF**	**F Value**	**Pr>F**
	RIO	P	2, 30	9.78	0.001 *
	REO	P	2, 30	0.56	0.574
	RES	P	2, 30	8.97	0.001 *
Tactaid	LES	P	2, 30	7.68	0.002 *
	LEO	P	2, 30	3.47	0.71
	LIO	P	2, 30	5.55	0.009 *
	ALL	P	2, 30	0.80	0.457
	RIO	P	2, 30	12.25	<0.0001 *
	REO	P	2, 30	0.04	0.963
	RES	P	2, 30	17.02	<0.0001 *
C2	LES	P	2, 30	8.86	0.001 *
	LEO	P	2, 30	0.44	0.648
	LIO	P	2, 30	10.64	<0.0001 *
	ALL	P	2, 30	0.35	0.706

Table 2.4.4. Statistical analysis results of the A/P RMS sway for tactor type (T), location (L), and period (P). *Statistical significance. RIO (Right Internal Oblique), REO (Right External Oblique), RES (Right Erector Spinae), LES (Left Erector Spinae), LEO (Left External Oblique), LES (Left Erector Spinae), and ALL (All locations).

Two-way ANOVA					
	Effects	**DF**	**F Value**	**Pr>F**	
	T	1, 420	13.49	<0.0001*	
Main	L	6, 420	51.32	<0.0001*	
	P	2, 420	70.37	<0.0001*	
	T X L	6, 420	2.59	0.018*	
	T X P	2, 420	0.71	0.492	
Interaction	L X P	12, 420	1.91	0.032*	
	T X L X P	12, 420	0.50	0.913	

One-way ANOVA					
Tactor type	**Location**	**Effects**	**DF**	**F Value**	**Pr>F**
	RIO	P	2, 30	12.66	<0.0001*
	REO	P	2, 30	1.08	0.35
	RES	P	2, 30	7.99	0.002*
Tactaid	LES	P	2, 30	11.93	<0.0001*
	LEO	P	2, 30	0.19	0.822
	LIO	P	2, 30	6.33	0.005*
	ALL	P	2, 30	1.72	0.196
	RIO	P	2, 30	11.52	<0.0001*
	REO	P	2, 30	0.04	0.965
	RES	P	2, 30	6.30	0.005*
C2	LES	P	2, 30	15.26	<0.0001*
	LEO	P	2, 30	1.67	0.206
	LIO	P	2, 30	19.56	<0.0001*
	ALL	P	2, 30	0.78	0.466

2.4.4. Power spectral density

The power spectral density (PSD) in both the M/L and A/P directions was computed in the 0.0 to 4Hz frequency range for each vibration period. Significant main effects of the per-vibration period were observed in the frequency range below 1.0 Hz for both tactor types. Thus the following results correspond to changes in the PSD magnitudes below 1.0 Hz. Average PSD values of the postural sway across the subjects in both M/L and A/P directions as a function of the tactor location with respect to pre-, per-, post-vibration period are illustrated in Figure 2.4.6.

The ANOVA applied to PSD indicated that the main effects of the tactor type, location, and period as well as the tactor type X location and the location X period interactions were significant in both the M/L and A/P directions, as shown in Table 2.4.5 (M/L PSD) and 2.4.6 (A/P PSD). Post-hoc analysis showed that the M/L and A/P PSD values were significantly greater during the per-vibration periods than during the pre- and post-vibration period when vibration was applied over the internal oblique and erector spinae locations, regardless of the tactor type. For each tactor type, however, the M/L and A/P PSD values during the pre- and post-vibration periods were statistically equivalent between the aforementioned four locations. Further, the M/L and A/P PSD values during the per-vibration period were similar for the left and right internal oblique and erector spinae locations for each tactor type. However, changes in the M/L and A/P PSD values were negligible when vibration was applied over the external obliques or at all locations, regardless of the tactor type.
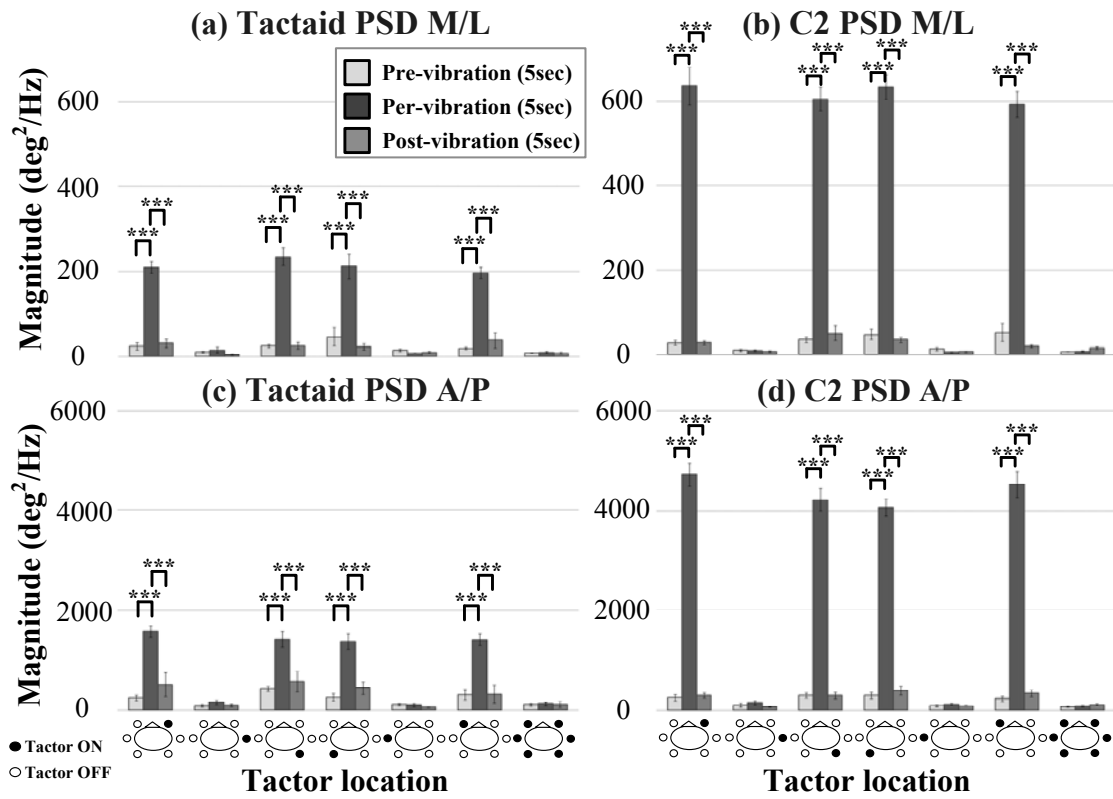
Figure 2.4.6. Average frequency power below 0.5 Hz as a function of tactor. Light, dark, and intermediate grey bars represent pre-, per-, and post-vibration periods, respectively. Error bars indicate standard error of the mean. (***p<0.0001). Bird's-eyeview drawings illustrate vibration locations. Note that the scale in (c) and (d) is ten times greater than that in (a) and (b).

Table 2.4.5. Statistical analysis results of the M/L PSD for tactor type (T), location (L), and period (P). *Statistical significance. RIO (Right Internal Oblique), REO (Right External Oblique), RES (Right Erector Spinae), LES (Left Erector Spinae), LEO (Left External Oblique), LES (Left Erector Spinae), and ALL (All locations).

Two-way ANOVA					
		Effects	DF	F Value	Pr>F
Main		T	1, 420	5.47	0.2 *
		L	6, 420	78.54	<0.0001 *
		P	2, 420	139.86	<0.0001 *
Interaction		T x L	6, 420	2.45	0.24 *
		T x P	2, 420	1.09	0.062
		L x P	12, 420	23.77	<0.0001 *
		T x L x P	12, 420	0.61	0.812

One-way ANOVA					
Tactor type	Location	Effects	DF	F Value	Pr>F
Tactaid	RIO	P	2, 30	26.42	<0.0001 *
	REO	P	2, 30	1.25	0.299
	RES	P	2, 30	71.88	<0.0001 *
	LES	P	2, 30	25.20	<0.0001 *
	LEO	P	2, 30	2.38	0.11
	LIO	P	2, 30	35.73	<0.0001 *
	ALL	P	2, 30	0.97	0.389
C2	RIO	P	2, 30	57.05	<0.0001 *
	REO	P	2, 30	2.68	0.084
	RES	P	2, 30	28.52	<0.0001 *
	LES	P	2, 30	37.51	<0.0001 *
	LEO	P	2, 30	1.80	0.182
	LIO	P	2, 30	91.62	<0.0001 *
	ALL	P	2, 30	1.09	0.346

Table 2.4.6. Statistical analysis results of the A/P PSD for tactor type (T), location (L), and period (P). *Statistical significance. RIO (Right Internal Oblique), REO (Right External Oblique), RES (Right Erector Spinae), LES (Left Erector Spinae), LEO (Left External Oblique), LES (Left Erector Spinae), and ALL (All locations).

Two-way ANOVA				
	Effects	DF	F Value	Pr>F
Main	T	1, 420	7.23	0.015 *
	L	6, 420	52.37	<0.0001 *
	P	2, 420	112.04	<0.0001 *
Interaction	T x L	6, 420	2.29	0.34 *
	T x P	2, 420	2.46	0.085
	L x P	12, 420	11.63	<0.0001 *
	T x L x P	12, 420	0.85	0.599

One-way ANOVA					
Tactor type	Location	Effects	DF	F Value	Pr>F
Tactaid	RIO	P	2, 30	11.69	<0.0001 *
	REO	P	2, 30	0.15	0.855
	RES	P	2, 30	4.72	0.017 *
	LES	P	2, 30	24.35	<0.0001 *
	LEO	P	2, 30	0.02	0.984
	LIO	P	2, 30	12.07	<0.0001 *
	ALL	P	2, 30	0.51	0.604
C2	RIO	P	2, 30	56.15	<0.0001 *
	REO	P	2, 30	1.52	0.235
	RES	P	2, 30	26.92	<0.0001 *
	LES	P	2, 30	41.65	<0.0001 *
	LEO	P	2, 30	2.90	0.085
	LIO	P	2, 30	43.67	<0.0001 *
	ALL	P	2, 30	0.90	0.416

Comparisons of the average PSD magnitudes during the per-vibration periods for each tactor type as a function of tactor location are illustrated in Figure 2.4.7. The A/P and M/L PSD magnitudes were significantly greater with the C-2 than the Tactaid tactors when vibration was applied over the internal oblique and erector spinae locations.
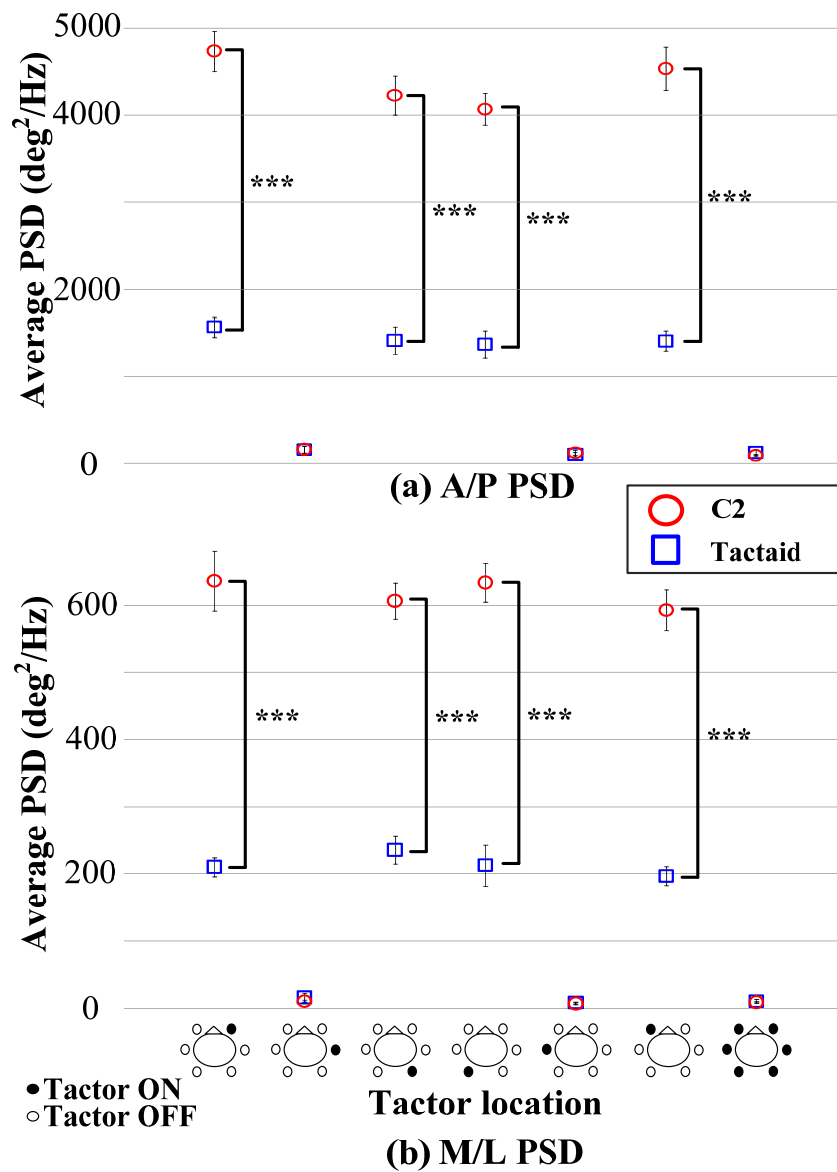
Figure 2.4.7. Average M/L (a) and A/P (b) PSD magnitude (less than 0.6Hz) for the C-2 (O) and Tactaid (☐) tactors during vibration periods as a function of tactor location. Error bars indicate standard error of the mean. ***$p<0.0001$. Bird's-eyeview drawings illustrate vibration locations. Note that the scale in (b) is ten times greater than that in (a).

2.4.5. Subjective perception

According to the post-test Likert questionnaire, the majority of subjects agreed that the duration of each vibrotactile stimulus appeared to be the same as a function of tactor location (Q1 – avg. 4.3 / 5). However, most subjects perceived neither vibration-induced postural changes (Q2 – avg. 2.7 / 5 and Q3 – avg. 1.9 / 5) nor corresponding post effects (Q4 – avg. 2.0 / 5). Furthermore, nine of eleven subjects indicated that vibration intensity was higher for the C-2 than the Tactaid tactors; one subject reported the opposite and one subject did not perceive a difference of vibration intensity.

2.5. Discussion

The results show that vibrations applied to the skin over the internal oblique and erector spinae muscles induce postural shifts in the direction of the vibration location; the average vibration-induced postural shift is 1.2°. This directional effect is not observed for vibrations applied over the external oblique locations or applied simultaneously at all locations around the torso.

The contribution of cutaneous afferents of the torso to an internal representation of the upper body and orientation was found. Previous results have shown that cutaneous receptors located in the skin around the finger [13, 16, 32], elbow [13, 33], ankle [11-12] and knee [13, 34] joints provide exteroceptive and proprioceptive information. Similar to muscle spindles, cutaneous receptors encode movement kinematics [14-15, 35] and show directional sensitivity [11, 14, 36]. The present results show that vibrotactile stimulation induces oriented compensatory postural shifts similar to those produced by muscle

vibration [37-43]. Indeed, for stimulations applied to the skin over the internal oblique and erector spinae locations, the observed direction of the shift was congruent with a postural response to skin stretch concomitant to muscle lengthening, as is the case when vibrations stimulate muscle spindles [27, 37, 41-44]. However, vibration applied to the skin over the external oblique locations did not induce a significant shift, as will be discussed below.

The directional involuntary compensatory response indicates that in the absence of vision, the CNS relies on proprioceptive information from peripheral sensory receptors (see for example Lackner et al. [45]; Massion [46]) during upright stance. In the present context it should be considered that the frequency response of muscle proprioceptive receptors is typically limited to approximately 120 Hz [27, 47-48], but may be up to 220 Hz for the most sensitive receptors [27]. However, the frequency response of cutaneous receptors can be as high as 280 Hz [25]. Therefore, it is postulated that the 260 Hz vibration was largely ineffective in stimulating the spindle primary endings while activating cutaneous receptors. Hence, the results suggest that the role of cutaneous information in postural stabilization and orientation is not negligible in the absence of vision and that cutaneous receptors in the skin over the torso's primary mover muscles supply proprioceptive information. This hypothesis is confirmed by the absence of postural shift when all locations around the trunk are stimulated simultaneously. This parallels the results obtained during simultaneous vibration at the same frequency of antagonist muscle pairs [28, 49-50], which did not produce movement illusions; co-vibration of the tibialis anterior and soleus muscles [51] and whole trunk vibration [42],

which did not induce postural effects. In these conditions, homogeneous stimulation of all receptors contributing to kinesthesia produced a neutral effect.

The present vibrotactile-induced shifts are smaller than movements induced by muscle vibration activating Ia afferents [40, 49, 52]. Although postural responses of proprioceptive or tactile origins are frequency dependent [40], they are also limited by the frequency response of the each type of receptor, the number of receptors stimulated, and the weight of each sensory input. Hence, considering that frequency may not be a major factor when stimulations correspond to the highest limit range for each receptor category, the difference between vibration-induced postural shifts of cutaneous and muscle proprioceptive origin are likely to reflect the influence of two factors: one is the difference in the number of receptors stimulated, the other is the interaction/incongruence between muscle and cutaneous information, since in the present case only information from tactile receptors was altered by vibration. Due to the magnitude of stimulation used in most experiments, it is usually assumed that most proprioceptive receptors are stimulated by tendon vibration [48]; however in the present case tactile vibration was of very small amplitude (<100 m) and limited to a small area (i.e., 330 mm^2 for Tactaid and 180 mm^2 for C2), Accordingly, the cutaneous vibration-induced afferent flow was relatively small. Therefore, significant postural shifts in spite of these two limitations (cutaneous afferent flow and incongruence between the two modalities) support a significant contribution of cutaneous information to proprioception in the tested areas and the integration of information from the two sensory modalities, as suggested previously [46, 53-54].

The lack of significant effects resulting from the external oblique locations is not surprising, since postural stability is greater in the M/L direction than the A/P direction during normal stance [42, 55]. This effect is commonly associated with the mechanical limitation of bipedal posture, which constrains torso lateral flexion [55-56]. Furthermore, the hip-width separation of the feet in this study contributes to a high lateral stability. Hence, a small vibration-induced change in sensory information in the lateral direction does not necessarily need to be compensated with a postural shift to avoid instability.

The magnitude of both the postural shifts and the RMS sway occurring in response to an applied vibrational stimulus was significantly larger when the C-2 tactor was employed in lieu of the Tactaid tactor. This was to be expected, as the C-2 tactor provides a more powerful stimulus in comparison to the Tactiad tactor. Vedel and Roll [48] and Ribot-Ciscar et al. [25] have shown that mechanoreceptors are very sensitive to mechanical vibration with stimulations in the range of 200-500 μm peak to peak displacement. In this study, subjects also reported that the perceived vibration intensity was greater for the C-2 than the Tactaid tactors. This difference in perception is in agreement with the difference in postural responses and well correlated with vibration strength. This finding is in agreement with investigations by Martin et al. [42] who showed that the strength of vibration-induced proprioceptive activity increases with the magnitude of the vibration stimulus. Furthermore, Kavounoudias et al. [40] and Wierzbicka et al. [43] have shown that muscle response increased with stimulation magnitude. Therefore, it is assumed that, due to the greater strength of the C-2 tactor, a larger number of tactile receptors are recruited during the mechanical stimulation that occurs on the skin during the application of a vibrational stimulus, which in turn

increases the associated compensatory response. It is also possible that the efficiency of the stimulation is larger for linear tactors, such as the C-2, than for inertial actuators, such as the Tactaid, as the former may produce a larger deformation of the skin due to the unique direction of travel of the pulse waves providing the stimulation. Hence, a better efficiency may be translated by a more secure drive (consistency of response better for normal stretch than shear stretch) of the cutaneous receptors. As indicated earlier, it is unlikely that the largest vibration of the C-2 tactors would significantly activate the primary endings of the muscles located under the skin. Hence, the contribution of these latter to the response difference between C-2 and Tactaid tactors may be ruled out.

The latency of vibration-induced postural shifts, when vibration was applied over the right and left internal oblique as well as right and left erector spinae locations, was observed to be approximately 800 msec after the onset of vibration. The latency of the postural response is greater than that of a reflex response, which is known to be less than 100 msec [57-58], and thus is not compatible with a reflex response. The time course, which is defined as the response time needed to reach the average values of vibration-induced postural shifts (i.e., approximately 1.2° for the C-2 tactor and 0.7° for the Tactaid tactor), was observed to be approximately 3.3 s for both the C-2 and Tactaid tactors. One interpretation of this outcome may be that the recruitment of a larger number of tactile receptors increases response speed. However, the average value of mean power frequency (less than 0.5 Hz for both M/L and A/P directions) was not significantly different in the presence or absence of vibrotactile stimulation, regardless of the tactor type or tactor location. Since the postural sway frequency measured lies within the

normal range of less than 1.0 Hz [7, 59], vibrotactile stimulation does not appear to induce disruptive higher frequency behavior.

The qualitative survey results indicate that vibration-induced postural shifts and corresponding post effects were not consciously perceived by the large majority of subjects (9 of 11 subjects) as is the case when vibrations are applied to muscle tendons or body segments [42]. This dissociation between perceptual and motor effects may result from the relatively small shift and thus an automatic motor response that does not require a cognitive intervention, as is commonly the case in postural regulation, since the displacement is not sufficient to compromise stability. Alternatively, attention may have been diverted by the stimulus, which was perceived, and thus the small postural change was missed at the conscious level.

To conclude, the results strongly support the use of cutaneous information from receptors located over the torso's primary mover muscles to facilitate posture regulation and thus an internal representation of the upper body or "postural body scheme", which has been attributed primarily to muscle proprioception [28, 44, 46]. The compensatory motor response associated with vibrotactile stimulation of these receptors corresponds to an attraction in the direction of the stimulated area, which indicates that proprioceptive information from cutaneous receptors in this area obeys the vector rule observed for other locations [11]. The C-2 tactor generated larger postural shifts compared with the Tactaid tactor. Therefore, study findings suggest that tactor type and application location should be carefully considered. Moreover, the instructions concerning reactive and/or corrective movements should be compatible with the non-volitional response to the vibrotactile stimulation in order to facilitate postural adjustments. These results may have clinical

implications, since vibrotactile stimulation can be used to indicate the direction in which an individual affected by a vestibular disorder should move in order to maintain a stable standing posture. To date, vibrotactile stimulation has been used to indicate the direction of postural tilt of the body, with accompanying instructions to "move away from the vibration" in analogy to an aversion response [5-7, 11, 21, 60]. This instruction seems to be poorly compatible with the natural tendency revealed here. Thus, the use of vibrotactile biofeedback should be carefully considered and instruction of reactive/corrective movements should be made compatible with the unconstrained response to stimulation in order to facilitate postural adjustments. It is presumed that optimizing this compatibility may result in reduced reaction time (response delay) for tactile cues and thus better stability of body posture.

References

[1]   J. R. Davis, M. G. Carpenter, R. Tschanz, S. Meyes, D. Debrunner, J. Burger, and J. H. Allum, "Trunk sway reductions in young and older adults using multi-modal biofeedback," *Gait Posture* vol. 31, no. 4, pp. 465-472, Apr. 2010.

[2]   F. B. Horak, M. Dozza, R. Peterka, L. Chiari, and C. Wall, "Vibrotactile biofeedback improves tandem gait in patients with unilateral vestibular loss," *Annals of the New York Academy of Sciences,* vol. 1164, pp. 279-281, May. 2009.

[3]   K. H. Sienko, M. D. Balkwill, L. I. Oddsson, and C. Wall, "Effects of multi-directional vibrotactile feedback on vestibular-deficient postural performance

during continuous multi-directional support surface perturbations," *Journal of Vestibular Research,* vol. 18, no. 5-6, pp. 273-285, Jan. 2008.

[4]   C. Wall and M. S. Weinberg, "Balance prostheses for postural control," *Engineering in Medicine and Biology Magazine,* vol. 22, no. 2, pp. 84-90, Mar. 2003.

[5]   C. Wall, M. S. Weinberg, P. B. Schmidt, and D. E. Krebs, "Balance prosthesis based on micromechanical sensors using vibrotactile feedback of tilt," *IEEE Transactions on Biomedical Engineering,* vol. 48, no. 10, pp. 1153-1161, Oct. 2001.

[6]   S. Haggerty, L. T. Jiang, A. Galecki, and K. H. Sienko, "Effects of vibrotactile feedback on response time and postural stability in older adults," *Gait & Posture,* 2012 (In press).

[7]   K. H. Sienko, V. V. Vichare, M. D. Balkwill, and C. I. I. I. Wall, "Assessment of vibrotactile feedback on postural stability during pseudorandom multidirectional platform motion," *IEEE Transactions on Biomedical Engineering,* vol. 57, no. 4, pp. 944-952, Apr. 2010.

[8]   D. A. Ross and B. B. Blasch, "Wearable Interfaces for Orientation and Wayfinding," in *Conf. Proc. 4th international ACM conference on Assistive technologies*, Arlington, VA, USA 2000, pp. 193-200.

[9]   J. B. F. Van Erp and H. A. H. C. Van Veen, "Vibro-Tactile Information Presentation in Automobiles," in *EuroHaptics* Birmingham, UK, 2001, pp. 99-104.

[10] H. A. H. C. Van Veen and J. B. F. Van Erp, "Tactile Information Presentation in the Cockpit," in *Haptic Human-Computer Interaction*, Tokyo, JAPAN, 2001, pp. 174-181.

[11] J. M. Aimonetti, V. Hospod, J. P. Roll, and E. Ribot-Ciscar, "Cutaneous afferents provide a neuronal population vector that encodes the orientation of human ankle movements.," *Journal of Physiology,* vol. 580, no. 2, pp. 649-658, Apr. 2007.

[12] D. F. Collins and A. Prochazka, "Ankle muscle stiffness in the control of balance during quiet standing," *Journal of Physiology,* vol. 496, no. 3, pp. 857-871, Nov. 1996.

[13] D. F. Collins, K. M. Refshauge, G. Todd, and S. C. Gandevia, "Cutaneous receptors contribute to kinesthesia at the index finger, elbow, and knee," *Journal of Neurophysiology,* vol. 94, no. 3, pp. 1699-1706, Sep. 2005.

[14] B. B. Edin, "Quantitative analysis of static strain sensitivity in human mechanoreceptors from hairy skin," *Journal of Neurophysiology,* vol. 67, no. 5, pp. 1105-1113, May. 1992.

[15] B. B. Edin and J. H. Abbs, "Finger movement responses of cutaneous mechanoreceptors in the dorsal skin of the human hand," *Journal of Neurophysiology,* vol. 65, no. 3, pp. 657-670, Mar. 1991.

[16] B. B. Edin and A. B. Vallbo, "Muscle afferent responses to isometric contractions and relaxations in humans," *Journal of Neurophysiology,* vol. 63, no. 6, pp. 1307-1313, Jun. 1990.

[17] J. A. Goebel, B. C. Sinks, B. E. Parker, Jr., N. T. Richardson, A. B. Olowin, and R. W. Cholewiak, "Effectiveness of head-mounted vibrotactile stimulation in

subjects with bilateral vestibular loss: a phase 1 clinical trial," *Otology & neurotology,* vol. 30, no. 2, pp. 210-216, Feb. 2009.

[18] A. A. Priplata, B. L. Patritti, J. B. Niemi, R. Hughes, D. C. Gravelle, L. A. Lipsitz, A. Veves, J. Stein, P. Bonato, and J. J. Collins, "Noise-enhanced balance control in patients with diabetes and patients with stroke," *Annals of Neurology,* vol. 59, no. 1, pp. 4-12, Jan. 2006.

[19] D. Ursu, L. T. Jiang, and K. H. Sienko, "Effect of vibrotactile trunk tilt feedback on postural stability in older adults," in *Annual American Society of Biomechanics Meeting*, Penn State University, Aug., 2009.

[20] R. J. Peterka, C. I. I. I. Wall, and E. Kentala, "Determining the effectiveness of a vibrotactile balance prosthesis," *Journal of Vestibular Research,* vol. 16, no. 1-2, pp. 45-65, Jan. 2006.

[21] K. H. Sienko, M. D. Balkwill, L. I. Oddsson, and C. Wall, "Effects of multi-directional vibrotactile feedback on vestibular-deficient postural performance during continuous multi-directional support surface perturbations," *Journal of Vestibular Research,* vol. 18, no. 5-6, pp. 273-285, Jan. 2008.

[22] R. W. Cholewiak and M. Wollowitz, "The design of vibrotactile transducers," in *Tactile Aids for the Hearing Impaired, I. Summers, ed, Whurr Publishers Ltd*, London, UK, Oct., 1992, pp. 57-82.

[23] B. J. Mortimer, G. A. Zets, and R. W. Cholewiak, "Vibrotactile transduction and transducers," *Journal of the Acoustical Society of America,* vol. 121, no. 5 Pt1, pp. 2970-1977, May. 2007.

[24] L. M. Brown, S. A. Brewster, and H. C. Purchase, " A first investigation into the effectiveness of Tactons," in *Conf. Proc. 1st World Haptics 2005*, Pisa, Italy, Mar., 2005, pp. 167-176.

[25] E. Ribot-Ciscar, J. P. Vedel, and J. P. Roll, "Vibration sensitivity of slowly and rapidly adapting cutaneous mechanoreceptors in the human foot and leg," *Neuroscience Letter,* vol. 104, no. 1-2, pp. 130-135, Sep. 1989.

[26] M. Knibestol and A. B. Vallbo, "Single unit analysis of mechanoreceptor activity from the human glabrous skin," *Acta Physiologica Scandinavica* vol. 80, no. 2, pp. 178-195, Oct. 1970.

[27] D. Burke, K. E. Hagbarth, L. Lofstedt, and B. G. Wallin, "The responses of human muscle spindle endings to vibration during isometric contraction," *Journal of Physiology,* vol. 261, no. 3, pp. 695-711, Oct. 1976.

[28] J. P. Roll, J. P. Vedel, and E. Ribot, "Alteration of proprioceptive messages induced by tendon vibration in man: a microneurographic study," *Experimental Brain Research,* vol. 76, no. 1, pp. 123-222, 1989.

[29] Polytec Inc. (2011, Jun). *Laser Doppler Vibrometer - User manual*. Available: http://www.polytec.com

[30] R. K. Otnes and L. Enochson, *Digital Time Series Analysis*. NewYork: John Wiley & Sons Inc, 1972.

[31] D. B. Chaffin, G. B. J. Andersson, and B. J. Martin, *Occupational Biomechanics*, 4th ed. New York: Wiley-Interscience, 2006.

[32] D. F. Collins, K. M. Refshauge, and S. C. Gandevia, "Sensory integration in the perception of movements at the human metacarpophalangeal joint," *Journal of Physiology,* vol. 529, no. 2, pp. 505-515, Dec. 2000.

[33] G. M. Goodwin, D. I. McCloskey, and P. B. Matthews, "The contribution of muscle afferents to kinaesthesia shown by vibration induced illusions of movement and by the effects of paralysing joint afferents," *Brain,* vol. 95, no. 4, pp. 705-748, 1972.

[34] B. B. Edin, "Cutaneous afferents provide information about knee joint movements in humans," *Journal of Physiology,* vol. 531, no. 1, pp. 289-297, Feb. 2001.

[35] M. Hulliger, E. Nordh, A. E. Thelin, and A. B. Vallbo, "The responses of afferent fibres from the glabrous skin of the hand during voluntary finger movements in man," *Journal of Physiology,* vol. 291, pp. 233-249, Jun. 1979.

[36] A. Kavounoudias, R. Roll, and J. P. Roll, "Specific whole-body shifts induced by frequency-modulated vibrations of human plantar soles," *Neuroscience letter,* vol. 266, no. 3, pp. 181-184, May. 1999.

[37] G. Eklund, "General features of vibration-induced effects on balance," *Upsala Journal of Medical Sciences,* vol. 77, no. 2, pp. 112-124, 1972.

[38] M. Gregoric, T. Takeya, J. B. Baron, and J. C. Bessineton, "Influence of vibration of neck muscles on balance control in man," *Agressologie,* vol. 19, no. A, pp. 37-38, 1978.

[39] T. Kasai, S. Yahagi, and K. Shimura, "Effect of vibration-induced postural illusion on anticipatory postural adjustment of voluntary arm movement in standing humans," *Gait & Posture,* vol. 15, no. 1, pp. 94-100, Feb. 2002

[40] A. Kavounoudias, R. Roll, and J. P. Roll, "Foot sole and ankle muscle inputs contribute jointly to human erect posture regulation," *Journal of Physiology,* vol. 532, no. Pt 3, pp. 869-878, May. 2001.

[41] J. R. Lackner, E. Rabin, and P. DiZio, "Fingertip contact suppresses the destabilizing influence of leg muscle vibration," *Journal of Neurophysiology,* vol. 84, no. 5, pp. 2217-2224, Nov. 2000.

[42] B. J. Martin, G. M. Gauthier, J. P. Roll, M. Hugon, and F. Harlay, "Effects of whole-body vibrations on standing posture in man," *Aviation, Space, and Environmental Medicine,* vol. 51, no. 1, pp. 778-787, Aug. 1980.

[43] M. M. Wierzbicka, J. C. Gilhodes, and J. P. Roll, "Vibration-induced postural posteffects," *Journal of Neurophysiology,* vol. 79, no. 1, pp. 143-150, Jan. 1998.

[44] J. R. Lackner and M. S. Levine, "Changes in apparent body orientation and sensory localization induced by vibration of postural muscles: vibratory myesthetic illusions," *Aviation, Space, and Environmental Medicine,* vol. 50, no. 4, pp. 346-354, Apr. 1979.

[45] J. R. Lackner, "Some proprioceptive influences on the perceptual representation of body shape and orientation," *Brain,* vol. 111 (Pt 2), pp. 281-297, Apr. 1988.

[46] J. Massion, "Movement, posture and equilibrium: interaction and coordination," *Progress in Neurobiology,* vol. 38, no. 1, pp. 35-56, Jan 1992.

[47] B. J. Martin and H. S. Park, "Analysis of the tonic vibration reflex: influence of vibration variables on motor unit synchronization and fatigue," *European journal of applied physiology and occupational physiology,* vol. 75, no. 6, pp. 504-511, 1997.

[48]   J. P. Roll and J. P. Vedel, "Kinaesthetic role of muscle afferents in man, studied by tendon vibration and microneurography," *Experimental Brain Research,* vol. 47, no. 2, pp. 177-190, 1982.

[49]   S. Calvin-Figuiere, P. Romaiguere, J. C. Gilhodes, and J. P. Roll, "Antagonist motor responses correlate with kinesthetic illusions induced by tendon vibration," *Experimental Brain Research,* vol. 124, no. 3, pp. 342-350, Feb. 1999.

[50]   J. C. Gilhodes, J. P. Roll, and M. F. Tardy-Gervet, "Perceptual and motor effects of agonist-antagonist muscle vibration in man," *Experimental Brain Research,* vol. 61, no. 2, pp. 395-402, 1986.

[51]   A. Kavounoudias, J. C. Gilhodes, R. Roll, and J. P. Roll, "From balance regulation to body orientation: two goals for muscle proprioceptive information processing?," *Experimental Brain Research,* vol. 124, no. 1, pp. 80-88, Jan. 1999.

[52]   J. P. Roll and R. Roll, *From eye to foot: a proprioceptive chain involved in postural control*. Amsterdam: Elsevier, 1988.

[53]   V. S. Gurfinkel, M. I. Lipshits, and F. G. Lestienne, "Anticipatory neck muscle activity associated with rapid arm movements," *Neuroscience Letter,* vol. 94, no. 1-2, pp. 104-108, Nov. 1988.

[54]   F. B. Horak and J. M. MacPherson, *Postural orientation and equilibrium*. New York: Oxford University Press, 1996.

[55]   D. A. Winter, A. E. Patla, F. Prince, M. Ishac, and K. Gielo-Perczak, "Stiffness control of balance in quiet standing," *Journal of Neurophysiology,* vol. 80, no. 3, pp. 1211-1221, Sep. 1998.

[56] J. L. Huffman, L. E. Norton, A. L. Adkin, and H. J. Allum, "Directional effects of biofeedback on trunk sway during stance tasks in healthy young adults," *Gait and Posture* vol. 32, no. 1, pp. 62-66, May. 2010.

[57] E. Kugelberg and K. E. Hagbarth, "Spinal mechanism of the abdominal and erector spinae skin reflexes," *Brain,* vol. 81, no. 3, pp. 290-304, Sep. 1958.

[58] B. J. Martin, J. P. Roll, and M. Hugon, "Modulation of cutaneous flexor responses induced in man by vibration-elicited proprioceptive or exteroceptive inputs," *Aviation, Space, and Environmental Medicine,* vol. 61, no. 10, pp. 921-928, Oct. 1990.

[59] R. J. Peterka, "Sensorimotor Integration in human postural control," *Journal of Neurophysiology,* vol. 88, no. 3, pp. 1097-1118, Sep. 2002.

[60] C. Wall, L. E. Oddsson, F. B. Horak, D. W. Wrisley, and M. Dozza, "Applications of vibrotactile display of body tilt for rehabilitation," in *Conf. Proc. 26th IEEE Ann. Int. Conf. Engineering in Medicine and Biology Society (EMBS' 04)*, San Francisco, CA, USA, 2004, pp. 4763-4765.

CHAPTER 3: A Wearable Device for Real-Time Motion Error Detection and Vibrotactile Instructional Cuing

3.1. Abstract

A Mobile Instrument for Motion Instruction and Correction (MIMIC) system has been developed to enable an expert (i.e., physical therapist) to map their movements onto a trainee (i.e., patient) in a hands-free fashion. MIMIC comprises an Expert Module (EM) and a Trainee Module (TM). Both the EM and TM are composed of six-degree-of-freedom inertial measurement units, microcontrollers, and batteries. The TM is equipped with an array of actuators to generate vibrotactile instructional cues. The expert wears the EM, and his/her relevant body position is computed by an algorithm based on an extended Kalman filter that provides asymptotic state estimation. The captured expert body motion information is transmitted wirelessly to the TM, which displays directional instructions via vibrotactile stimulation to the skin, based on the computed difference between the expert and trainee motions. Three proof-of-concept studies involving young healthy adults were conducted using a simplified version of the MIMIC system (employing pre-specified target trajectories representing ideal expert movements and

only two TM actuators) during anterior–posterior trunk movements. For the first two studies, each subject was instructed to move in the direction of the vibration sensation until the vibration was eliminated. The first study was designed to investigate the effects of changing the expert-trainee error thresholds (0.5°, 1.0°, and 1.5°) and varying the nature of the control signal (proportional, proportional plus derivative). Expert-subject cross-correlation values were maximized (0.99) and average position errors (0.33°) and time delays (0.2 s) were minimized when the controller used a 0.5° error threshold and proportional plus derivative feedback control signal. The second study used the best performing activation threshold and control signal determined from the first study to investigate subject performance when the motion task complexity and speed were varied. Subject performance decreased as motion speed and complexity increased. The third study was designed to investigate the effects of attractive versus repulsive vibrotactile instructional cues as a function of motion speed and task complexity. Thus, each subject completed two trial sets consisting of two distinct cues (attractive and repulsive) during two days of testing. Preliminary results suggest that repulsive vibrotactile instructional cues provide the greatest correlation, cause the least time delay, and the lead to the least position error between expert and subject motion.

3.2. Motivation and objective

Physical rehabilitation has been shown to improve sensory integration, motor coordination, and strength in patient populations with balance or vestibular disorders, stroke, and traumatic brain injuries [1-4]. During conventional rehabilitation and training,

physical therapists communicate proper execution of an exercise to patients through a combination of verbal instruction, demonstration, and/or physical guidance. Instruction and demonstration are provided prior to and/or during the execution of the rehabilitation exercise and are typically used in combination with extrinsic (or augmented) feedback [5]. The impact of feedback on motor learning varies as a function of the frequency, delay, and precision with which information is provided [6]. Physical guidance involves the manual manipulation of a patient's body or body segment(s) in order to facilitate the completion of a task that a patient may not otherwise be able to perform on his/her own [7]. While physical guidance improves the patient's ability to accurately replicate the desired trajectory or movement, it does so at the expense of providing a patient with the ability to detect and correct errors [7], a critical aspect of motor learning [8-9].

Technologies that augment traditional rehabilitation practices in the clinical setting or increase compliance in at-home based exercise programs have the potential to provide both instructions regarding the intended movements and real-time or delayed feedback. Lieberman and Breazeal developed a real-time wearable vibrotactile feedback suit to facilitate upper limb human motor learning [10]. Subjects were asked to replicate upper limb motion presented via pre-recorded video while receiving vibrotactile feedback based on passive motion tracking measurements whenever an error between the target motion and the subject's motion occurred. The feedback control signal used in this study was solely based on errors of joint angles. Vibrotactile feedback contributed to a decrease in motion errors and an accelerated motor task-learning rate compared to pre-recorded video-based instructional cues when the arm motion was produced using a hinge joint. Rotational joint motions were not improved with any statistical significance. The authors

79

noted that video or optical-based motion tracking of the human body is not feasible for use outside of a laboratory environment due to the expense and size of the equipment.

Several other recent studies have developed and assessed kinesthetic motion guidance systems for upper limb motion guidance that use a control signal proportional to the position error between the target and subject [11-13]. Both the Sergi et al. (2008) and Kapur et al. (2010) kinesthetic guidance systems employ magnetic motion tracking technologies. Recent advances in micro-electro-mechanical system technology such as the miniaturization of inertial measurement units (IMUs) have provided a platform for real-time motion tracking in unconstrained environments [14-17]. Van der Linden et al. (2009) leveraged this portable and low-cost technology for their upper limb motion study focused on teaching violin bowing techniques [13].

The majority of kinesthetic-based motion guidance techniques explored to date have provided a control signal proportional to the position error between the target and the subject, which may or may not be varied in terms of magnitude or frequency based on the magnitude of the error. However, based on the known time delay associated with perceiving, processing, and responding to vibrotactile cues, hypothesize is that performance might be further improved if the rate of change of position or other predictive information were used to generate the feedback control signal. In a recent study performed by Wall and Kentala [18], several control signals were used to activate vibrotactile trunk feedback during computerized dynamic posturography in a subject population with vestibular loss. Specifically, they evaluated the following control signals: proportional to the measured tilt angle (P), proportional to the rate of change of tilt angle (D), and a combination of the P and D signals (PD). Their findings demonstrated that all

evaluated control signals reduced trunk tilt, but that the PD control signal produced significantly smaller trunk tilt values compared to either P or D feedback.

Attractive cues, during which individuals are instructed to move in the direction of the sensed vibration, have previously been used to provide turning guidance during walking [19], driving [20], and flying [21] tasks and to provide pilots with information about the attitude of an aircraft with respect to gravity [21]. Repulsive cues, for which individuals are instructed to move in the direction opposite the sensed vibration, have been used by Wall et al. in the first vibrotactile feedback balance device. This system functioned based on the notion that such repulsive vibrations may provoke a similar aversional response of the kind that occurs when people bump into a wall [22]. Although individuals can use either attractive or repulsive cuing to make volitional movements, it is possible that one of the two cues may result in superior performance or may better leverage non-volitional responses during certain tasks. For example, it has been shown that stimulation of muscle proprioception by vibration may lead to non-volitional balance-correcting responses, generate illusions of movement, and modify reflex responses [23-25]. Chapter 2 demonstrated that random, vibrotactile stimulation in the absence of instructions (i.e., subjects were not told how to respond to the sensed vibrotactile cues) over the internal obliques and erector spinae muscle groups resulted in small postural deviations on the order of 1.0° in the direction of the vibration stimulation. Therefore, it is possible that repulsive cuing is actually acting in opposition to natural impulses, and hence vibrotactile feedback may, in some circumstances, work better by supporting reflexive responses rather than forcing the brain to think about opposing them.

This chapter presents the design, development, and initial assessment of a wearable, wireless, IMU-based expert-trainee motion error detection and vibrotactile instructional cuing technology called MIMIC (Mobile Instrument for Motion Instruction and Correction). This technology enables an expert to map his/her movements to a trainee in hands-free fashion using IMUs, microcontrollers, and vibrating actuators. The goal of this technology is to provide vibrotactile instructional cues to a trainee based on the motion of an expert. In what follows, this chapter will 1) describe the MIMIC's hardware and software components, 2) quantitatively assess a simplified version of the MIMIC's effectiveness in a young healthy pilot subject population during simple trunk bend exercises, 3) determine the best control signal and movement error threshold for slow trunk-based vibrotactile instructional cuing, and 4) determine whether or not young healthy subjects exhibit a difference in performance as quantified by the expert-subject cross-correlation value, time delay, and the average position error when using attractive versus repulsive vibrotactile cues.

3.3. Methods

3.3.1. MIMIC Design Overview

An overall schematic representation of the MIMIC is given in Figure 3.3.1. The wearable IMU-based expert-trainee motion error detection and vibrotactile instructional cuing device is composed of an Expert Module (EM) and Trainee Module (TM) that are utilized by a physical therapist and patient, respectively. Each module includes a six-degree-of-freedom inertial measurement unit (IMU), microcontroller unit (MCU),

Bluetooth module, data-saving module, and battery. The TM additionally has an array of tactors that provide vibrotactile stimulation to the skin. The expert's body motions are sensed by the EM IMU and processed by an extended Kalman filter (EKF) estimation algorithm embedded in the MCU. The estimated expert motion is transmitted wirelessly to the TM through Bluetooth communication, and based on the computed difference between the expert and trainee motion, directional instructions are displayed via vibrotactile stimulation to the skin. The trainee is instructed to move in the direction of the vibration until the stimulus ceases. All information related to the body motion of the expert and trainee and the tactor stimulation history are recorded in the data-saving module for post-processing and analysis.
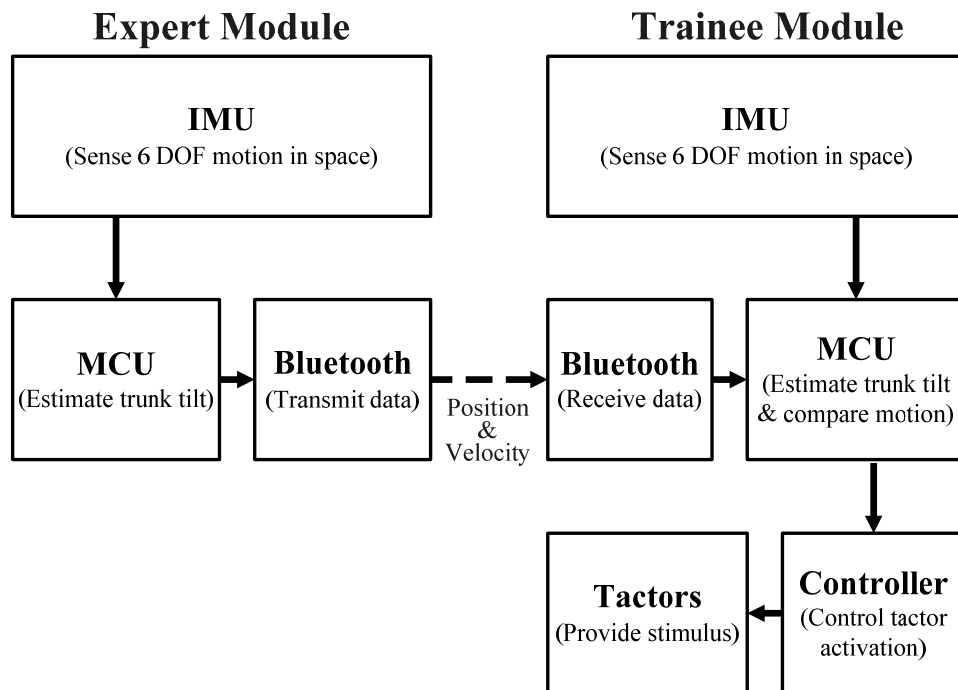
Figure 3.3.1. MIMIC system configuration.

3.3.2. Hardware

The hardware architecture is organized in layers to minimize size and enable easy access for replacement or maintenance. The main layer is equipped with an MCU, Bluetooth module, and data saving module. Communication between the main layer and sensor layer is achieved with serial data communication through a wired connection.

The primary purpose of the MCU is to log IMU data, capture raw angular rates and linear accelerations, estimate body motion using an EKF, generate a control signal for vibrotactile stimulation, manage data communication, and store data in a text format on a data-saving module. For embedded application systems, MCUs such as the ATMEL ATmega 128 provide acceptable computational performance with minimal power consumption and low cost.

The sensory layer comprises a tri-axial linear accelerometer (Freescale Semiconductor, Inc., MMA7260Q) and two gyroscopes (InvenSense, Inc., IDG-300). The accelerometers used in this prototype have a sensitivity range of ±4g with a bandwidth of 350 Hz along each axis. The gyroscopes have a range of ±500°/s. IMU data is sampled at 300 Hz.

Two coin-style eccentric mass pager motors (Samsung Electro-Mechanics, DMJBRK30O), shown in Figure 3.3.2 (c) and subsequently referred to as tactors, were selected to provide vibrotactile stimulation based on their small size and weight, low cost, and minimal power consumption. The spin-up time for the selected tactors to reach maximum rotational vibration is on the order of 90 ms. Each has an operating voltage range of 2.5-3.5 V at 65 mA, a frequency of 200 Hz at 3.0 V, a weight of 1.2 g, and a vibration quantity of 0.84 g root-mean-square.
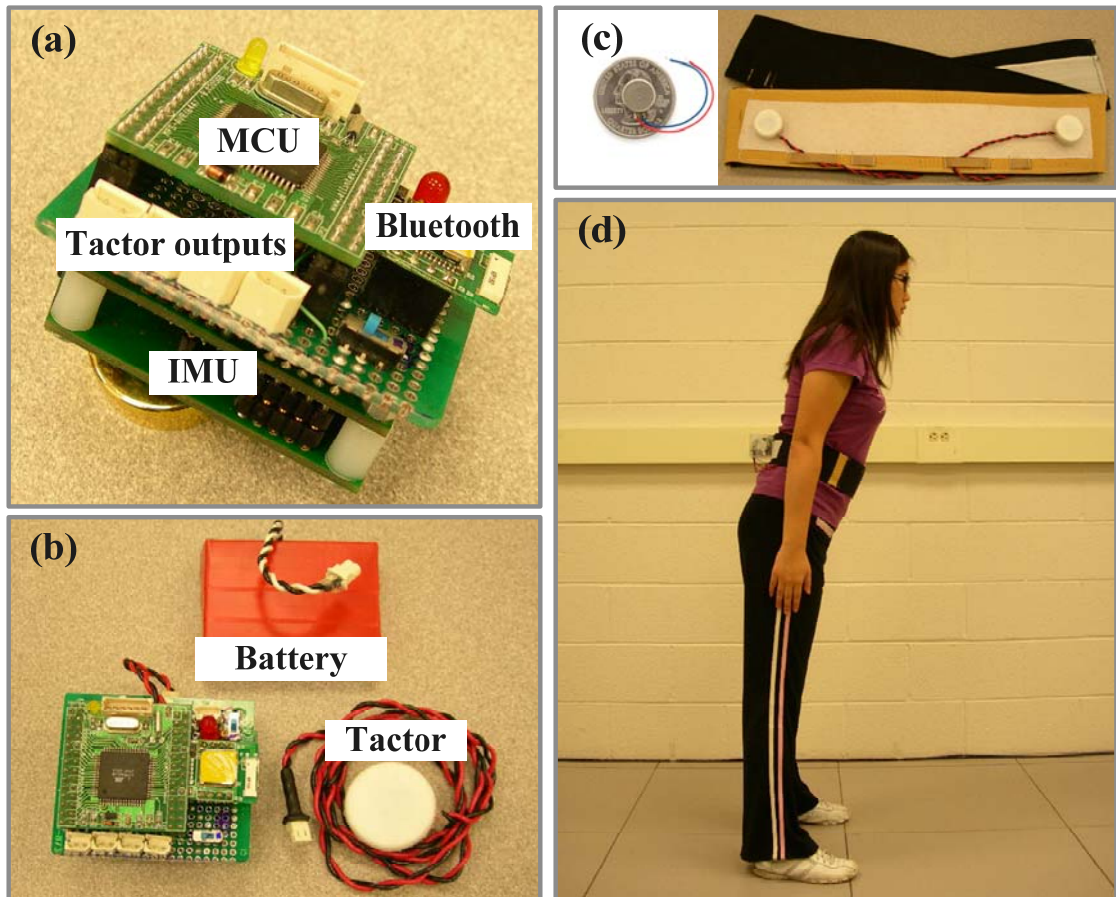
Figure 3.3.2. Hardware architecture. (a) Hardware layers. (b) Hardware system components. (c) Coin-style pager motors and belt. (d) Trainee wearing MIMIC device.

Wireless communication of estimated expert motion data is provided by the Bluetooth module (Comfile Technology Inc, ACODE 330). This module supports Bluetooth 2.0 with SPP interface and also supports simultaneous operation of multiple devices thereby enabling an expert to engage with more than one trainee. The Bluetooth protocol provides sufficient bandwidth to transmit data - approximately 0.23 Mbit per second in symmetric mode.

The data-saving module allows the main processor to store numeric data such as raw or state space representation 3D motion data on an SD memory card for post-processing. Each module is powered by a rechargeable lithium ion battery with a rating of 900 mAh.

3.3.3. Software

To maximize the embedded MCU performance, a component-based software architecture was designed to carefully manage computational resources, prioritizing real-time motion capture and estimation, data transmission, and saving capabilities. The core software architecture implemented in the MCU is the same in both the EM and TM. The only difference between the two modules is the number of data packets communicated to/from peripheral interfaces; the TM acquires raw linear accelerations and angular velocities from the trainee IMU as well as estimated tilt data from the EM.

Tilt estimates were computed based on an Euler-angle-based EKF [26] with four state variables. Two of the state variables (roll and pitch angular positions) were calculated from the output of the tri-axial accelerometer [27]. The remaining two state variables (roll and pitch angular velocities) were acquired directly from the gyroscopes. The EKF, based on a first-order linear state transition model and non-linear measurement model, estimated tilt at a rate of 100 Hz with accuracy better than 0.25° confirmed by tilt table testing. The implemented EKF continuously measures tri-axial accelerations in order to correct for drift error based on the assumption that human trunk acceleration is bounded and averages to zero over any extended period of time [14]. Note that Appendix B

provides a detailed description of the software architecture and the EKF algorithm implemented on the MCU.

For the two control signals chosen for separate evaluation in this study, the difference in position between the expert and trainee was used to generate the error term for the proportional (P) control signal, while differences in both position and velocity between the expert and trainee were used to generate error terms for the proportional plus derivative (PD) control signal:

$$\text{Error} = (\theta_{\text{expert}} - \theta_{\text{trainee}}) + K_d(\dot{\theta}_{\text{expert}} - \dot{\theta}_{\text{trainee}}) \qquad (3.3.1)$$

where θ represents the estimated tilt angle in degrees and $\dot{\theta}$ represents the angular velocity of tilt in °/ms. The angular velocity was calculated by subtracting sequential tilt angle estimates and dividing by the 10 ms estimation interval (corresponding to the 100 Hz tilt estimation rate). K_d is a constant chosen to be 0.5 ms based on a previous study [28-29]. Because this control signal incorporated velocity as well as position error terms, it effectively reduced the tactor activation threshold, theoretically enabling the subjects to quicken their response. The use of a control signal based solely on velocity error was eliminated from consideration based on the results of a pilot study in which this signal produced excessive oscillatory trunk movements in subjects. If the absolute value of the error signal exceeded the specified expert-trainee error threshold, an "attractive" vibrotactile cue was provided to the trainee until the error signal dropped below the

threshold value. Vibrotactile stimulation was not graded according to the magnitude of the error signal; tactor activation was binary in nature (either on or off).

3.3.4. Subjects

The first study using the MIMIC system employed five young (23.4±3.3 yrs) healthy naïve subjects (3 male, 2 female). The second study employed eight young (26.5±1.3 yrs) healthy naïve subjects (5 male, 3 female) and the third study involved 12 young (24.8±3.7 yrs) healthy naïve subjects (8 male, 4 female). The University of Michigan Institutional Review Boards approved the experimental protocol, which conformed to the Helsinki Declaration. Informed consent was obtained from each subject prior to the start of the experiment.

3.3.5. Experimental Protocol

The first study was designed to investigate the effects of changing the vibrotactile stimulation activation threshold and varying the nature of the control signal. The second study used the best performing activation threshold and control signal determined from the first study to investigate subject performance as a function of increasing motion task complexity and speed. The third study was designed to investigate the effects of attractive versus repulsive vibrotactile instructional cues while varying motion speed and task complexity. Subjects participating in these three studies were instrumented with the TM and instructed to 1) stand with their feet parallel approximately 15 cm apart (as indicated

by floor markings) and 2) "move either in the direction of the sensed vibration (attractive) or in the direction opposite the sensed vibration (repulsive) until the vibration stops". Standard foam earplugs and earmuffs were provided to eliminate environmental and tactor noise. One tactor was placed near the navel and another near the spine at approximately the L4/L5 lumbar level. Prior to data collection, subjects were provided with acclimatizing tactor stimulation.

In the first study, subjects were asked to replicate a pre-specified anterior-posterior (A/P) trunk movement, subsequently referred to as "expert motion", by moving toward the vibrotactile instructional cues. The expert motion consisted of an anterior 20° trunk bend followed by a 6 s static hold at 20° and a posterior trunk bend to return to neutral upright stance (refer to solid line in Figure 3.3.3). The anterior and posterior 20° trunk bends were performed at a rate of approximately 1.12°/s. Note that each subject was asked to bend only at the waist in response to the vibrotactile cues while they were performing the task. In this study, three expert-trainee error thresholds (0.5°, 1.0°, and 1.5°) and two control signals (P and PD) were evaluated. Each subject performed three repetitions of the six possible control signal and error threshold combinations, totaling eighteen trials. The presentation of trial type was randomized and no practice trials were provided. In addition, pre-/post-baseline data were collected to assess any potential training effects. All experimental trials were performed with eyes closed.
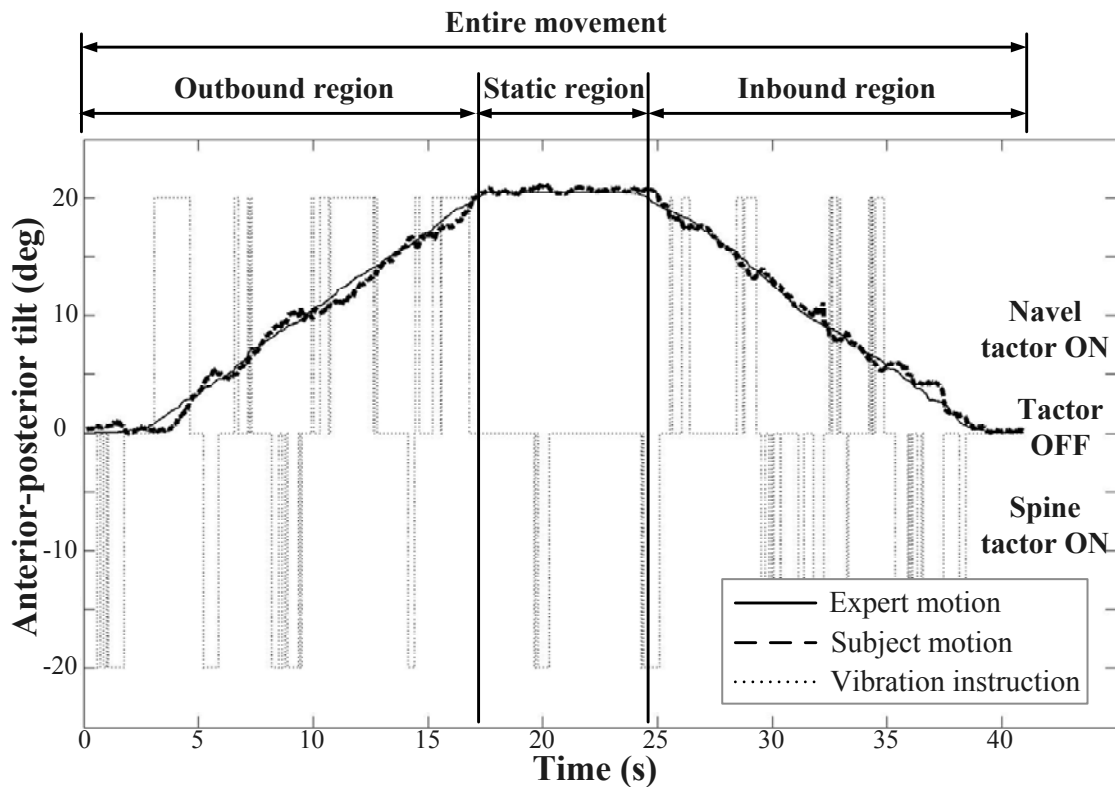
Figure 3.3.3. Representative sample data from one subject after parameter optimization was completed. Light grey, grey, and black lines represent the expert motion, subject motion, and simulation motion, respectively.

In the second study, subjects were presented with the same pre-specified anterior-posterior (A/P) trunk movement used during the first study, but at three different speeds: slow (approximately 1.12°/s), medium (approximately 2.0°/s), and fast (approximately 4.0°/s). Subjects were also asked to use the vibrotactile cues to replicate four additional and more challenging A/P expert trunk motion patterns with variable speeds (Figure 3.3.4), by moving toward the vibrotactile instructional cues. The second study leveraged the results from the first study and therefore only the best performing control signal (PD) and error threshold (0.5°) were used. Each subject performed three repetitions for each

90

speed of the simple motion and three repetitions of each of the four more challenging patterns, totaling twenty-one trials. The presentation of both speed and pattern type were randomized. One practice trial for each speed and pattern was provided.
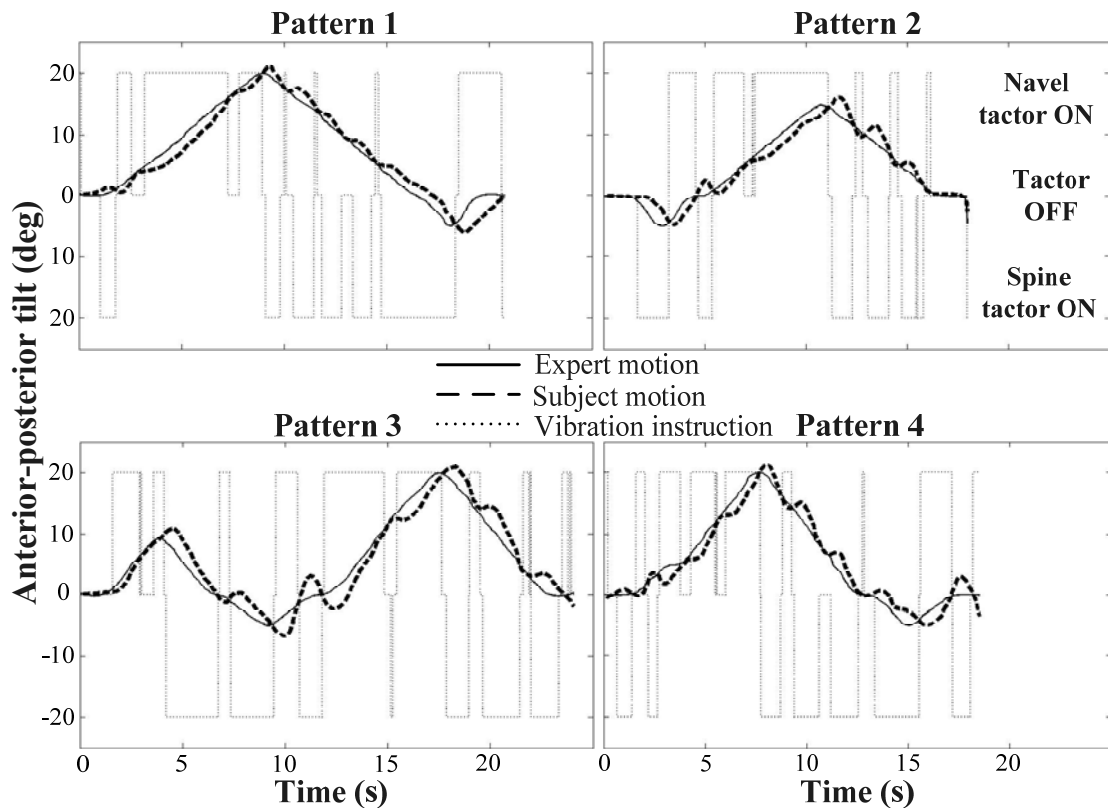
Figure 3.3.4. Representative sample data in which the four different patterns were provided. Solid, dashed, and dotted lines represent the expert motion, subject motion, and vibration instruction, respectively. Positive and negative values indicate movement in the anterior and posterior directions, respectively.

In the third study, subjects were divided into two groups. Group 1 (G1) subjects completed the first day of testing using attractive cues and the second day of testing using repulsive cues. The second group (G2) completed the testing in the opposite order. All

subjects participated on both testing days, which were separated by approximately 48 hours. Subjects performed four device-instructed movement patterns (identical to the ones used in the second study) at three different speeds. Three practice trials for each speed and pattern were performed prior to the experimental session. In the experimental session, subjects completed three repetitions for each speed and pattern. Presentation of trial type was randomized. Note that the best performing control signal (PD) and error threshold (0.5°) were used based on the results from the first study.

3.3.6. Data Analysis Methodologies

All post-processing was performed using MATLAB (The MathWorks, Natick, MA). To characterize subjects' ability to replicate the expert motion, a cross-correlation analysis of the expert and subject trunk tilt angle was performed. The output of the cross-correlation analysis was 1) a cross-correlation value ranging between 0 and 1, with 1 indicating perfectly matched motion and 2) a time delay, with a positive delay indicating a time lag between the trainee and expert motion. Position error was defined as the average difference between the expert and subject position in degrees. For the purpose of data analysis, each trial from the first study was split into outbound, static, and inbound regions (shown in Figure 3.3.3) corresponding to the anterior trunk bend, static hold at 20°, and posterior trunk bend to the neutral upright position, respectively. The composite movement was defined as the entire sequence of regions. The position error in the outbound and inbound regions characterizes performance during dynamic motion, while

the position error in the static region characterizes performance during the static trunk bend.

Statistical analysis was performed using linear mixed effects models (LMM). One particularly desirable feature of this analytical methodology is that it takes into account the likely correlation of repeated measurements performed on the same subject. Dependent variables were cross-correlation value, time delay, and position error. The primary focus of the analysis was to estimate the effects of activation threshold and control signal on the dependent variables while accounting for the correlation of the observations' random intercepts associated with subjects and replicated measures. Hypotheses for the main effects of activation threshold and control signal and their interactions were tested using an F-test. Post-hoc analysis for each dependent variable was performed using Sidak's method. To assure the assumptions of the LMM (in particular normality and constant variance of residual variance for the time delay and position error), the dependent variable was expressed on a logarithmic scale. Furthermore, a two-way analysis of variance was conducted to determine the main effects of cue instruction (attractive vs. repulsive) and motion condition (speed and pattern) for each dependent variable. Hypotheses for the main effects and their interactions were tested using an F-test. Post-hoc analysis for each dependent variable was performed using Tukey Honestly Significant Differences.

3.4. Results

3.4.1. System performance

Figure 3.4.1 shows the recorded angular position measurement noise for the A/P and M/L directions. The data were normally distributed and resembled white Gaussian noise. The Gaussian curves shown in Figure 3.4.1 (c) and (d), were computed using the curve fitting toolbox provided by MATLAB (The MathWorks, Natick, MA). The R^2 value quantifies the goodness of fit and is defined as the square of the correlation between the sensor data values and the predicted Gaussian values. Note that the MIMIC device was placed on a vibration isolated optical table for an extended period of time to eliminate the addition of the measureable table noise.

Figure 3.4.2 shows the performance of the EKF tilt estimation algorithm implemented in the MIMIC system while the representative subject was performing the motion replication task with A/P trunk movement. Without the EKF algorithm, the noise of the angular position accelerometer output computed by Equation B.3 (Appendix) was shown to be approximately ±0.5°, while the employment of the EKF algorithm reduced the noise to approximately 0.2° in the A/P direction without significant estimation delay.
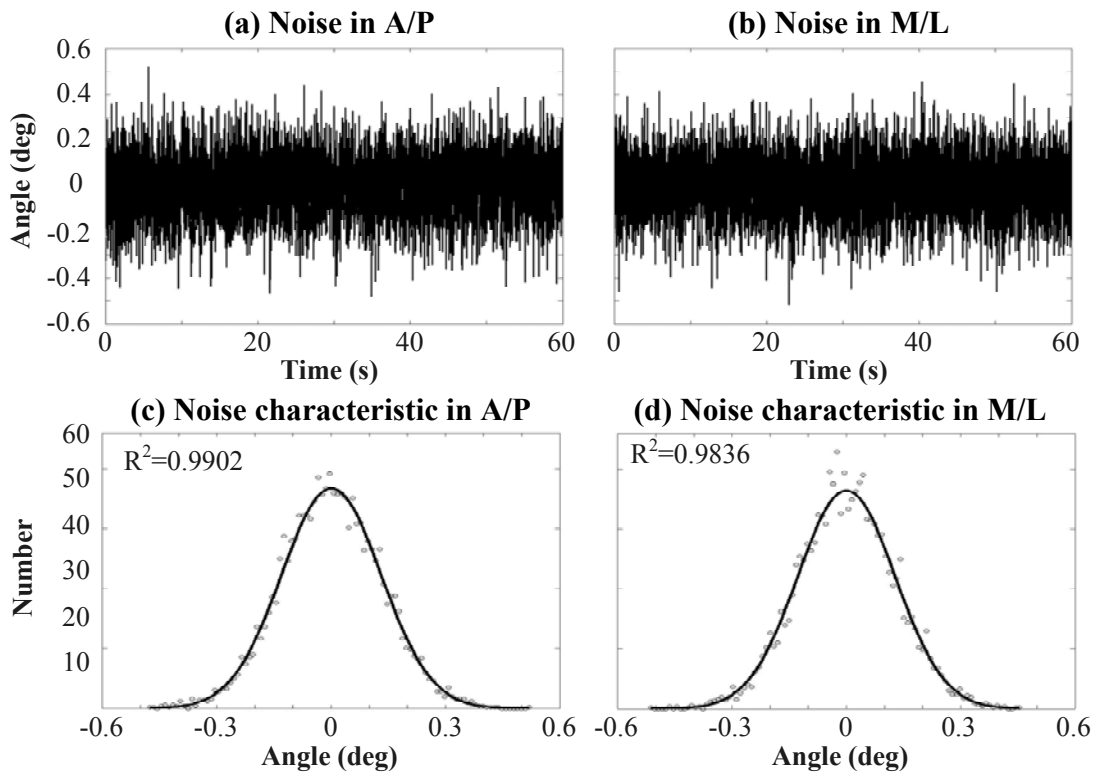
Figure 3.4.1. Noise analysis and characteristics of angular positions in A/P and M/L directions when the MIMIC is resting in the postion corresponding to the axis of sensitivity of the respective accelerometers and gyroscopes. (a) Noise in A/P direction without the EKF estimation. (b) Noise in M/L direction without the EKF estimation. (c) A/P predicted Gaussian curve (solid line) and measured data (point). (d) M/L predicted Gaussian curve (solid line) and measured data (point). Note that values for R^2 range from 0 to 1 and indicate the goodness of fit between the predicted Gaussian curve and the noise distribution.
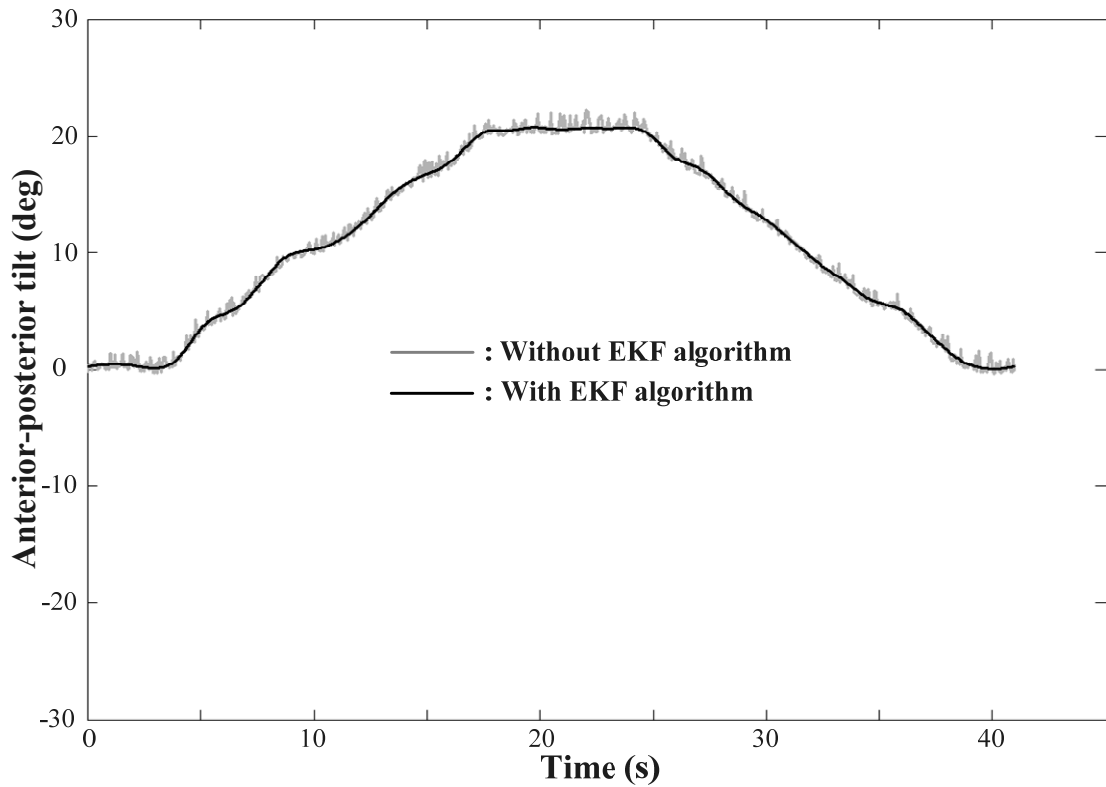
Figure 3.4.2. Effect of EKF algorithm on tilt estimation performance: light and dark solid lines represent the estimated tilt angle of the MIMIC system without or with the EKF algorithm, respectively.

3.4.2. Effects of activation threshold and control signal

Table 3.4.1 reports the estimates and standard errors for the effects of activation threshold and control signal conditions used during the first study.

Table 3.4.1. Statistical analysis results (n=5) for control signal (CS) and activation threshold (AT). Results for all dependent variables except cross-correlation are expressed on a logarithmic scale. *In the presence of significant control signal by activation threshold interaction, estimates of main effects are not interpretable and therefore not reported.

Dependent variable	Effects	Estimate	Std error	DF	F Value	Pr>F
Cross-correlation	CS (P vs PD)	-0.02874	0.00464	1,72	38.29	<0.0001
	AT (1 vs 3)	0.03184	0.00569	2,72	15.86	<0.0001
	AT (2 vs 3)	0.01286	0.00569			
Position error (Outbound)	CS (P vs PD)	0.6627	0.0434	1,72	233.1	<0.0001
	AT (1 vs 3)	-0.5300	0.05316	2,72	50.64	<0.0001
	AT (2 vs 3)	-0.2022	0.05316			
Position error (Static)	CS (P vs PD)	0.6516	0.09638	1,72	45.71	<0.0001
	AT (1 vs 3)	-0.4245	0.118	2,72	7.09	0.0016
	AT (2 vs 3)	-0.0983	0.118			
Position error (Inbound)	CS			1,70	223.81	<0.0001
	AT			2,70	52.28	<0.0001
	CS X AT (*)			2,70	4.49	0.0147
Position error (Entire)	CS (P vs PD)	0.6906	0.03308	1,72	435.84	<0.0001
	AT (1 vs 3)	-0.5571	0.04051	2,72	95.09	<0.0001
	AT (2 vs 3)	-0.2423	0.04051			
Time delay	CS (P vs PD)	1.1466	0.2426	1,72	22.34	<0.0001
	AT (1 vs 3)	-0.7599	0.2971	2,72	3.4	0.0388
	AT (2 vs 3)	-0.2489	0.2971			

Figure 3.4.3 depicts the average cross-correlation results for the three activation thresholds and two control signals used during the first study. Analysis of the cross-correlation of the expert-trainee movement showed significant main effects of the activation threshold ($p<0.0001$) and control signal ($p<0.0001$) conditions. However, the analysis did not show a significant interaction of the activation threshold X control signal conditions ($p=0.1773$). A post-hoc analysis showed that the best cross-correlation values were achieved with the PD control signal regardless of the activation threshold and with the smallest activation threshold regardless of the control signal.
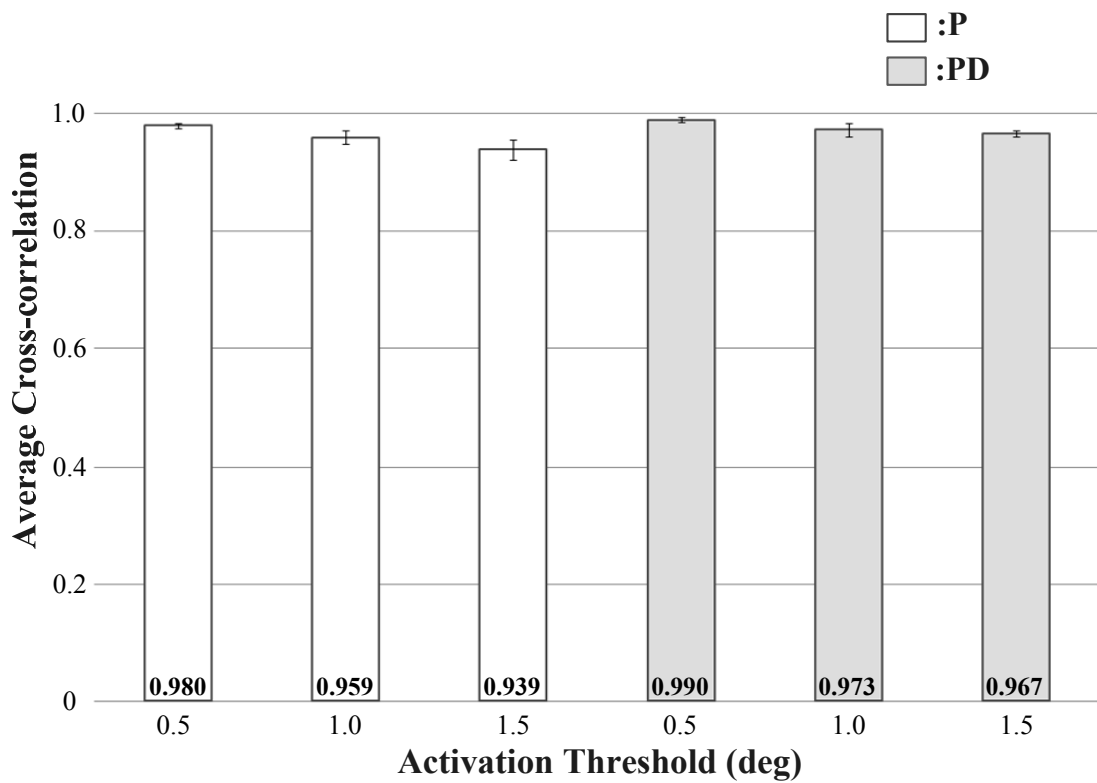
Figure 3.4.3. Average expert-trainee cross-correlation results as a function of activation threshold and control signal. White and gray bars represent P and PD control signals, respectively. Error bars represent standard error of the mean.

Figure 3.4.4 depicts the average expert-trainee position error for the outbound region (a), static region (b), inbound region (c), and entire movement (d). Analysis of the position error of the expert-trainee movement showed significant main effects of the activation threshold condition and control signal condition, respectively, for the outbound region ($p<0.0001$ and $p<0.0001$), static region ($p<0.0001$ and $p=0.0016$), inbound region ($p<0.0001$ and $p<0.0001$), and entire movement ($p<0.0001$ and $p<0.0001$). However, the analysis did not reveal a significant interaction of the activation threshold X control signal conditions for the outbound region ($p=0.2416$), static region ($p=0.8349$), or entire movement ($p=0.3113$). Only the inbound region revealed a significant interaction of activation threshold X control signal conditions ($p=0.0147$). A post-hoc analysis for the outbound and static regions and entire movement showed that subjects had smaller average position errors when using the PD control signal regardless of the activation threshold and when using the smallest activation threshold regardless of the control signal. For the inbound region, however, a post-hoc analysis showed that the 0.5° activation threshold with the PD control signal resulted in the smallest average position error, but the three post-hoc pair-wise comparisons were not significant.

Figure 3.4.5 represents the average time delay between the expert and subject movements over the entire movement. Analysis of the time delay of the expert-trainee movement showed significant main effects of activation threshold ($p<0.0001$) and control signal ($p=0.03888$) conditions, respectively. However, the analysis did not reveal a significant interaction of the activation threshold X control signal conditions ($p=0.9941$). A post-hoc analysis showed that subjects had the shortest time delays with the PD control

signal regardless of activation threshold and with the smallest activation threshold regardless of control signal.
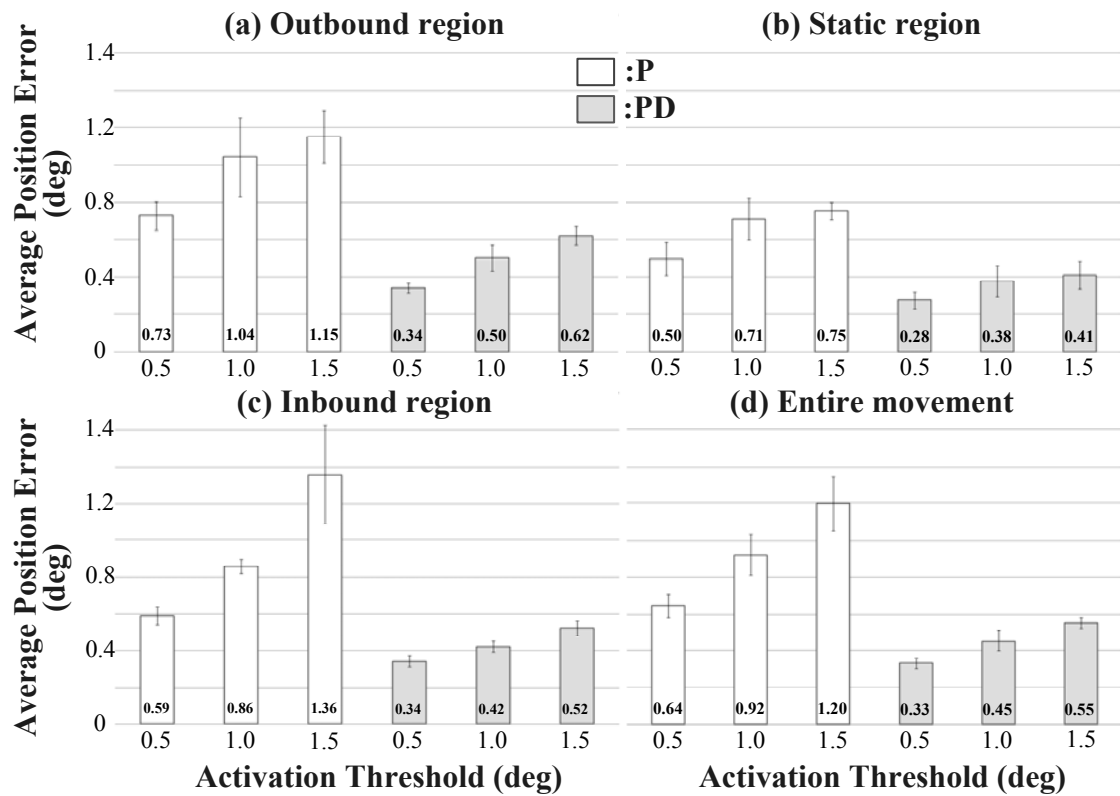
Figure 3.4.4. Average expert-trainee position error results in degrees as a function of activation threshold and control signal by region. (a) Outbound region. (b) Static region. (c) Inbound region. (d) Entire movement. White and gray bars represent P and PD control signals, respectively. Error bars represent standard error of the mean.
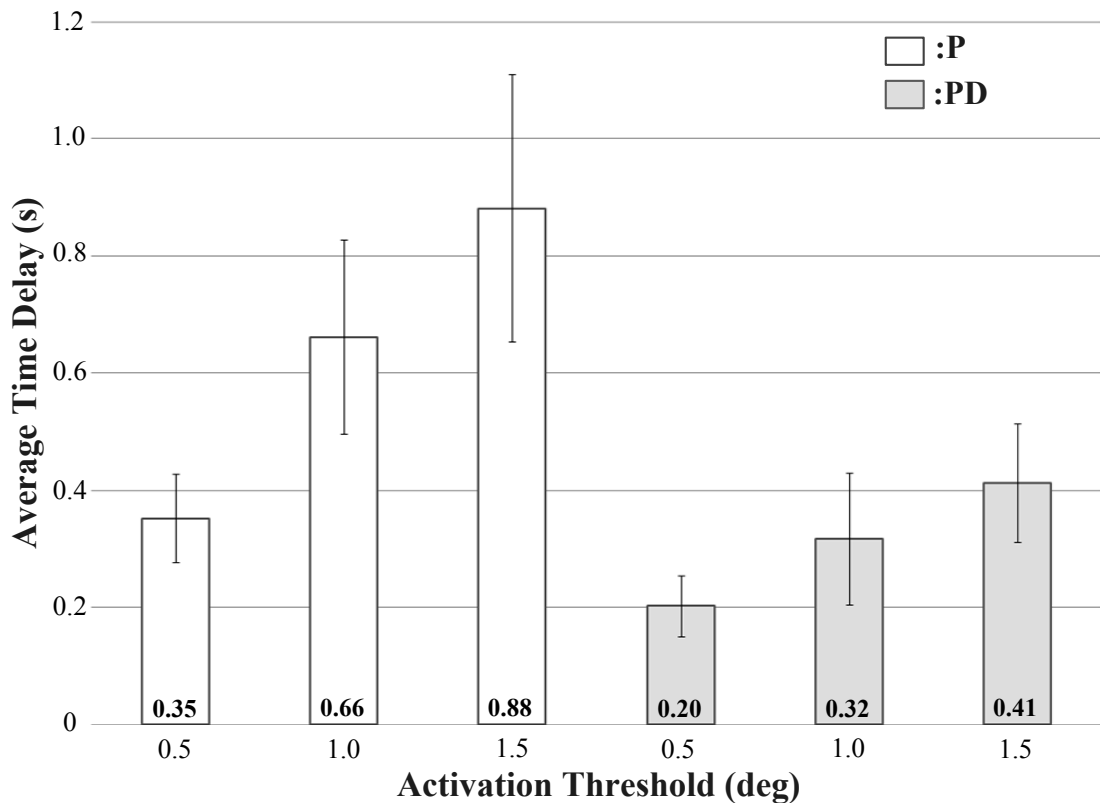
Figure 3.4.5. Average expert-trainee time delay results in seconds as a function of activation threshold limit and control signal. White and gray bars represent P and PD control signals, respectively. Error bars represent standard error of the mean.

3.4.3. Effects of speed and pattern

Table 3.4.2 reports the estimates and standard errors for the effects of three speeds and four patterns used during the follow up study.

Figure 3.4.6 depicts the average expert-trainee cross-correlation value results as a function of speed (Figure 3.4.6 (a)) and motion pattern (Figure 3.4.6 (b)). Analysis of the expert-trainee cross-correlation values showed significant main effects on the speed ($p<0.0001$) and pattern ($p<0.0001$) conditions. A post-hoc analysis showed that subjects had the best cross-correlation values when they replicated the motion with the slowest

speed (i.e., 1 deg/s) and the simplest pattern (i.e., pattern 1). However, the pair-wise comparisons of cross-correlation values between patterns 2, 3, and 4 were not significant for patterns.

Figure 3.4.7 depicts the average expert-trainee position error for the entire movement as a function of speed (Figure 3.4.7 (a)) and motion pattern (Figure 3.4.7 (b)). Analysis of the expert-trainee position error showed significant main effects on speed ($p<0.0001$) and pattern ($p<0.0001$) conditions.

A post-hoc analysis showed that subjects had the least amount of position error when they performed the motion replication for the slowest speed (i.e., 1 deg/s). This analysis also showed that neither pattern 1 vs. pattern 2 nor pattern 3 vs. pattern 4 were significant in terms of position error. However, the subjects showed the least amount of position error when they performed either pattern 1 or 2 compared to pattern 3 and 4.

Figure 3.4.8 depicts the average expert-trainee time delay results as a function of speed (Figure 3.4.8 (a)) and motion pattern (Figure 3.4.8 (b)). Analysis of the average expert-trainee time delay showed significant main effects on pattern ($p=0.0166$) conditions. A post-hoc analysis showed that subjects had the least amount of time delay when they replicated the motion with the simplest pattern (i.e., pattern 1). However, the pair-wise comparisons between patterns 2, 3, and 4 were not significant.

Table 3.4.2. Statistical analysis results (n=8) for speed (S) and pattern (P). Results for all dependent variables except cross-correlation are expressed on a logarithmic scale.

Dependent variable	Effects	Estimate	Std error	DF	F Value	Pr>F
Cross-correlation	S (1 vs 3)	0.01214	0.00106	2,46	65.15	<0.0001
	S (2 vs 3)	0.0061	0.00106			
Position error	S (1 vs 3)	-0.9461	0.05729	2,46	141.56	<0.0001
	S (2 vs 3)	-0.3128	0.05729			
Time delay	S (1 vs 3)	0.05399	0.07255	2,46	3.12	0.0535
	S (2 vs 3)	0.1769	0.07255			
Cross-correlation	P (1 vs 4)	0.02066	0.00389	3,69	20.53	<0.0001
	P (2 vs 4)	0.00059	0.00389			
	P (3 vs 4)	-0.0088	0.00389			
Position error	P (1 vs 4)	-0.272	0.05587	3,69	16.18	<0.0001
	P (2 vs 4)	-0.1521	0.05587			
	P (3 vs 4)	0.08538	0.05587			
Time delay	P (1 vs 4)	-0.1936	0.07189	3,69	3.65	0.0166
	P (2 vs 4)	0.01347	0.07189			
	P (3 vs 4)	-0.016	0.07189			
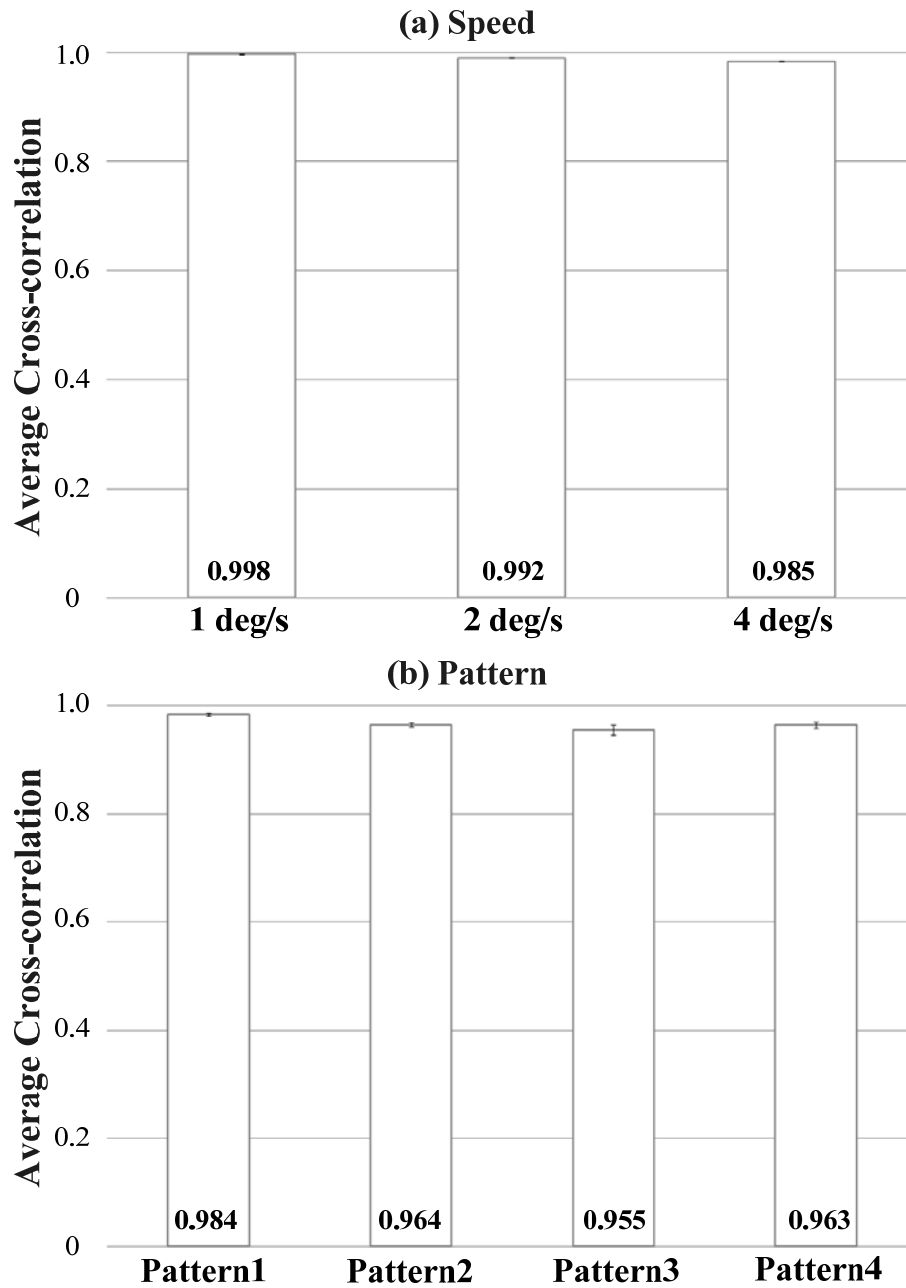
Figure 3.4.6. Average expert-trainee cross-correlation value results as a function of (a) different speed conditions and (b) different pattern conditions. Error bars represent standard error of the mean.
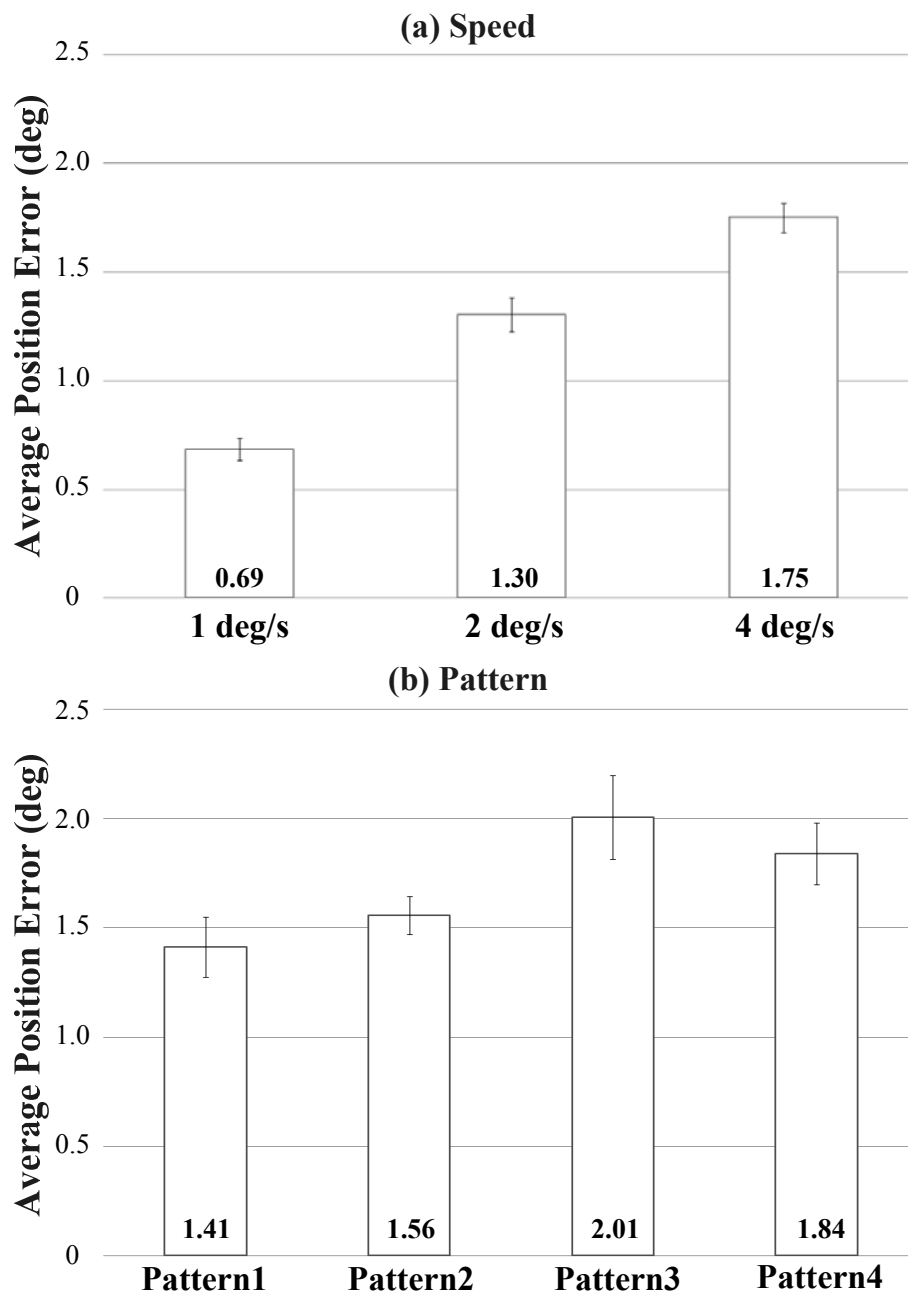
Figure 3.4.7. Average expert-trainee position error results in degrees as a function of (a) different speed conditions and (b) different pattern conditions. Error bars represent standard error of the mean.
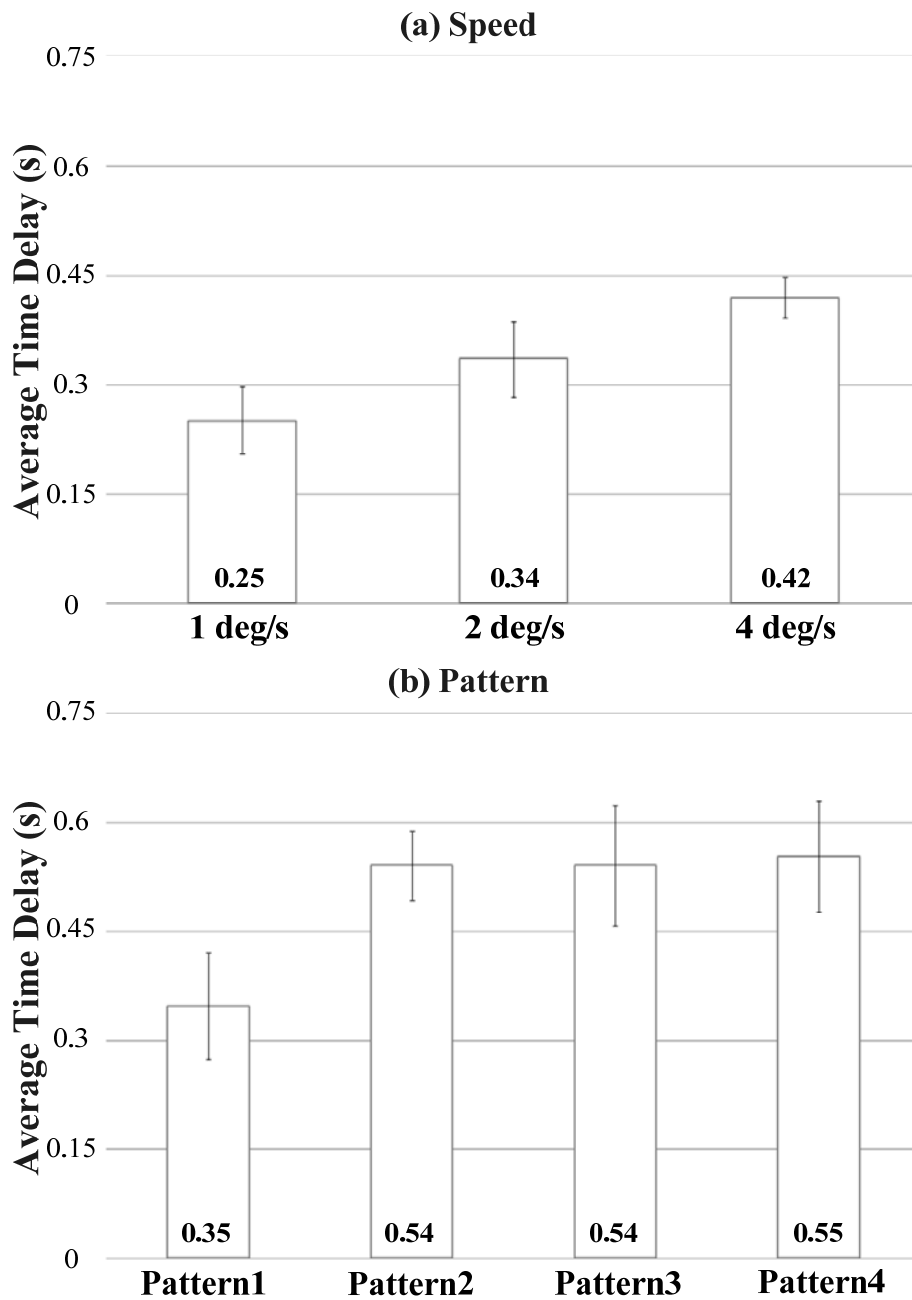
(a) Speed

(b) Pattern

Figure 3.4.8. Average expert-trainee time delay results in degrees as a function of (a) different speed conditions and (b) different pattern conditions. Error bars represent standard error of the mean.

3.4.4. Effects of instructional cues

Figure 3.4.9(a) presents the average position error between expert and subject motion as a function of speed. Analysis of the expert-subject cross-correlation values (cue: $F(1,60)=6.86$, $p=0.011$; speed: $F(2,60)=8.72$, $p<0.001$), position errors (cue: $F(1,60)=33.90$, $p<0.001$; speed: $F(2,60)=59.09$, $p<0.001$), and time delays (cue: $F(1,60)=13.49$, $p=0.001$; speed: $F(2,60)=7.58$, $p=0.001$) showed significant main effects of vibrotactile instructional on cue type and speed. Subjects from both groups had the smallest position errors and time delays and largest cross-correlation values when repulsive cues were provided. Moreover, as motion speed increased, performance decreased. The smallest position errors and largest cross-correlation values occurred when the motion was replicated at the slowest speed. G2 subjects consistently outperformed G1 subjects during this protocol. Four of the six G1 subjects stated a preference for repulsive cuing while four of the six G2 subjects stated a preference for attractive cuing.

Figure 3.4.9 (b) presents the average position error between expert and subject motion as a function of movement pattern. Analysis of the expert-subject cross-correlation values (cue: $F(1,80)=23.78$, $p<0.001$; pattern: $F(3,80)=4.69$, $p=0.005$), position errors (cue: $F(1,80)=47.89$, $p<0.001$; pattern: $F(3,80)=16.32$, $p<0.001$), and time delays (cue: $F(1,80)=51.29$, $p<0.001$; pattern: $F(3,80)=4.27$, $p=0.008$) showed significant main effects of vibrotactile instructional on cue type and pattern. Subjects consistently performed best in terms of minimizing position errors and time delays and maximizing cross-correlation values when repulsive cues were provided during patterns 1, 2, and 3. No differences in

performance were observed when subjects performed pattern 4, which was considered to be the most difficult since it included a short static hold while the other three patterns did not. G2 subjects outperformed G1 subjects for patterns 1-3.
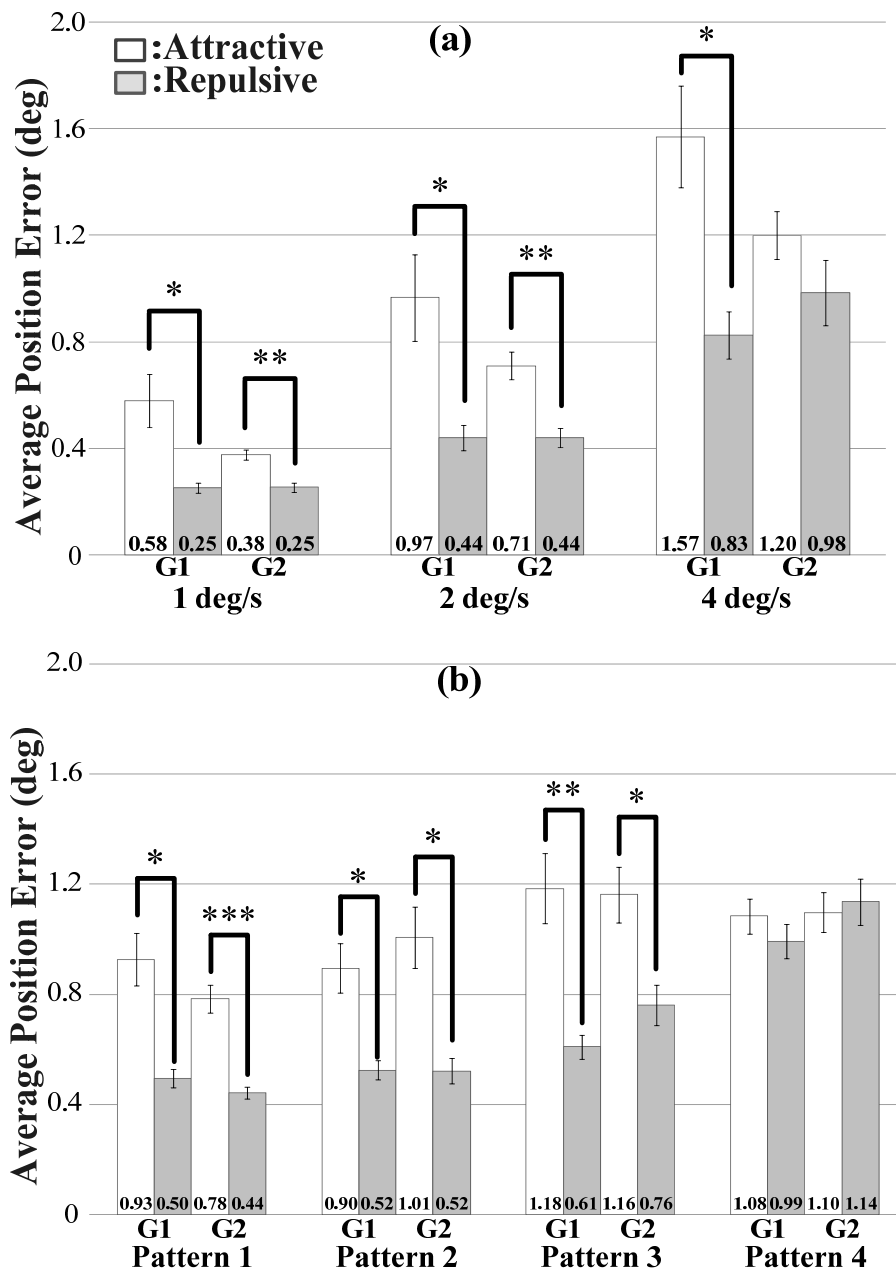
Figure 3.4.9. Average expert-subject position error for each group as a function of (a) protocol 1 motion speed and (b) protocol 2 pattern. White and gray bars represent attractive and repulsive vibrotactile instructional cues, respectively. Error bars represent standard error of the mean (*$p<0.05$, **$p<0.01$, ***$p<0.001$).

Figure 3.4.10 presents the average position error between expert and subject motion as a function of the number of trials performed. Trial order consisted of three practice trials followed by three experimental trials for each of the four patterns of the second protocol while using attractive (Figure 3.4.10(a)) and repulsive (Figure 3.4.10(b)) cuing. Attractive cuing consistently exhibited a greater initial error as well as a greater decrease in error over the course of the trials, suggesting that a longer training/practice time is required for attractive cuing to achieve position error comparable to repulsive cuing.

Table 3.4.3 presents the average position error between expert and subject motion for the four motion patterns delimited by group, preference, and cue type. The G1 subjects who stated a preference for repulsive cuing performed significantly better using repulsive cuing for all patterns.

Table 3.4.3. Average expert-subject position error for the four motion patterns by group (G), preference (P), and cue type (attractive (A), repulsive (R)). *$p < 0.05$.

G	P	Cue	Pattern 1	Pattern 2	Pattern 3	Pattern 4
1 (n=6)	A (n=2)	A	0.48	0.60	0.78	0.64
		R	0.30	0.51	0.40	0.40
	R (n=4)	A	0.85	0.86	0.88	1.01
		R	0.44 *	0.42 *	0.48 *	0.50 *
2 (n=6)	A (n=4)	A	0.56	0.70	0.92	0.99
		R	0.40 *	0.54	0.60	0.75
	R (n=2)	A	0.67	0.85	0.70	0.84
		R	0.18 *	0.33 *	0.49	0.34
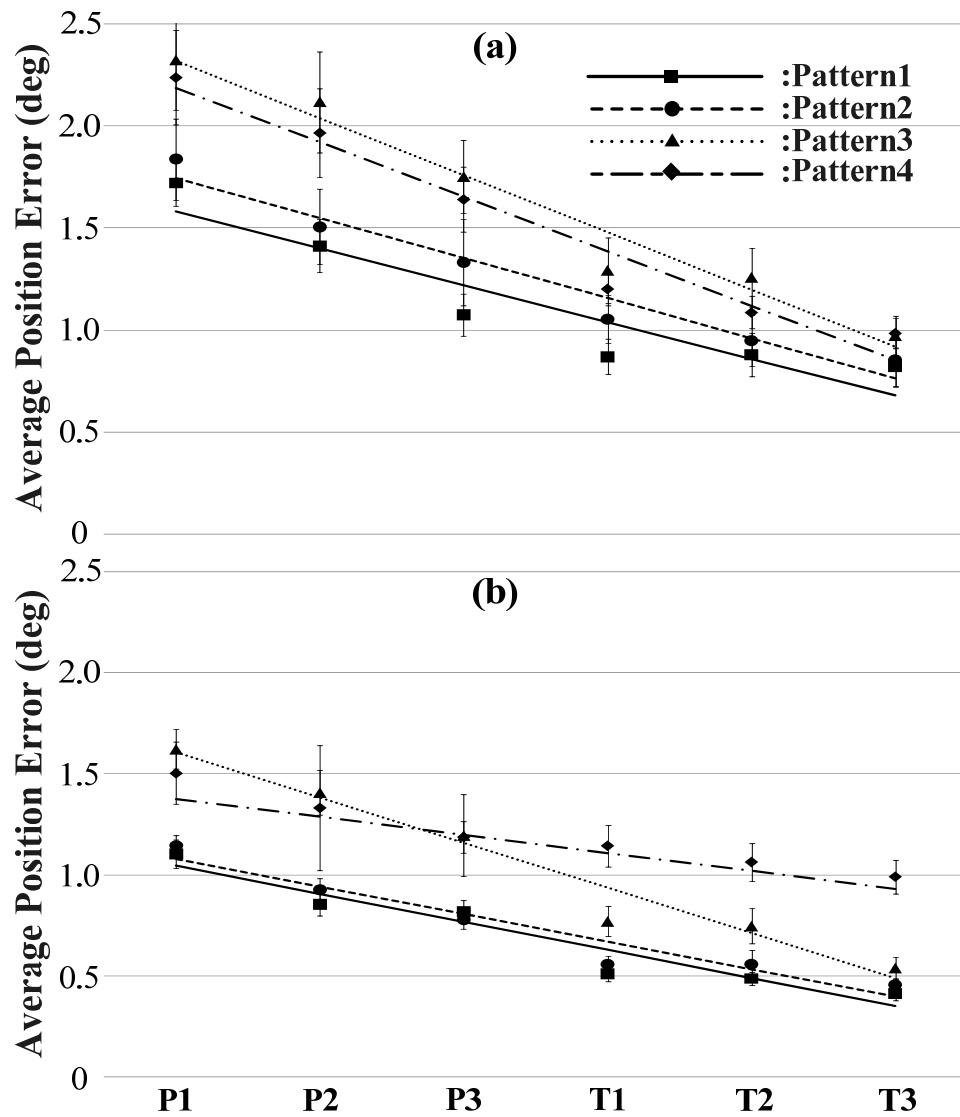
Figure 3.4.10. Average expert-subject tilt error versus trial number for the four patterns of protocol 2 under (a) attractive and (b) repulsive cuing. P and T represent practice and experimental trials, respectively. Error bars represent standard error of the mean.

3.5. Discussion

The first proof-of-concept study conducted in five healthy young adults demonstrated that subjects could accurately mimic the simple task of slowly bending at the waist using attractive vibrotactile instructional cues. The smallest error threshold (0.5°) combined with a proportional plus derivative (PD) control signal resulted in the greatest correlation between the expert and trainee motion, the least amount of time delay, and the least amount of average position error. Subjects showed lower position errors during the static component of the entire movement than during the dynamic (inbound/outbound) components.

The PD control signal consistently produced significantly better motion replication in terms of cross-correlation, time delay, and average position error values compared to the P control signal for all error thresholds. This finding was not unexpected given that there is an inherent delay associated with perceiving, processing, and responding to vibrotactile cues [30]. The inclusion of a rate of change of position term in the control signal effectively reduces the tactor activation threshold limit so that subjects receive information regarding their performance earlier than they would with a proportional-based control signal alone. Based on the average time delay results, the PD control signal decreased the lag in subject motion replication by 0.15 s, 0.34 s, and 0.47 s, for the 0.5°, 1.0°, and 1.5° error thresholds, respectively. In other words, as the error threshold increased, the PD control signal increasingly reduced the time lag compared to the P control signal. It may be possible to achieve equivalent performance using only a P control signal if the threshold limit were further reduced; however, if the limit is too

small, motion will no longer be smooth. The choice of 0.5 ms as the constant weighting factor for the difference between expert and trainee velocity was chosen based on the study of Wall and Kentala [18]; it may be possible to further improve performance by manipulating this weighting factor since it was chosen arbitrarily in their study.

The results of the second study in eight healthy young adults showed that the ability to accurately replicate motion decreased as a function of the motion speed and complexity. Average position error increased as the required speed of the task increased. The slow speed from the first study was included as a control for the second study given that different subjects were involved. The average position error for the slow motion was smaller for the first study subjects compared to the second study subjects. This is likely due to the fact that the first group performed 18 practice trials compared to the three practice trials performed by the second group of subjects.

To date, vibrotactile feedback displays for standing balance [29, 31-32] have used repulsive cues in which subjects are instructed to move away from the vibration. For the first two proof-of-concept studies, an attractive cue was used in which subjects were instructed to move toward the vibration. This decision was based on the results of the study presented in Chapter 2, which showed that tactors placed over the internal oblique and erector spinae muscles resulted in small postural shifts on the order of 1.0° in the direction of the tactor stimulation.

Repulsive vibrotactile instructional cues resulted in the greatest correlation between expert and subject motion, the least amount of time delay, and the least amount of average position error when the motion speed and task complexity were varied. Subject preference for a particular type of cue was dependent on the order of vibrotactile cues

provided; G1 subjects received attractive cues first, but preferred repulsive, while G2 subjects received repulsive cues first, but preferred attractive. This outcome may indicate that subjects were more comfortable with the experimental protocol on the second day of testing. However, subjects' position errors were minimized with repulsive cues even if they indicated a preference for attractive cues. All in all, subjects performed best when using repulsive cues regardless of whether they completed repulsive cuing trials on the first or second day of testing.

Analysis of learning effects suggests that additional training trials beyond those conducted herein are required to reach steady-state performance and draw definitive conclusions as to whether one cuing strategy is better than the other during long-term MIMIC use. However, for short-term applications such as a physical rehabilitation sessions during which training time may be limited, this study suggests that repulsive cues may be preferable. Such cues may be more intuitive because they mimic the light touch of a therapist guiding the patient toward a desired target position.

References

[1]   C. Y. Crooks, J. M. Zumsteg, and K. R. Bell, "Traumatic brain injury: a review of practice management and recent advances," *Physical Medicine & Rehabilitation Clinics of North America* vol. 18, no. 4, pp. 681-710, Nov. 2007.

[2]   F. B. Horak, C. Jones-Rycewicz, F. O. Black, and A. Shumway-Cook, "Effects of vestibular rehabilitation on dizziness and imbalance," *Otolaryngology - Head and Neck Surgery* vol. 106, no. 2, pp. 175-180, Feb. 1992.

[3]   C. D. Mulrow, M. B. Gerety, D. Kanten, J. E. Cornell, L. A. DeNino, L. Chiodo, C. Aguilar, M. B. O'Neil, J. Rosenberg, and R. M. Solis, "A randomized trial of physical rehabilitation for very frail nursing home residents," *Journal of the American Medical Association* vol. 271, no. 7, pp. 519-524, Feb. 1994.

[4]   K. Ones, E. Y. Yalcinkaya, B. C. Toklu, and N. Caglar, "Effects of age, gender, and cognitive, functional and motor status on functional outcomes of stroke rehabilitation," *NeuroRehabilitation,* vol. 25, no. 4, pp. 241-249, Dec. 2009.

[5]   P. M. van Vliet and G. Wulf, "Extrinsic feedback for motor learning after stroke: What is the evidence?," *Disability and Rehabilitation,* vol. 28, no. 13-14, pp. 831-840, Jul. 2006.

[6]   C. J. Winstein, "Knowledge of results and motor learning-implications for physical therapy," *Journal of Physical Therapy,* vol. 71, no. 2, pp. 140-149, Feb. 1991.

[7]   A. Domingo and D. P. Ferris, "Effects of physical guidance on short-term learning of walking on a narrow beam," *Gait & Posture,* vol. 30, no. 4, pp. 464-468, Nov. 2009.

[8]   S. G. Lisberger, "The neural basis for learning of simple motor skills," *Science,* vol. 242, no. 4879, pp. 728-735, Nov. 1988.

[9]   D. E. Rumelhart, G. E. Hinton, and R. J. Williams, "Learning representations by back-propagating errors," *Nature,* vol. 323, no. 6088, pp. 533-536, Oct. 1986.

[10] J. Lieberman and C. Breazeal, "Development of a wearable vibrotactile feedback suit for accelerated human motor learning," in *Conf. Proc. IEEE Int. Conf. Robotics and Automation (ICRA' 09)*, Kobe, Japan, Oct., 2007, pp. 4001-4006.

[11] P. Kapur, S. Premakumar, S. A. Jax, L. J. Buxbaum, A. M. Dawson, and K. J. Kuchenbecker, "Vibrotactile feedback system for intuitive upper-limb rehabilitation," in *Conf. Proc. World Haptics 2009 - Third Joint EuroHaptics conf. and IEEE Inter. Symp. Haptic Interfaces for Virtual Environment and Teleoperator Systems*, Salt Lake City, UT, USA, Mar., 2009, pp. 621-622.

[12] F. Sergi, D. Accoto, D. Campolo, and E. Guglielmelli, "Forearm orientation guidance with a vibrotactile feedback bracelet: On the directionality of tactile motor communication," in *Biomedical Robotics and Biomechatronics, 2008. BioRob 2008. 2nd IEEE RAS & EMBS International Conference on*, Scottsdale, AZ, USA, 2008, pp. 433-438.

[13] J. van der Linden, E. Schoonderwaldt, and J. Bird, "Towards a real-time system for teaching novices correct violin bowing technique," in *Haptic Audio visual Environments and Games, 2009. HAVE 2009. IEEE International Workshop on*, Lecco, Italy, 2009, pp. 81-86.

[14] E. R. Bachmann, Y. Xiaoping, D. McKinney, R. B. McGhee, and M. J. Zyda, "Design and implementation of MARG sensors for 3-DOF orientation measurement of rigid bodies," in *Conf. Proc. IEEE Int. Conf. Robotics and Automation (ICRA' 03)*, Taipei, Taiwan, Sep., 2003, pp. 1171-1178.

116

[15] Z. Rong and Z. Zhaoying, "A real-time articulated human motion tracking using tri-axis inertial/magnetic sensors package," *IEEE Transactions on Neural Systems and Rehabilitation Engineering,* vol. 12, no. 2, pp. 295-302, Jun. 2004.

[16] A. M. Sabatini, C. Martelloni, S. Scapellato, and F. Cavallo, "Assessment of walking features from foot inertial sensing," *IEEE Transactions on Biomedical Engineering,* vol. 52, no. 3, pp. 486-494, Mar. 2005.

[17] M. S. Weinberg, C. Wall, J. Robertsson, E. O'Neil, K. Sienko, and R. Fields, "Tilt determination in MEMS inertial vestibular prosthesis," *Journal of Biomedical Engineering,* vol. 128, no. 6, pp. 943-956, Dec. 2006.

[18] C. Wall and E. Kentala, "Effect of displacement, velocity, and combined vibrotactile tilt feedback on postural control of vestibulopathic subjects," *Journal of Vestibular Research,* vol. 20, no. 1, pp. 61-69, Jan. 2010.

[19] D. A. Ross and B. B. Blasch, "Wearable Interfaces for Orientation and Wayfinding," in *Conf. Proc. 4th international ACM conference on Assistive technologies*, Arlington, VA, USA 2000, pp. 193-200.

[20] J. B. F. Van Erp and H. A. H. C. Van Veen, "Vibro-Tactile Information Presentation in Automobiles," in *EuroHaptics* Birmingham, UK, 2001, pp. 99-104.

[21] H. A. H. C. Van Veen and J. B. F. Van Erp, "Tactile Information Presentation in the Cockpit," in *Haptic Human-Computer Interaction*, Tokyo, Japan 2001, pp. 174-181.

[22] C. Wall, M. S. Weinberg, P. B. Schmidt, and D. E. Krebs, "Balance prosthesis based on micromechanical sensors using vibrotactile feedback of tilt," *IEEE*

Transactions on Biomedical Engineering, vol. 48, no. 10, pp. 1153-1161, Oct. 2001.

[23] G. Eklund, "General features of vibration-induced effects on balance," *Upsala Journal of Medical Sciences,* vol. 77, no. 2, pp. 112-124, 1972.

[24] A. Kavounoudias, R. Roll, and J. P. Roll, "Foot sole and ankle muscle inputs contribute jointly to human erect posture regulation," *Journal of Physiology,* vol. 532, no. Pt 3, pp. 869-878, May. 2001.

[25] O. Oullier, A. Kavounoudias, C. Duclos, F. Albert, J. P. Roll, and R. Roll, "Countering postural posteffects following prolonged exposure to whole-body vibration: a sensorimotor treatment," *European Journal of Applied Physiology,* vol. 105, no. 2, pp. 235-245, Jan. 2009.

[26] D. E. Leader, "Kalman filter estimation of underwater vehicle position and attitude using a doppler velocity aided inertial motion unit," Ph. D., Joint Program in Oceanographic Engineering, Massachusetts Institute of Technology, Boston, Massachusetts, 1994.

[27] J. Vaganay, M. J. Aldon, and A. Fournier, "Mobile robot attitude estimation by fusion of inertial data," in *Robotics and Automation, 1993. Proceedings., 1993 IEEE International Conference on*, Atlanta, Georgia, USA, 1993, pp. 277-282.

[28] A. D. Goodworth, C. Wall, and R. J. Peterka, "Influence of Feedback Parameters on Performance of a Vibrotactile Balance Prosthesis," *IEEE Transactions on Neural Systems and Rehabilitation Engineering,* vol. 17, no. 4, pp. 397-408, Aug. 2009.

[29]   E. Kentala, J. Vivas, and C. Wall, "Reduction of postural sway by use of a vibrotactile balance prosthesis prototype in subjects with vestibular deficits," *The Annals of otology, rhinology, and laryngology,* vol. 112, no. 5, pp. 404-409, May. 2003.

[30]   P. P. Kadkade, B. J. Benda, P. B. Schmidt, and C. Wall, 3rd, "Vibrotactile display coding for a balance prosthesis," *IEEE Transactions on Neural Systems and Rehabilitation Engineering,* vol. 11, no. 4, pp. 392-399, Dec. 2003.

[31]   K. H. Sienko, M. D. Balkwill, L. I. Oddsson, and C. Wall, "Effects of multi-directional vibrotactile feedback on vestibular-deficient postural performance during continuous multi-directional support surface perturbations," *Journal of Vestibular Research,* vol. 18, no. 5-6, pp. 273-285, Jan. 2008.

[32]   C. Wall and E. Kentala, "Control of sway using vibrotactile feedback of body tilt in patients with moderate and severe postural control deficits," *Journal of Vestibular Research,* vol. 15, no. 5-6, pp. 313-325, Apr. 2005.

CHAPTER 4: Modeling and Simulation of the Mobile Instrument for Motion Instruction and Correction (MIMIC)

4.1. Motivation and Objective

Chapter 3 introduced the development of the Mobile Instrument for Motion Instruction and Correction (MIMIC) system and evaluated the effects of varying the nature of the control signal (proportional (P), proportional plus derivative (PD)). The previous study also evaluated the effects of varying the activation error threshold (0.5°, 1.0°, and 1.5°) while the subjects performed a pre-specified trunk bending tasks in the A/P direction. The results from these experiments suggest that the smallest activation threshold (0.5°) combined with a PD control signal results in the lowest average error and highest cross-correlation values. The control signal for the tactor activation in the previous chapter was chosen to be P+0.5D based on previous studies [1-2]. However, a different combination of controller gains might produce even better results.

In a recent study performed by Wall and Kentala, several control signals for a trunk-based vibrotactile feedback device were compared during computerized dynamic

posturography in a population of subjects with vestibular loss [2]. Their findings demonstrated that although all of the evaluated control signals reduced body tilt, the PD control signal produced a significantly smaller body tilt angle when compared to either the P or D feedback control signal alone. Goodworth et al. also investigated the influence of vibrotactile feedback parameters (i.e., P and D gains) on subject performance during continuous support surface perturbations [1]. Their findings were consistent with the findings reported by Wall and Kentala. However, Goodworth et al. reported that no single combination of position and velocity feedback performed significantly better than the others.

The primary goal of this chapter is to determine whether or not there is a particular combination of position and velocity gains that would minimize the average position error and maximize the cross-correlation values for subjects replicating simple motions using a system such as the MIMIC. Identification of the internal body parameters for the neural controller and evaluation of the MIMIC controller gains are accomplished through simulation and optimization. In this study, only the upper body is modeled since subjects only performed the simple task of slowly bending at the waist using the MIMIC system (Chapter 3). The internal body parameters for generating both active and passive torques (exerted by the neural controller) are initially identified by a nonlinear optimization process, coupled with experimental data obtained from the previous chapter. The effects of the P and D gains in the MIMIC controller on performance are evaluated by varying the values of the position and velocity gains. The overall approach and terminology used herein are adapted from the study performed by Goodworth et al. [1].

4.2. Modeling

4.2.1. MIMIC System Model

Figure 4.2.1. shows a schematic representation of the MIMIC system. The MIMIC system model used in this study is based on the "independent channel model" presented by Goodworth et al. [1], which decomposes complex biomechanical systems involved in human postural control into vibrotactile biofeedback (i.e., MIMIC system), sensory, neuromuscular, and body subsystems.
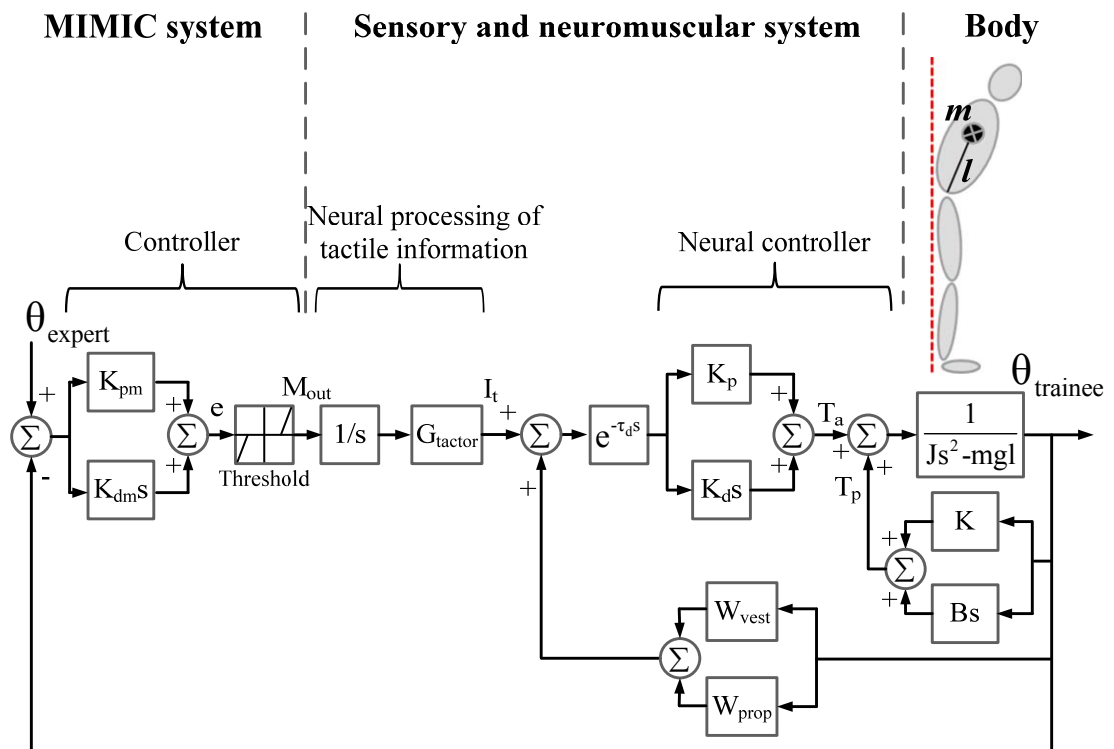
Figure 4.2.1. Block diagram of the MIMIC system model in frequency domain.

The subject's body is represented by a linearized inverted pendulum model, which is

widely used as a simple control system model of human postural control [1, 3-5]. Since the MIMIC system's IMU is only measuring the angular position of the upper body, the inverted pendulum's kinematics represents the motion from the human hip joint to the center-of-mass (COM) of the upper body. Furthermore, the subject's body movement can be numerically described by the differential equation of a single-link inverted pendulum:

$$J\frac{d^2\theta}{dt^2} = mgl\sin(\theta_{trainee}) + T_a \qquad (4.2.1)$$

where J is the upper body moment of inertia about the hip joint axis, m is the mass of the upper body, g is the action of gravity on the COM of the upper body, l is the location of the upper body COM with respect to the hip joint axis, $\theta_{trainee}$ is the angular position of the torso with respect to earth vertical, and T_a is active torque generated from the hip joint, which produces the upper body rotation. In Equation 4.3.1, a nonlinear term (i.e., $\sin(\theta_{trainee})$) is approximated as $\theta_{trainee}$ based on the comparison of two values (i.e., $\sin(\theta_{trainee})$ vs. $\theta_{trainee}$) at 20°, which is the maximum bending angular position given in the experiment with the MIMIC system, presented in Chapter 3. The approximated $\theta_{trainee}$ value at 20° is close to 98% of the $\sin(\theta_{trainee})$ (i.e., $\sin(20°) = 0.342\,rad$ vs. $20°\pi\big/180° = 0.349\,rad$). After making the small angle approximation ($\sin(\theta_{trainee}) \approx \theta_{trainee}$) without significant loss of accuracy and taking the Laplace transform, equation 4.2.1 can be expressed as a transfer function relating

123

$\theta_{trainee}$ to T_a :

$$\frac{\theta_{trainee}(s)}{T_a(s)} = \frac{1}{Js^2 - mgl} \qquad (4.2.2)$$

where s is the Laplace transform variable.

According to this model, the input to the inverted pendulum model (representing the body) is determined from the summation of both active (T_a) and passive (T_p) torques exerted about the hip joint. The active torque is determined by the neural controller and is generated in proportion to the vibrotactile biofeedback signal (I_t), (with a "stiffness" proportionality factor, K_p) and the time derivative of I_t (with a "damping" factor, K_d). This type of controller, commonly used in man-made control systems, is referred to as a proportional and derivative control (PD) controller [1, 3, 5-6]. Data regarding the angular motions of the ankles and knees were not collected. It was assumed that the contributions of the lower body segment movements were minimal. Thus, a corrective (passive) torque that acts without time delay is defined [6-7]. This passive torque contributes to the input of the body model and is assumed to contain both a musculoskeletal stiffness component (K) and damping component (B). The units of these constants, as they are used in Figure 4.3.2, are N·m/deg for K_p and K , and N·m·s/deg for K_d and B , respectively.

τ_d is a time delay that includes sensory transduction, neural processing, transmission, and muscle activation delays [5-6]. The time delay was selected as 100 ms based on previous studies [1, 5-6].

The values for both W_{vest} and W_{prop} were based on an assumption made by Goodworth et al. that the vestibular and proprioceptive systems provide "wide bandwidth orientation information" [1]. Thus, no information about body orientation is lost among vestibular, W_{vest}, and proprioceptive, W_{prop}, inputs and so these gains always sum to 1:

$$W_{vest} + W_{prop} = 1$$

In the MIMIC controller, the differences in both position and velocity between the expert and trainee were used to generate error terms for the proportional plus derivative (PD) control signal described in Chapter 3. If the absolute value of the error signal (e) exceeds the specified expert-trainee error threshold, M_{out} takes on the values of 1 for the anterior direction or -1 for the posterior direction. These values correspond to tactor activation in the anterior and posterior directions, respectively. The central neural processing of M_{out} is represented by a mathematical integration of M_{out} and multiplication by a gain factor, G_{tactor}. The value for G_{tactor} is a proportional gain determined by the length of the time that the tactors are activated. The variable gain for G_{tactor} ranges from 0 to 1 and increases by 0.1 every 100 ms the tactors are activated. If the tactor activation exceeds 1 s, the gain remains at 1. The output (M_{out}) from the

feedback loop of the MIMIC system is used to generate trunk motion through the neural processing of vibrotactile biofeedback, shown in Figure 4.3.2.

Taking the above into account, the overall transfer function for the MIMIC system, sensory and neuromuscular system, and body is given as:

$$\frac{\theta_{\text{trainee}}(s)}{\theta_{\text{expert}}(s)} = \frac{G_{\text{tactor}}\{P_1 s^2 + (P_2 + P_3)s + P_4\}e^{-\tau_d s}}{Js^3 - Bs^2 - (mgl + K)s + (P_6 s^2 + P_7 s + P_8)e^{-\tau_d s}} \qquad (4.2.3)$$

$P_1 = K_d K_{dm}, P_2 = K_d K_{pm}, P_3 = K_p K_{dm}, P_4 = K_p K_{pm}, P_5 = K_p K_d$

$P_6 = G_{\text{tactor}} P_1 - K_d (W_{\text{prop}} + W_{\text{vest}})$

$P_7 = G_{\text{tactor}} (P_2 + P_5) - K_p (W_{\text{prop}} + W_{\text{vest}})$

$P_8 = G_{\text{tactor}} P_4$

4.2.2. Parameter Identification and Simulation Protocol

Internal parameter gains for K_p, K_d, K , and B, which contribute to generating both active and passive muscle torques at the hip joint, were found by a nonlinear optimization process, coupled with experimentally obtained data from Chapter 3. Model data related to mass (m), moment of inertia (J), and height of the center of mass (l) of the upper body were obtained from body measurements of each subject who participated in the preliminary MIMIC evaluation study [8]. The MIMIC controller gains were chosen to be P+0.5D. Furthermore, experimentally obtained data (i.e., θ_{expert} and θ_{trainee}) were used for the parameter identification process. Using the aforementioned experimental data, a constrained nonlinear optimization routine, "fmincon" (Matlab Optimization

Toolbox, The MathWorks, Natick, MA), was utilized to identify the remaining model parameters (i.e., K_p, K_d, K , and B) for each subject. The optimization objective was to find the optimal gains of each parameter that minimize the mean-squared-error (MSE) between the subject's angular position ($\theta_{subject}$) and the model's angular position (θ_{model}) in terms of the desired angular position (θ_{expert}).

$$\min \sum \left\| \theta_{subject} - \theta_{model} \right\|^2 \tag{4.2.4}$$

The parameter identification process is an iterative process used to find the parameters' optimal gain. Thirteen experimental data sets, which showed the slowest A/P trunk movement (approximately 1.12°/s) with the smallest error threshold (0.5°) combined with a P+0.5D control signal, were chosen to determine the optimal values for the model parameters, since the aforementioned conditions resulted in the optimum performance during the A/P trunk motion replication tasks described in Chapter 3. Note that the constant MIMIC controller gains (K_{pm} and K_{dm}) were set to 1.0 and 0.5 ms, respectively. Figure 4.2.2 shows the representative sample data from the parameter identification process for one of the subjects.

After determining the optimal values for K_p, K_d, K , and B, simulations were performed using MATLAB Simulink (The MathWorks, Natick, MA) by varying each K_{pm} and K_{dm} gain, ranging from 0 to 1 with 0.25 intervals, to find the optimal MIMIC

controller gains. Note that the simulated expert motion (θ_{expert}) was identical to the provided expert motion. Both the expert angular position and the angular position resulting from the model simulations were saved for further data analysis.
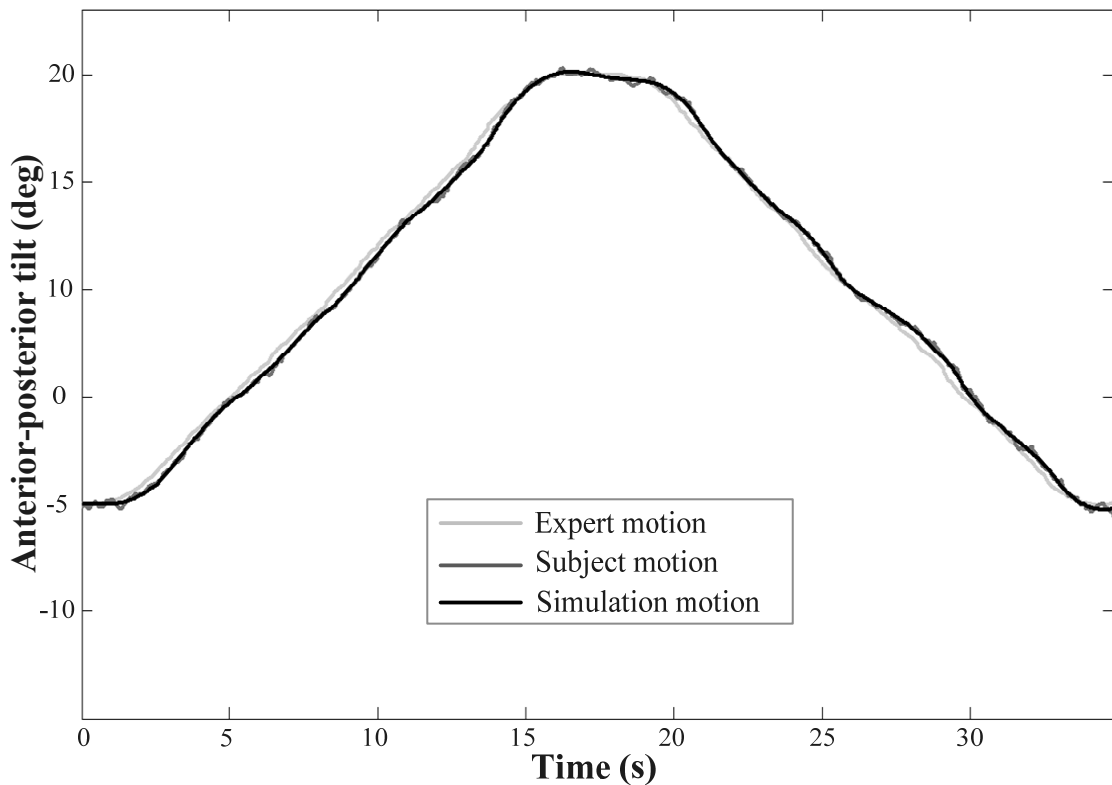
Figure 4.2.2. Representative sample data from one subject after parameter optimization was completed. Light grey, grey, and black lines represent the expert motion, subject motion, and simulation motion, respectively.

4.2.3. Data Analysis Methodologies

All post-processing was performed using MATLAB. Three performance metrics were used to assess the goodness of fit.

The first metric is the absolute position error between the experimental measurement (i.e., subject's A/P motion) and the simulation output for the parameter identification study. This metric also evaluates the goodness of fit between the simulation input (i.e., expert motion) and the simulation output for the optimal MIMIC controller gain study with respect to the change of the MIMIC controller gains (i.e., K_{pm} and K_{dm}).

The second, normalized mean square error (NMSE) is defined as:

$$NMSE = \frac{\sum_{i=1}^{N} \left| f_{m,i} - f_{s,i} \right|^2}{\sum_{i=1}^{N} \left| f_{s,i} \right|^2} \tag{4.2.5}$$

where the indices "*m*" and "*s*" indicate model data and subject's data, respectively. In addition, N represents the length of the measurement vector. Note that the NMSE metric was only used to evaluate the goodness of fit between the simulation output and the experimental measurement (i.e., subject's A/P motion) in the parameter identification study.

The second metric, the crossover frequency (f_c), is defined as the frequency at which the magnitude frequency response crosses the 0 dB axis.

These metrics are based on the crossover model introduced by McRuer [9]. The McRuer model was originally developed to analyze human performance with or without a controller when a human performs a pursuit tracking task by maneuvering a plant (e.g., vehicle or aircraft) [9-12]. The principal idea behind this model is that the human adapts

his behavior to the plant. Hence, he behaves as a 'good servo' in the region of the crossover frequency. As a result, a small absolute position error, a small NMSE, and a large crossover frequency indicate good motion replication performance.

A one-way analysis of variance (ANOVA) was conducted to determine the main effect of the combination of MIMIC controller gains on the dependent variable (i.e., the average position error between the simulation input (i.e., expert motion) and the simulation output). Hypotheses for the main effects of the combination of MIMIC controller gains were tested using an F-test. Post-hoc tests (Tukey Honestly Significant Differences - HSD - for multiple comparisons) were conducted to determine which combinations of the MIMIC controller gains have the largest influence on position error. The level of significance was set at $p < 0.05$. Note that the dependent variable was expressed on a logarithmic scale in order to assure the assumptions of normality and constant variance of residual variance.

4.3. Results

4.3.1. Parameter Identification

Figure 4.3.1 represents the results of the parameter identification process from thirteen subjects' experimental data sets collected in the preliminary evaluation study of the MIMIC system. The average optimal parameters of the model, which are active proportional gain (K_p), active derivative gain (K_d), passive promotional gain (K), and passive derivative gain (B), were 3.48 N·m/deg, 2.00 N·m·s/deg, 1.44 N·m/deg, and

-1.29 N·m·s/deg, respectively, as shown in Figure 4.3.1 (a). Simulation outputs with these optimal model parameters (i.e., K_p, K_d, K, and B), resulted in an average NMSE of 0.019% and position error of 0.43° between the subject's angular position ($\theta_{subject}$) and the model angular position (θ_{model}), respectively, as shown in Figure 4.3.1 (b) and (c).
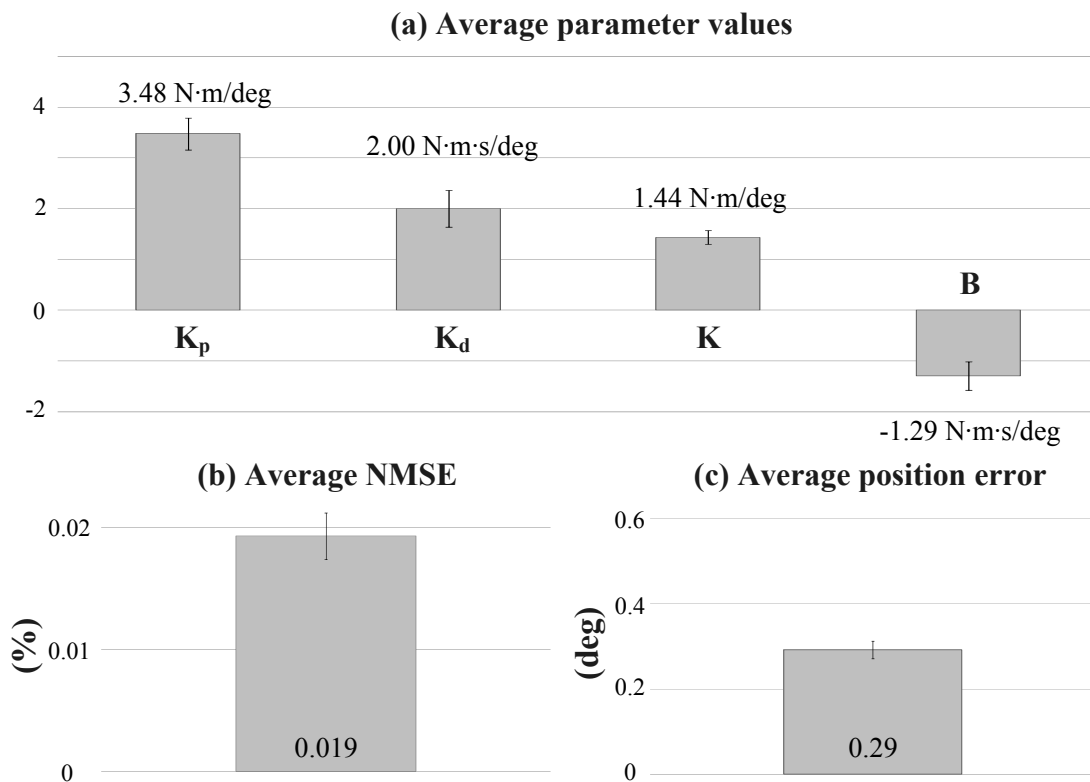
Figure 4.3.1. Parameter identification results (n=13). (a) Average gains of the each parameter. (b) average NMSE between model data and subject's data. (c) average position error between model data and subject's data. Error bars represents standard error of the mean.

Figure 4.3.2 shows the open loop transfer function of the motion replication simulation based on the determined optimal parameters for the model across thirteen subjects. In Figure 4.3.2, the average crossover frequency is observed at 0.78 Hz and the

average crossover frequency range (across all subjects) is 0.43 Hz to 1.87 Hz. Using a method of least squares, a straight line with a slope constrained to -20 dB/dec was fit to the magnitude curves from the frequency domain plots on a subject-by-subject basis, shown as black dash line in Figure 4.3.2 (a). Furthermore, gain and phase margins were derived from the open-loop transfer function of the model. Average values of gain and phase margin were 8.07 dB and 33.53°, respectively. Note that either a negative gain margin or phase margin implies instability, and that a combination of larger positive gain and phase margins suggests a more robust system in general.
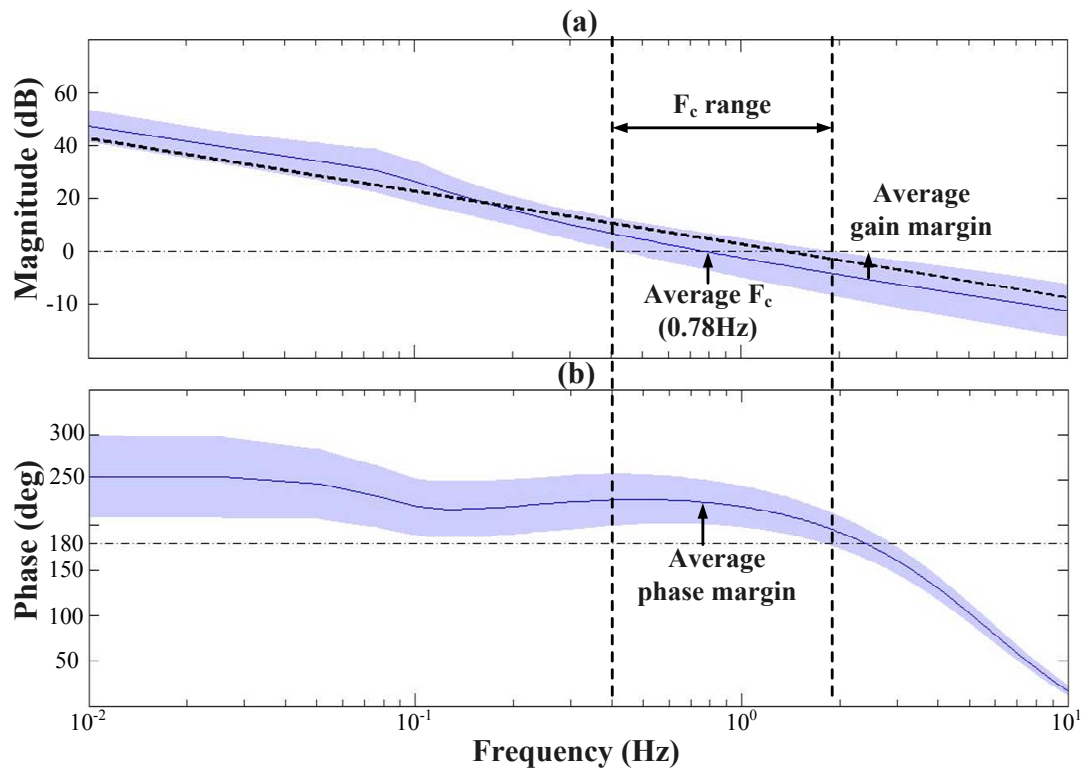
Figure 4.3.2. Open loop transfer function of the motion replication simulation (n=13). (a) magnitude frequency response plot. (b) phase frequency response plot. Shaded areas represent standard deviation of each metric, magnitude and phase, and solid lines indicate average values of each metric.

4.3.2. Optimal MIMIC Controller Gains

Figure 4.3.3 shows the representative simulation results in terms of the variation of D gains. Note that the expert motion is identical to the slowest A/P trunk movement (approximately 1.12°/s) described in Chapter 3.
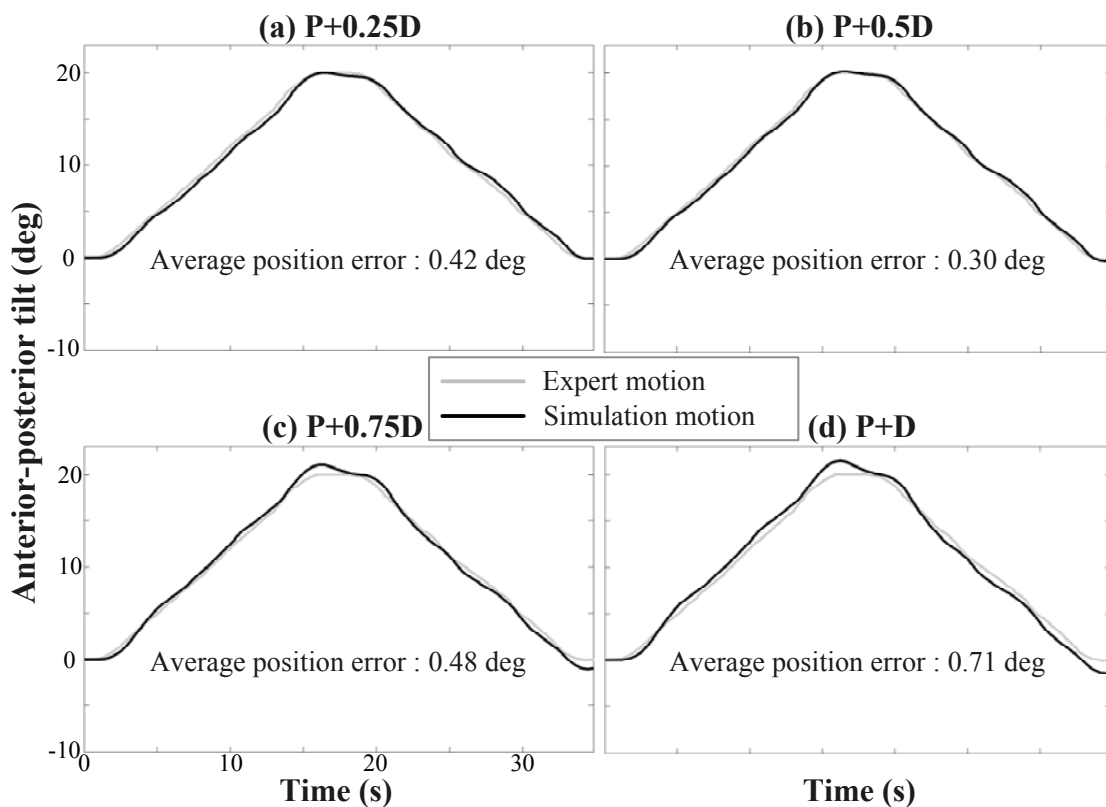
Figure 4.3.3. Representative simulation results in terms of the variation of D gain. Light grey and black lines represent the expert motion and simulation motion, respectively. (a) P+0.25D control signal. (b) P+0.5D control signal. (c) P+0.75D control signal. (d) P+D control signal.

Figure 4.3.4 depicts exemplary simulation results of the average expert-simulation position error for the entire movement with respect to the variation of D gain. Analysis of the position error of the expert-simulation movement showed a significant main effect of

133

the control signal condition ($F(23,288)=9.01$, $p<0.0001$). A post-hoc analysis showed that the smallest average position error (0.39°) was achieved with the use of the P+0.5D control signal (best control signal group). The 0.75P+1.0D (0.44°) and P+0.25D (0.47°) control signals (2nd best control signal group) produced the second smallest average position errors. Furthermore, the third smallest average position error was observed with the 1.0P (0.53°), 0.75P+0.75D (0.51°), and P+0.75D (0.52°) control signals (3rd best control signal group). Note that significant differences in average position errors between/across control signals within each group were not observed.
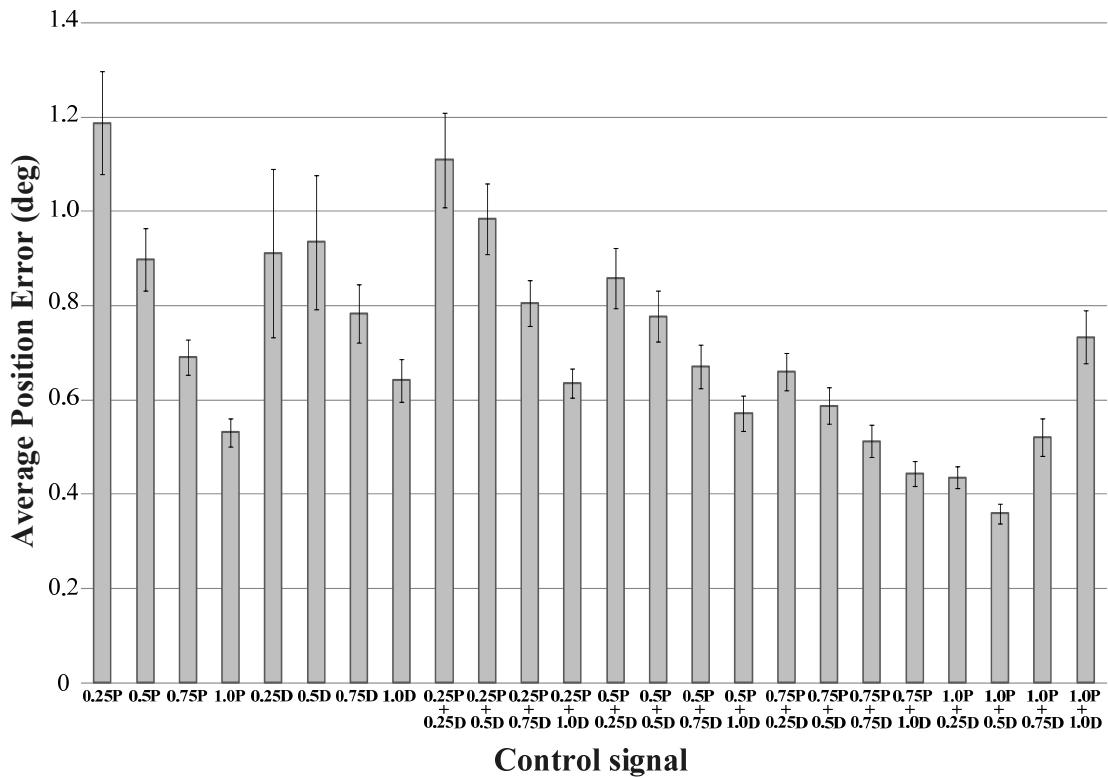
Figure 4.3.4. Average expert-simulation position error results (n=13) in degrees as a function of the control signal. Error bars represent standard error of the mean.

Figure 4.3.5 represents the box plot of crossover frequencies as a function of the top three control signal groups determined from the average expert-simulation position error analysis, shown in Figure 4.3.4.
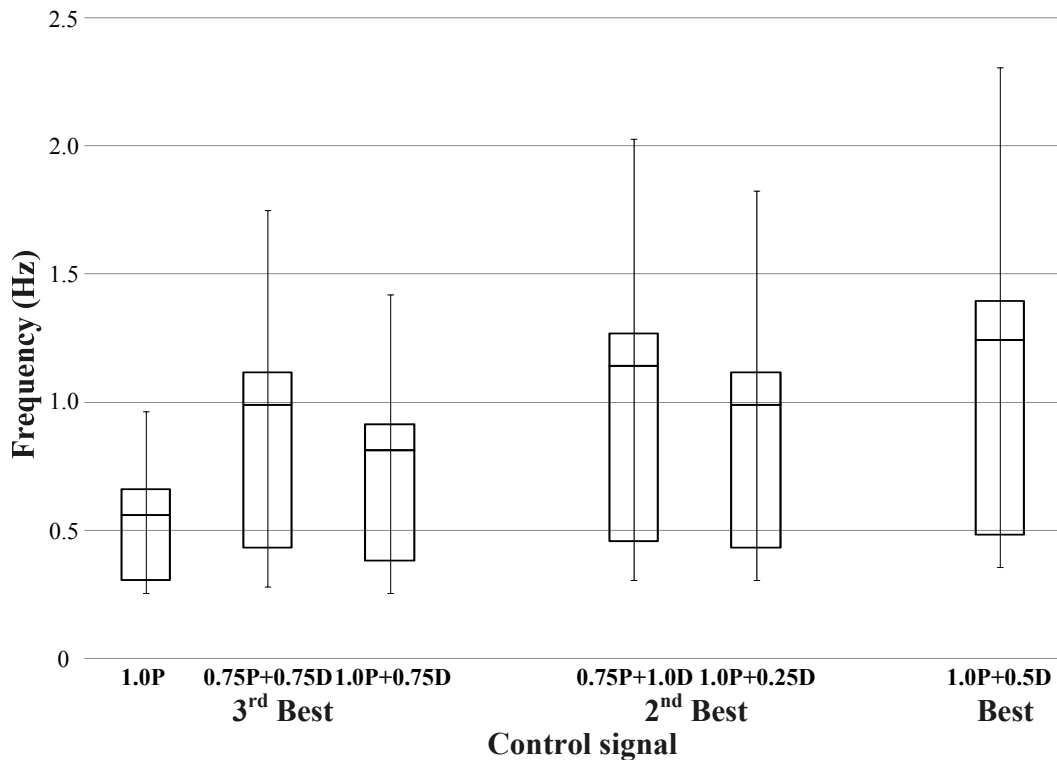
Figure 4.3.5. Box plot of crossover frequencies as a function of top three control signal groups across the thirteen subjects.

Frequency ranges of the 1.0P, 0.75P+0.75D, and P+0.75D control signals were 0.25~0.96 Hz with a mean value of 0.52, 0.28~1.75 Hz with a mean value of 0.85, and 0.25~1.42 Hz with a mean value of 0.70, respectively. In the second best performing group, frequency ranges of the 0.75P+1.0D and P+0.25D control signals were 0.30~2.03 Hz with a mean value of 0.97 and 0.30~2.31 Hz with a mean value of 0.86, respectively.

Furthermore, the frequency range for the best control signal (i.e., P+0.5D) was 0.36~2.31 Hz with a mean value of 1.06. However, analysis of the crossover frequency of the open loop transfer function did not show any main effect of control signal ($F(5,78)=2.17$, $p=0.067$) conditions.

4.4. Discussion

This chapter has shown how model-based simulation can be used to determine the controller gains for K_{pm} and K_{dm} in the MIMIC system. Independent model components, which indicate MIMIC, sensory, neuromuscular, and body subsystems, were adapted based on careful consideration of their contributions during the trunk bend motion replication task. Based on the results of the parameter identification test, the simulated angular position was well matched with the subject's angular position, producing a 0.02% NMSE and 0.43° position error across the thirteen subjects in Chapter 3. From the simulation results, active and passive torque were approximately less than 20 Nm. These values are consistent with previously reported values from studies involving human postural responses to support surface translations and during the performance of voluntary forward bending tasks [13-14]. Based on the McRuer crossover analysis, it was observed that high gains below the crossover frequency support good tracking performance of slower components of given the expert motion [10]. In addition, observed low gains beyond the crossover frequency guarantee good tracking performance by suppressing high frequency oscillation [10]. Furthermore, positive average gain and

phase margins from the open-loop system analysis suggest that the MIMIC system promotes smooth motion replication behaviors in subjects.

The PD control signal produced smaller average position errors compared to either the P or D control signals alone. This finding also confirms the results of the experimental data in Chapter 3. This finding was expected given the inclusion of velocity information (i.e., the D control signal) in the simulation, which effectively reduces the tactor activation threshold limit and leads to the CNS receiving information regarding performance of the motion replication task earlier than it would with the P control signal [2]. However, a higher D gain, combined with the unit P gain, results in larger position errors compared with the P+0.5D control signal. This means that the high D gain can produce excessive oscillatory movements. In addition, the results suggest that other combinations of gains (e.g., 0.75P+1.0D or P+0.25D) could also be used for the trunk bend motion replication task.

However, there are several limitations to this study. The model did not capture lower limb contributions to the trunk bend movement. The simulation was conducted using an inverted pendulum that only represented the upper body, even though multiple-body segments are generally involved in the generation of human motion. Furthermore, the study for deciding the optimal controller gain was limited to position and velocity gains. The future work on the modeling and simulation of the MIMIC controller might include using various body segments and reference movements in order to enhance the usability of the MIMIC system in balance rehabilitation exercises. Additionally, finding the optimal controller gains may be performed with the addition of acceleration (suggested

by Loughlin et al. [15]) or predictive information (suggested by Wall and Kentala [2]) in order to develop a MIMIC controller with higher fidelity.

References

[1]   A. D. Goodworth, C. Wall, and R. J. Peterka, "Influence of Feedback Parameters on Performance of a Vibrotactile Balance Prosthesis," *IEEE Transactions on Neural Systems and Rehabilitation Engineering,* vol. 17, no. 4, pp. 397-408, Aug. 2009.

[2]   C. Wall and E. Kentala, "Effect of displacement, velocity, and combined vibrotactile tilt feedback on postural control of vestibulopathic subjects," *Journal of Vestibular Research,* vol. 20, no. 1, pp. 61-69, Jan. 2010.

[3]   R. Johansson, M. Magnusson, and M. Akesson, "Identification of human postural dynamics," *IEEE Transactions on Biomedical Engineering,* vol. 35, no. 10, pp. 858-869, Oct. 1988.

[4]   R. J. Peterka, "Postural control model interpretation of stabilogram diffusion analysis," *Biological Cybernetics,* vol. 82, no. 4, pp. 335-343, Apr. 2000.

[5]   K. Masani, A. H. Vette, and M. R. Popovic, "Controlling balance during quiet standing: proportional and derivative controller generates preceding motor command to body sway position observed in experiments.," *Gait & Posture,* vol. 23, no. 2, pp. 164-172, Feb. 2006.

[6]   R. J. Peterka, "Sensorimotor Integration in human postural control," *Journal of Neurophysiology,* vol. 88, no. 3, pp. 1097-1118, Sep. 2002.

[7]   R. J. Peterka, "Simplifying the complexities of maintaining balance," *IEEE Engineering in Medicine and Biology Magazine,* vol. 22, no. 2, pp. 63-68, Mar/Apr. 2003.

[8]   D. A. Winter, *Biomechanics and motor control of human movement*, 2nd ed.: Wiley-Interscience, 1990.

[9]   D. T. McRuer and H. R. Jex, "A Review of Quasi-Linear Pilot Models," *IEEE Transactions on Human Factors in Electronics* vol. HFE-8, no. 3, pp. 231-249, Sep. 1967.

[10]   R. B. Gillespie and S. Sovenyi, "Model-based cancellation of biodynamic feedthrough using a force-reflecting joystick " *ASME Journal of Dynamic Systems, Measurement, and Control,* vol. 128, no. 1, pp. 94-103, Mar. 2006.

[11]   D. Feth, R. Groten, A. Peer, and M. Buss, "Control-theoretic model of haptic human-human interaction in a pursuit tracking task," in *The 18th IEEE International Symposium on Robot and Human Interactive Communication (RO-MAN' 09)*, Sept/Oct., 2009, pp. 1106-1111.

[12]   S. Soveyni and R. B. Gillespie, "Cancellation of Biodynamic Feedthrough in Vehicle Control Tasks," *IEEE Transactions on Control Systems Technology,* vol. 15, no. 6, pp. 1018-1029, Nov. 2007.

[13]   A. V. Alexandrov, A. A. Frolov, and J. Massion, "Biomechanical analysis of movement strategies in human forward trunk bending. II. Experimental study," *Biological Cybernetics,* vol. 84, no. 6, pp. 435-43, Jun. 2001.

[14] G. A. Mirka and W. S. Marras, "A stochastic model of trunk muscle coactivation during trunk bending," *Spine (Phila Pa 1976),* vol. 18, no. 11, pp. 1396-1409, Sep. 1993.

[15] P. Loughlin, A. Mahboobin, and J. Furman, "Designing vibrotactile balance feedback for desired body wway reductions," in *Ann. Int. Conf. of the IEEE Engineering in Medicine and Biology Society (EMBC '11)*, 2011, pp. 1310-1313.

CHAPTER 5: Cell Phone Based Balance Trainer

5.1. Abstract

A cell phone based vibrotactile feedback system has been designed and developed for potential use in balance rehabilitation training in clinical and home environments. It comprises an iPhone with an embedded tri-axial linear accelerometer, custom software to estimate trunk tilt, a "tactor bud" accessory that plugs into the headphone jack to provide vibrotactile cues of trunk tilt, a small external controller to translate the audio signals from the iPhone into vibrotactile cues, and a battery. Five young healthy subjects (24 ± 2.8 yrs, 3 females and 2 males) and four subjects with vestibular involvement (42.25 ± 13.5 yrs, 2 females and 2 males) participated in a proof-of-concept study to evaluate the effectiveness of the system. Healthy subjects used the system with eyes closed during Romberg, semi-tandem Romberg, and tandem Romberg stances. Subjects with vestibular involvement used the system with both eyes-open and eyes-closed conditions during semi-tandem Romberg stance. Vibrotactile feedback was provided when the subject exceeded either an anterior-posterior (A/P) or a medial-lateral (M/L) trunk sway threshold. Subjects were instructed to move away from the vibration. The system was

capable of providing real-time vibrotactile cues that informed corrective trunk tilt responses. When feedback was available, both healthy subjects and those with vestibular involvement significantly reduced their A/P or M/L RMS trunk sway (depending on the direction of feedback), had significantly smaller elliptical area fits to their sway trajectory, spent a significantly greater mean percentage time within the no feedback zone, and showed a significantly greater A/P or M/L mean power frequency. The results suggest users can use the real-time feedback provided by this system to reduce their trunk sway. Its advantages over more complex laboratory-based and commercial balance training systems in terms of cost, size, weight, functionality, flexibility, and accessibility make it a good candidate for further home-based balance training evaluation.

5.2. Motivation and objective

Balance disorders increase the risk of non-fatal and fatal falls, leading to direct medical costs of approximately 19 billion USD annually [1]. Among the treatments available for balance disorders, physical balance rehabilitation has the advantage of being non-invasive while providing interventions that can be tailored to patient's specific needs. These clinical balance rehabilitation programs are designed to recover, retrain, or develop new sensorimotor strategies, in order to facilitate functional mobility, decrease dizziness, and re-establish effective coordination [2-4]. Rehabilitation programs that incorporate motor, sensory, and cognitive systems are more effective than muscular training alone in reducing balance and coordination deficits [5-6].

Post-treatment, patients are instructed to continue exercises on their own at home, but lack of expert feedback has been shown to limit improvement, causes a loss in motivation, and eventually leads to exercise discontinuation [7-9]. In addition, compliance decreases over time due to a lack of proper instruction (i.e., feedback on the appropriateness of exercise movements) and consequent loss of motivation due to the absence of feedback from physical therapy aids [8]. Furthermore, practical considerations (e.g., financial, patient schedule, or therapist load) constrain the number of training sessions that can be performed in a clinical setting under expert supervision.

Augmented/substituted sensory biofeedback is a technique currently being explored as a means of supplementing/replacing compromised sensory information during rehabilitation in order to retrain sensorimotor functions [10]. In the clinical setting, balance rehabilitation training incorporating biofeedback has been accomplished by providing visual displays [11-14], auditory tones [15-18], and/or tactile stimulations [19-31], which include surface electrode stimulation of the vestibular nerve (i.e., galvanic vestibular stimulation) [21, 23, 26, 31], electric currents applied to the tongue [19-20, 27-28], or vibration applied to the body segment [22, 24-25, 29-30]. Existing biofeedback systems employing sophisticated inertial or center-of-pressure measurement devices [32-33], complex and high-resolution arrays of vibrating actuators (tactors) or electrodes [25, 34], and estimation algorithms for capturing body tilt [35] have been investigated for the purpose of task-oriented training in neuromotor rehabilitation [10].

Among these various biofeedback modalities, vibrotactile feedback has the advantage of discreetly providing motion cues that may not interfere with a person's activities of daily living (e.g., hearing or speaking). Vibrotactile feedback displays can be co-located

143

with the inertial measurement units (IMUs) used to detect the kinematics of a particular body segment, thereby providing more intuitive operation [36]. While positioning these components on the trunk offers less spatial resolution and increased reaction times compared to locations on the tongue, head, or finger [37], trunk positioning offers a significant advantage for rehabilitation purposes, since it maps directly to the body segment that primarily dictates the location of the center-of-mass with respect to the base-of-support. We have previously shown that real-time trunk-based vibrotactile feedback significantly decreases postural sway during multidirectional perturbed stances in individuals with vestibular involvement [25] and during normal and semi-tandem Romberg stances in older adults [38-39].

In their current laboratory-based form, vibrotactile device technologies are impractical for use in home rehabilitation training regimens due to their size, weight, complexity, calibration procedures, cost (due to high-performance IMUs and computational processors), and fragility. Very recently, commercial balance training systems have become commercially available [40-41]. The BalanceFreedom™ [40] measures angular deviations and angular velocities of the trunk and provides auditory, vibrotactile, and visual cues through a headband. The VertiGuard® RT [41] is a vibrotactile feedback system that measures body sway and provides vibrotactile cues on the trunk with an intensity proportional to the magnitude of body sway in the direction corresponding to/ associated with a tactor.

Both the BalanceFreedom™ and VertiGuard® RT systems were developed in order to improve patients' balance stability during stance and gait in the clinical environment. However, wider use of vibrotactile feedback for balance rehabilitation can be achieved by

taking advantage of technologies already widespread. Smartphones in particular stand out for this purpose, as they feature increasingly powerful microprocessors, considerable memory capacity, large screens, open source operating systems, tri-axial accelerometers, and high-resolution video, making them ideal candidates for easily programmable and customizable balance feedback. Supplying vibrotactile balance training through a smartphone obviates the need to purchase and carry a dedicated system (such as BalanceFreedom™ or VertiGuard® RT) for those within the rapidly-expanding smartphone market, which is projected to reach 1 billion users by 2014 [42]. Furthermore, smartphones offer features that dedicated vibrotactile feedback systems do not, such as the ability to wirelessly communicate with a hospital or therapist through internet or Bluetooth data connections, the support of a large programming community, and the ability to integrate balance training into a larger suite of smartphone-based medical applications that include real-time monitoring of physiological signals such as blood pressure [43], body temperature [44], and heart rate [45-46].

Recognizing the potential advantages in terms of increased functionality and improved access for at-home physical rehabilitation, this chapter presents design, development, and assessment of a low-cost, small, lightweight, easy-to-use, cell phone-based vibrotactile feedback system for balance rehabilitation training. The primary goal of this study is to develop an effective system that can be used in the home to assist a patient with therapist-assigned balance exercises or in an environment where access to balance therapy is limited (i.e., rural regions in the developing world, where health care access is difficult but cell phone networks are increasingly prevalent [47]). In what follows, this chapter will 1) describe the hardware and software design, 2) quantitatively assess the

effectiveness of the proposed system in young healthy subjects and subjects with vestibular involvement, and 3) discuss the potential applications of this technology to clinical and home-based balance rehabilitation training.

5.3. Methods

5.3.1. Hardware design

Figure 5.3.1 shows the prototype of a cell phone-based balance training system. The hardware accessory referred to as a "tactor bud", which plugs into and receives sinusoidal signals from the cell phone audio jack was developed to provide a vibrotactile feedback. The tactor bud consists of a controller, a battery, and two tactors as shown in Figure 5.3.1. Note that the tactor bud is much smaller and much lower in cost than the dedicated vibrotactile systems discussed above. The controller is composed of a microcontroller unit (MCU) (ATMEL, ATmega 32), quad operational amplifier (MC33204), and two band-pass filters with frequency bandwidths of 100–600 Hz and 1.9–3.0 kHz, respectively. The controller detects the frequency of the cell phone generated sine wave (either 250 Hz or 2 kHz) and provides a 3.0 V DC voltage signal to drive a selected tactor based on which cell phone generated sine wave is detected. All controller functions are managed by the MCU, which provides acceptable computational performance (each command is executed at a frequency of 16 MHz) with minimal power consumption at a low cost (less than $20 / MCU).

146
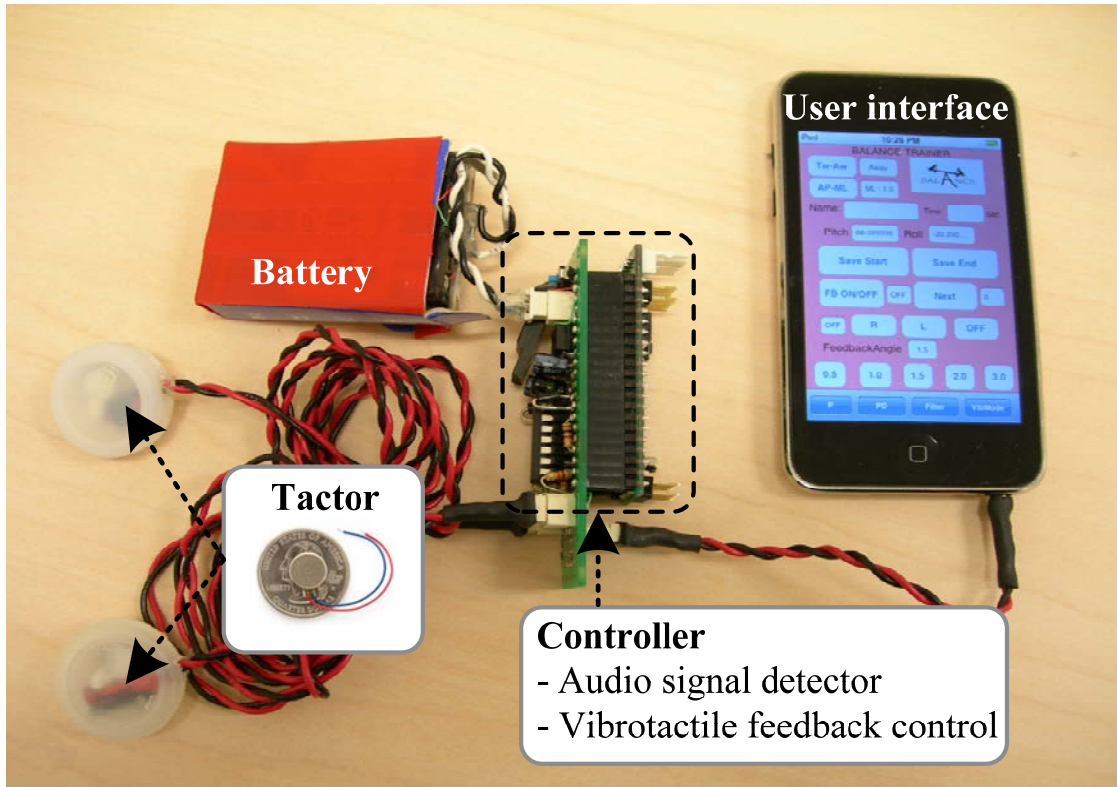
Figure 5.3.1. Prototype of cell phone based balance trainer.

The choice of tactor was based on a number of design considerations including availability, size, weight, power consumption, cost, and signal strength as perceived by the user. While previous studies demonstrated balance improvements in healthy subjects, older adults, and patients with vestibular involvement using laboratory-based vibrotactile feedback systems that employ C2 and Tactaid tactors [25, 30, 38, 48-49], the high power consumption and cost of these tactors make them less suited for mobile battery-powered applications. Consequently, the tactor was chosen to be small, low-power, and coin-style (Samsung Electro-Mechanics, DMJBRK30O, $4 each) actuated via eccentric mass pager motors with rotation speed that vary as a function of the DC voltage input. These round tactors each have a diameter of 10 mm, weight of 1.2 grams, operation range of 2.5 V to

3.5 V at 65 mA, vibration frequency of 200 Hz at 3.0 V, and spin-up time to reach maximum rotational velocity of approximately 90 ms. Since they can be actuated by DC voltage alone, no complex controllers are required for signal generation. In order to create a larger skin contact area, 25mm diameter plastic caps was used to house each tactor.

5.3.2. Cell phone platform and software algorithm

For our initial design we sought to develop a cell phone platform that provided real-time operation, simple setup and use by the programmer and end user, integrated motion sensing, and the ability to save training data for subsequent performance analysis. Therefore, the iPhone (Apple, Inc. iPhone 3GS) was chosen for this purpose, as it includes a built-in tri-axial linear accelerometer (STMicoelectronics, LIS302DL), an adequately powerful microprocessor (ARM Cortex A8, 600 MHz), substantial memory capacity (16 GB storage), a touch screen interface (3.5 inches with 320 x 480 pixels), and a software development toolkit (SDK) provided by Apple, Inc. [50]. Mounted on the waist via an elastic belt, the phone was used to measure trunk acceleration, estimate both A/P and M/L trunk tilt, provide tactor activation commands to the "tactor bud" vibrotactile stimulation hardware, and store body tilt data as well as vibration onset and duration for later performance analysis.

Tilt estimates were computed using an Euler-angle-based extended Kalman filter (EKF) described in detail in Appendix B.2. However, the two state variables (i.e., roll and pitch angular velocities) are calculated from time derivatives of the roll and pitch angular

positions. The EKF can typically be applied to nonlinear systems with additive white noise (i.e., measurement noise) by continually updating around the previous state estimate, starting with an initial guess [51]. In order to quantify measurement noise and drift, the phone (containing the tri-axial linear accelerometer sensor) was placed on a vibration isolated optical table for an extended period of time.

Figure 5.3.2 shows a flow chart of the software architecture implemented in the cell phone platform. If the trunk tilt angle estimated by the EKF surpassed a preset positive angle limit with respect to the vertical, a 250 Hz sine wave was transmitted to the tactor bud through the iPhone's audio output jack. Similarly, if the estimated body tilt angle was less than the negative angle limit with respect to the vertical, a 2 kHz sine wave was transmitted. The generated sine waves were detected by the audio signal detector in the tactor bud hardware controller, which activated the proper tactor based on the sine wave frequency. The update rate from sensing to displaying vibrotactile feedback was nominally 50 Hz.
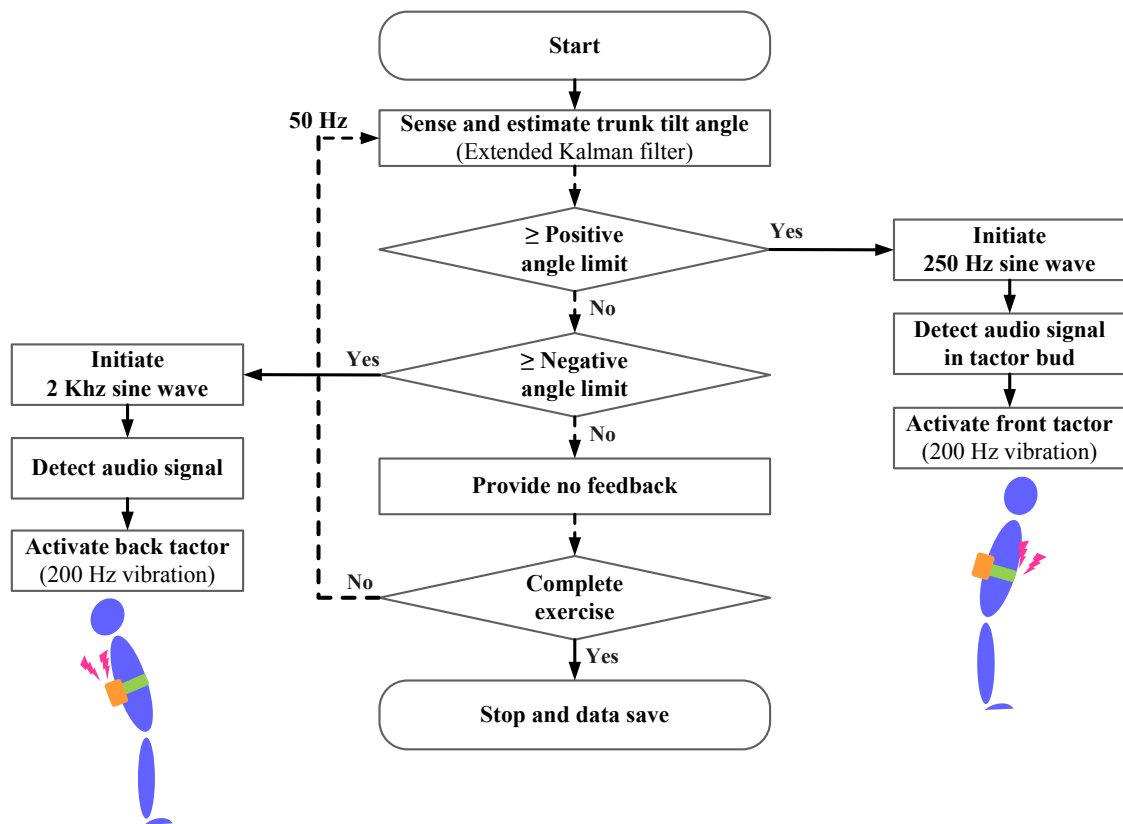
Figure 5.3.2. Software architecture flow chart.

5.3.3. Subjects

Five young (24 ± 2.8 yrs) healthy naïve subjects (3 female, 2 male) and four subjects (2 female, 2 male) with vestibular involvement (42.2±13.5 yrs) participated in this proof-of-concept study. Three of this latter group were patients with unilateral vestibular deficits, and one had bilateral vestibulopathy. Patients were eligible to participate in this study if they had a diagnosed peripheral vestibular impairment, caloric weakness of 25% or greater on either side, and recommendation by a physical therapist for balance

rehabilitation. Subjects with vestibular involvement were excluded if they had severe visual impairment, history of fainting, idiopathic vestibulopathies, or neurological disease affecting balance (e.g., Parkinson's). The University of Michigan Institutional Review Boards approved the experimental protocol, which conformed to the Helsinki Declaration. Informed consent was obtained from each subject prior to the start of the experiment.

5.3.4. Experimental protocol

Both subject groups were instrumented with the cell phone based balance trainer. Healthy subjects were tested using three different stance conditions: Romberg, semi-tandem Romberg, and tandem Romberg stance [52]. For the Romberg stance condition, tactors were placed on the trunk midline (navel and spine) at approximately the L4/L5 vertebrae level. For the semi-tandem Romberg and tandem Romberg stance conditions, tactors were placed on the medial and lateral sides of the trunk at approximately the L4/L5 vertebrae level. Both subject groups were instructed to move away from a vibrotactile cue until the vibration stopped [24-25, 29]. The angle limit (i.e., dead zone) that dictated the onset of vibrotactile feedback was selected as 1.0° in the A/P direction for Romberg stance, 1.0° in the M/L direction for semi-tandem Romberg stance, and 1.5° in the M/L direction for Romberg stance.

Each subject performed practice trials for each stance condition before the experimental protocol began. Each practice trial consisted of a 40 s balance task followed by a 20 s break. Healthy subjects performed 12 practice trials (~15 min. total) with their eyes closed for each stance condition, including 10 trials with vibrotactile feedback and

two trials without vibrotactile feedback. Subjects with vestibular involvement participated in a separate study involving a lab-based vibrotactile feedback system immediately before completing the cell phone study and consequently were well acquainted with the challenging nature of the tandem Romberg stance both in the presence and in the absence of vibrotactile feedback.

For both subject groups, the experimental protocol comprised eight separate trials consisting of two trials without vibrotactile feedback, followed by four trials with vibrotactile feedback, followed by two trials without vibrotactile feedback. Healthy subjects were instructed to keep their eyes closed and arms crossed over their chest during all three stance conditions. The subjects with vestibular involvement were tested using only the semi-tandem Romberg stance, with their arms crossed over their chest during both the eyes open and eyes closed conditions, as the tandem Romberg stance proved too challenging to perform. The study team assisted all subjects with both donning and operating the cell phone system.

Following the completion of the experimental protocol, each subject answered a six-question comparative Likert scale survey (strongly disagree (1), disagree (2), neither disagree nor agree (3), agree (4), or strongly agree (5)) which assessed the subject's preference for the device, balance confidence, and impression of the system's intuitiveness. The survey questions were: Q1) My body was more stable when feedback was available than when it was not available, Q2) The feedback did not distract me from performing the given balance task, Q3) When the feedback was available, I felt more confident in my ability to maintain my balance during the given balance task, Q4) I could use this type of feedback at home by myself if I was given the appropriate equipment, Q5)

I understood how to use the feedback, and Q6) I would prefer to use no feedback rather than use this type of feedback.

5.3.5. Data analysis

All data processing was performed off line using MATLAB (The MathWorks, Natick, MA). The metrics used to quantify subjects' balance performance were root mean square (RMS) of trunk tilt, elliptical area (EA) of trunk sway trajectory, percent time spent in the dead zone where no tactor activation took place (PZ), and mean power frequency (MPF) of trunk sway, calculated for each trial from the power spectral density of trunk tilt. The RMS trunk tilt in the A/P and M/L directions was computed by taking the square root of the time average of the squared A/P and M/L tilt values. The trunk tilt trajectory of each trial was fit with a 95% confidence interval ellipse in order to capture the sway area. In addition, PZ analysis was conducted by calculating the percentage of time that the trunk tilt was within the specified angle limits for a given stance condition. The MPF parameters of A/P and M/L tilt were computed to characterize the mean spectral decompositions of sway motions in specific bandwidths (0–1.0 Hz). Note that the first two non-feedback trials were averaged with the last two non-feedback trials and four feedback trials were averaged for each subject for each metric in order to perform a statistical analysis.

Statistical analysis was performed using linear mixed effects models (LMM). One particularly desirable feature of this analytical methodology is that it takes into account the likely correlation of repeated measurements performed on the same subject.

Dependent variables were RMS trunk tilt, EA, PZ, and MPF. The primary focus of the analysis was to estimate the effects of vibrotactile feedback during different stance conditions on the dependent variables while accounting for the correlation of the replicated measures obtained from the same subject. Hypotheses for the main effects of vibrotactile feedback were tested using an F-test. The averages of the dependent variables during the first two trials (which were performed without feedback) were used as baseline values in order to evaluate the effects of vibrotactile feedback and facilitate comparisons among subjects. Significance was defined at $p \leq 0.05$.

The rank of vibrotactile feedback for all six survey questions was averaged over all subjects to determine an overall rank of the proposed system efficacy, with five being the highest rank and the "most preferred" or "most helpful in maintaining balance."

5.4. Results

5.4.1. Performance evaluation of cell phone based balance trainer

Figure 5.4.1 shows the performance of the EKF tilt estimation algorithm implemented in the cell phone based balance trainer. To evaluate accelerometer noise and drift, the cell phone was attached to a tilt table that was manually manipulated. Without the EKF algorithm, the noise of the angular position accelerometer output computed by Equation 1 was observed to be approximately $\pm 1.2°$, while employment of the EKF algorithm reduced the noise to $0.2°$ in both pitch (i.e., A/P) and roll (i.e., M/L) directions without significant estimation delay.

To benchmark the resolution of the cell phone accelerometer and tilt estimation algorithm, the computed tilt was compared with that of a high fidelity motion tracking IMU (Xsens, Xsens Technologies B.V., Enschede, NL.), as shown in Figure 5.4.1 (b). Both the cell phone and Xsens IMU were attached to a tilt table that was oriented manually. At a tilt frequency of 2.5 Hz, the sensing resolution of the cell phone based system was better than 0.2°, while the high fidelity Xsens IMU resolution was better than 0.1°. Note that the data from the cell phone was recorded in the phone internal memory while the data from the Xsens IMU was recorded by a laptop computer. It is important to note that the refresh rates of the iPhone and the laptop computer were not equal to each other even when both refresh rates were set at 20 ms; the refresh rate variations in the iPhone and the laptop computer are ±3.2 ms (±16 %) and ±0.5 ms (±2.5 %), respectively. Due to time step variation of each refresh rate, a synchronization discrepancy between the two signals, shown in Figure 5.4.1 (b), existed.
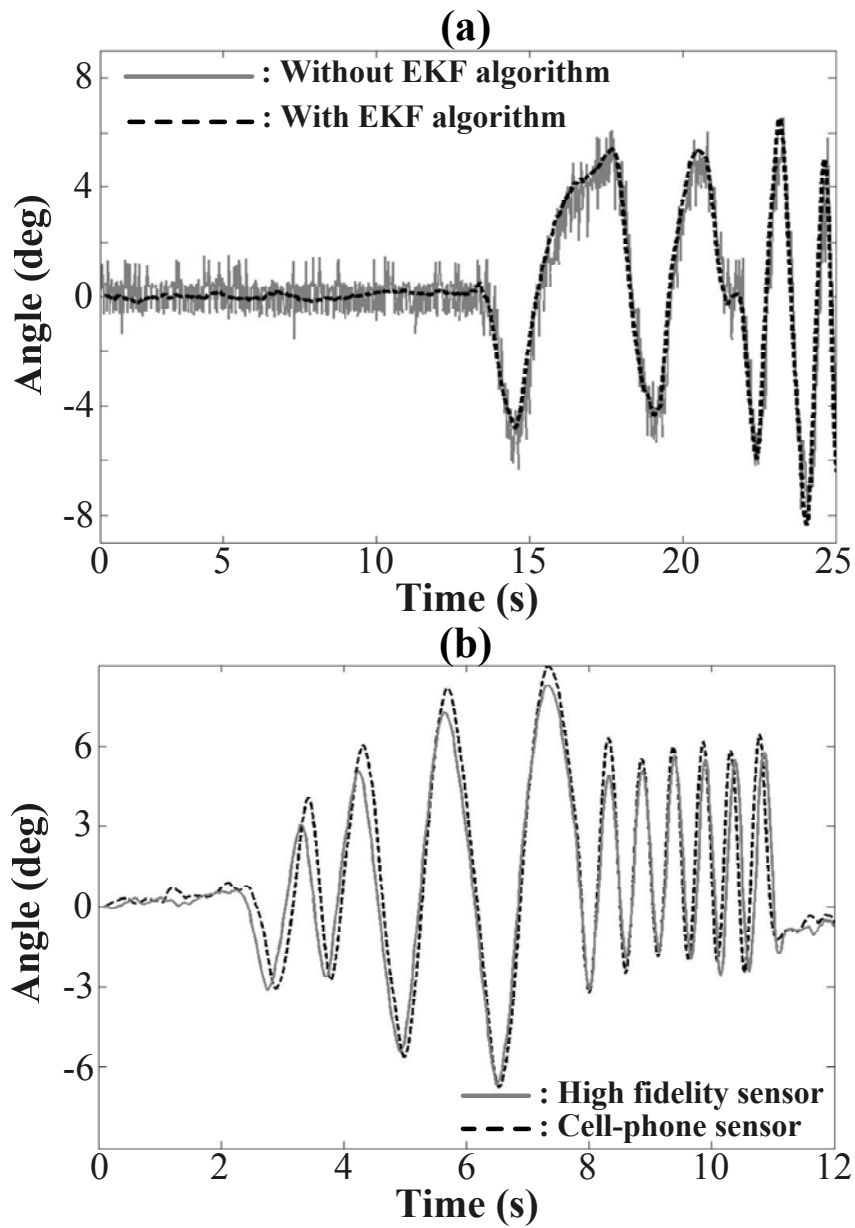
Figure 5.4.1. (a) Effect of EKF algorithm on tilt estimation performance: solid and dashed lines represent estimated tilt angle of the cell phone without or with EKF algorithm, respectively. (b) Benchmarking of tilt estimation: blue solid and red dashed lines represent tilt angle estimated by a high fidelity sensor and the cell phone sensor, respectively. Tilt angle was sampled at a rate of 50 Hz for both sensors.

5.4.2. Healthy subjects

Figure 5.4.2 shows elliptical fits and RMS tilt values for example trunk sway trajectories obtained from a healthy subject for the three different stance conditions. The subject exhibited a decreased EA for each stance condition when cell phone based vibrotactile feedback was applied, as well as decreased RMS. All healthy subjects demonstrated larger EA during tandem Romberg stance than during the other two stances, presumably due to the more challenging nature of the tandem Romberg stance.

Figure 5.4.3 presents the statistical analysis and significance levels of the average A/P RMS, M/L RMS, PZ, EA, A/P MPF, and M/L MPF metrics for healthy subjects during all stance conditions. For Romberg stance, significant main effects were found for the A/P RMS, M/L RMS, PZ, EA, and A/P MPF metrics when vibrotactile feedback was provided. Subjects showed a significant decrease in A/P RMS, M/L RMS, and EA, and a significant increase in PZ and A/P MPF. For semi-tandem Romberg stance, significant main effects were found for the M/L RMS, PZ, EA, and M/L MPF metrics when vibrotactile feedback was provided. Subjects showed a significant decrease in M/L RMS, and EA, and a significant increase in PZ and M/L MPF. For tandem Romberg stance, significant main effects were found for the A/P RMS, M/L RMS, PZ, and EA metrics when vibrotactile feedback was provided. Subjects showed a significant decrease in A/P RMS, M/L RMS, and EA, and a significant increase in PZ.

Frequency domain analysis of trunk tilt (MPF) for healthy subjects shows that provision of vibrotactile feedback significantly increases low frequency power in the 0.1

Hz to 0.4 Hz range for A/P MPF with Romberg stance and M/L MPF with semi-tandem

Romberg stance.
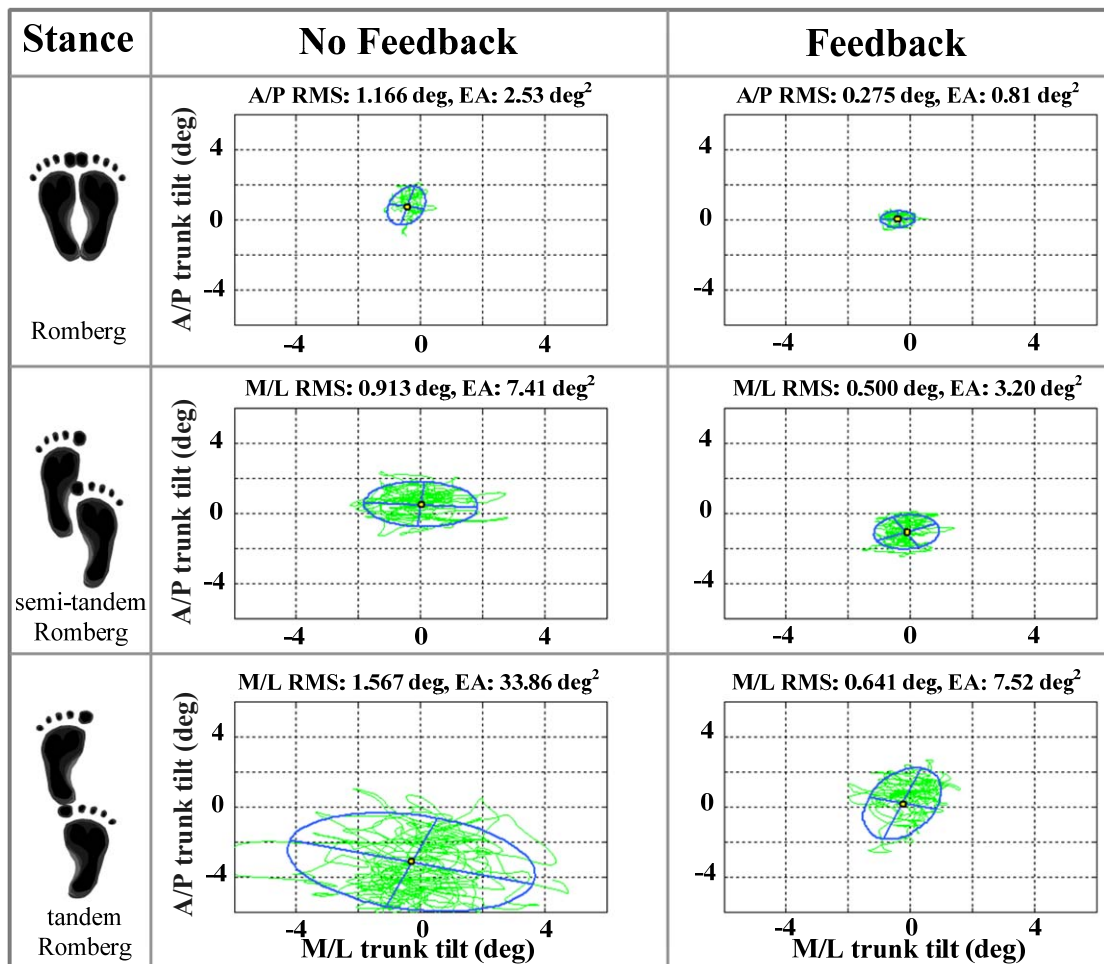
Figure 5.4.2. Elliptical fits and RMS values for one healthy subject trial under each stance condition without (left column) and with (right column) feedback. The blue line represents the elliptical fit with major and minor axes, and the green line represents the actual trunk tilt trajectory.
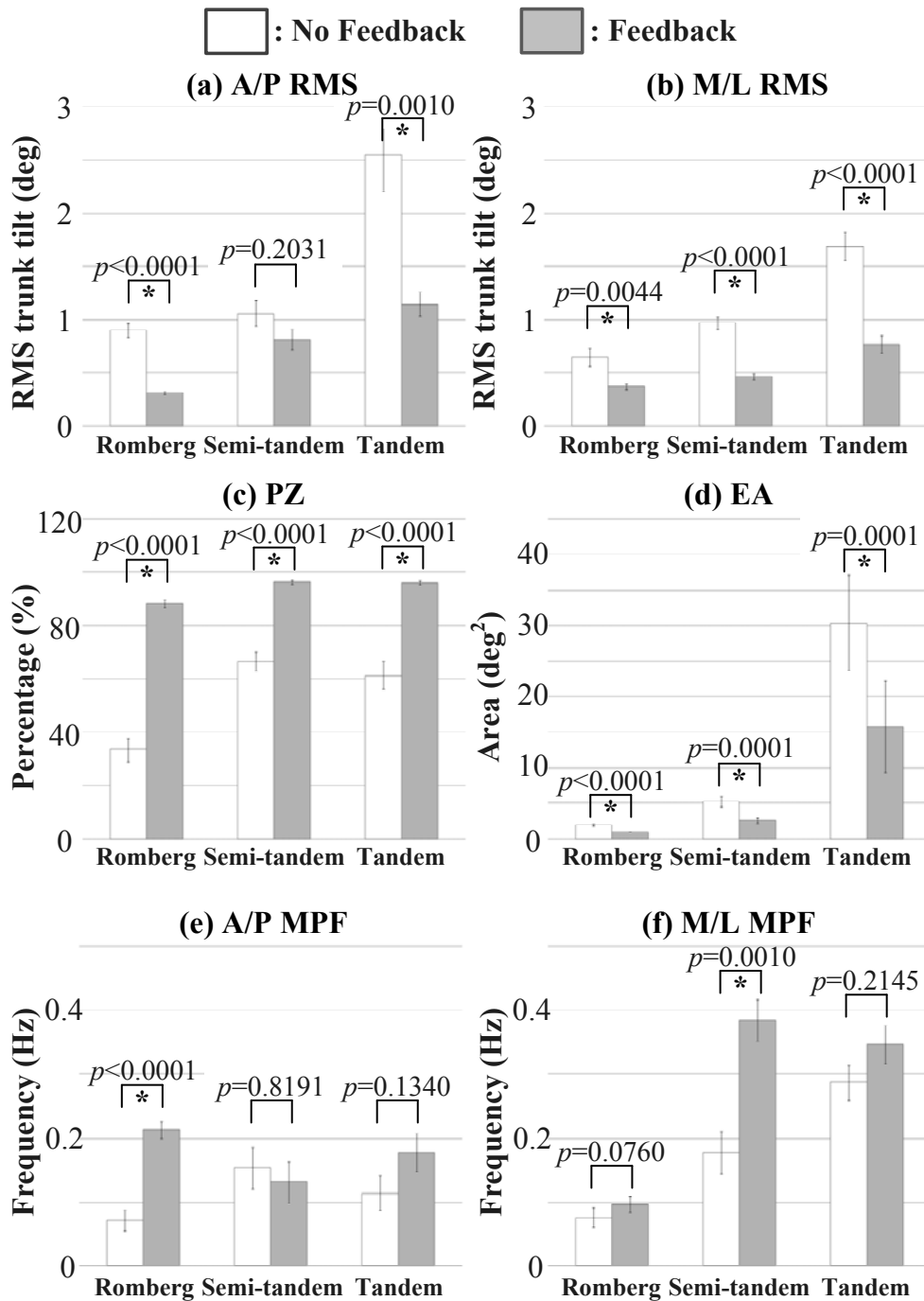
Figure 5.4.3. Balance metric results for healthy subjects. All values were computed by averaging the values of each subject's average value. (a) RMS tilt in the A/P direction. (b) RMS tilt in the M/L direction. (c) Percent time spent in the dead zone. (d) Elliptical area. (e) Mean power frequency in the A/P direction. (f) Mean power frequency in the A/P direction. Error bars indicate standard error of the mean.

5.4.3. Subjects with vestibular involvement

Figure 5.4.4 shows elliptical fits and RMS tilt values for example trunk sway trajectories obtained from a subject with vestibular involvement during eyes-open and eyes-closed testing in the semi-tandem Romberg stance. While an increase in EA was observed for the eyes-closed condition relative to the eyes-open condition for both feedback conditions, the subject exhibited a decrease in EA and RMS for both eyes-open and eyes-closed conditions when cell phone based vibrotactile feedback was applied.
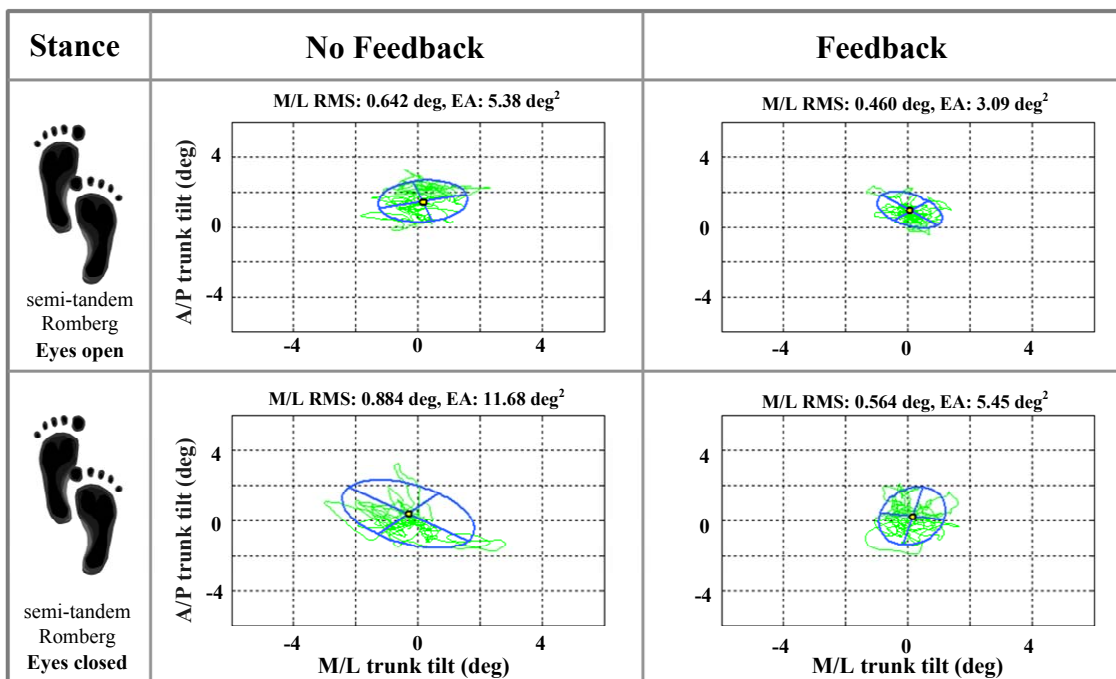
Figure 5.4.4. Elliptical fits and RMS values for one subject with vestibular involvement under eyes-open and eyes-closed conditions. Left and right column indicates subject's performance without and with feedback, respectively. The blue line represents the elliptical fit with major and minor axes, and the green line represents the actual trunk tilt trajectory.

Figure 5.4.5 presents the statistical analysis and significance levels of the A/P RMS, M/L RMS, PZ, EA, A/P MPF, and M/L MPF metrics during all stance conditions for subjects with vestibular involvement. Significant main effects were found for the M/L RMS, PZ, EA, and M/L MPF metrics when vibrotactile feedback was provided, regardless of whether subjects had their eyes open or closed. Subjects showed a significant decrease in M/L RMS and EA, and a significant increase in PZ and M/L MPF. When subjects had their eyes closed, the M/L RMS, EA, and M/L MPF metrics trended larger, and PZ smaller, for both feedback conditions.

The MPF for subjects with vestibular involvement shows that provision of vibrotactile feedback significantly increases low frequency power of the M/L direction in the 0.1 Hz to 0.4 Hz range for Romberg stance with eyes open and with eyes closed condition.
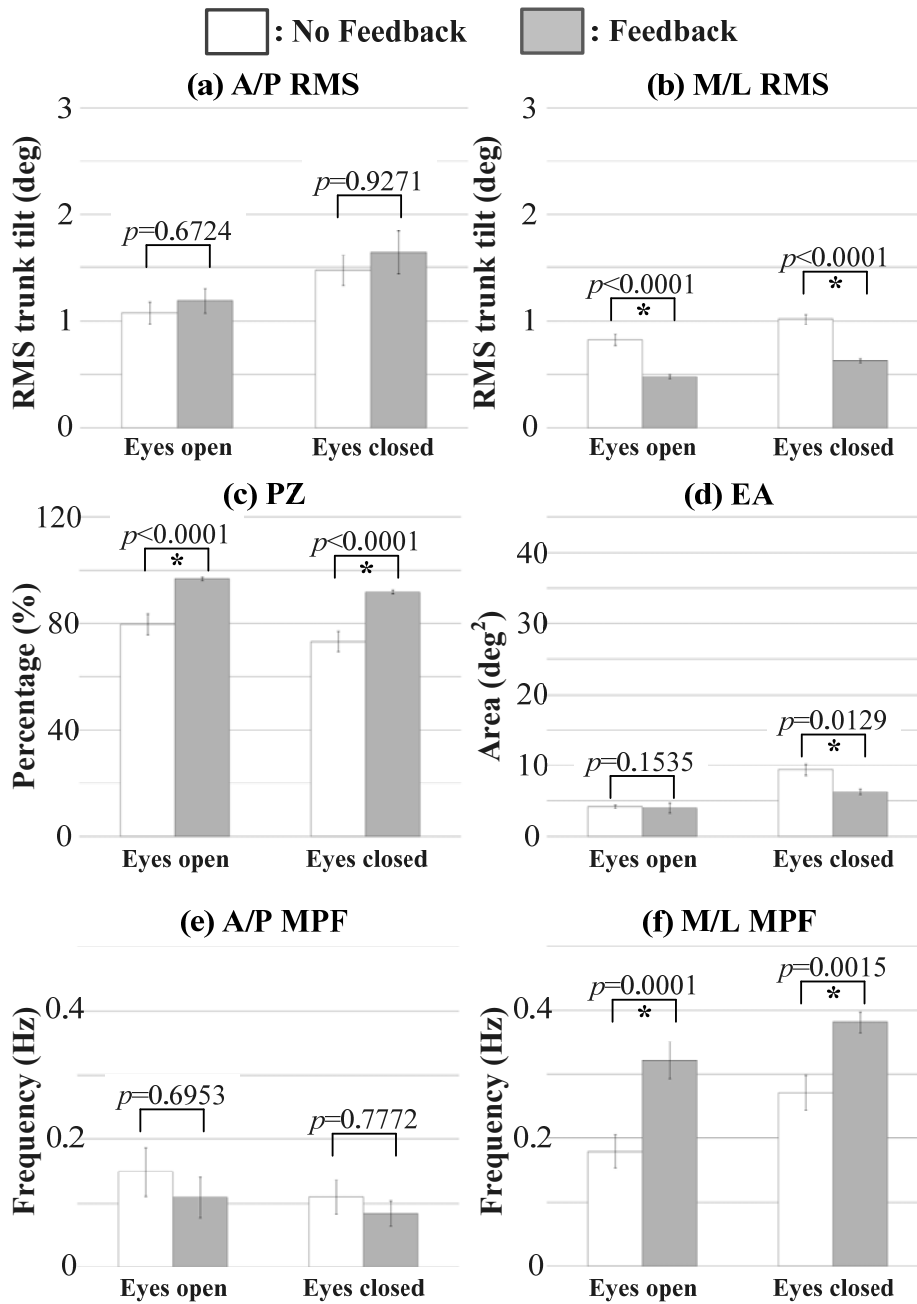
Figure 5.4.5. Balance metric results for subjects with vestibular involvement. All values were computed by averaging the values of each subject's average value. (a) RMS tilt in the A/P direction. (b) RMS tilt in the M/L direction. (c) Percent time spent in the dead zone. (d) Elliptical area. (e) Mean power frequency in the A/P direction. (f) Mean power frequency in the A/P direction. Error bars indicate standard error of the mean.

5.4.4. Subjective evaluation of balance trainer by all subjects

According to the post-experimental Likert questionnaire, the majority of subjects (healthy and those with vestibular involvement) agreed that their body was more stable when vibrotactile feedback was available than when it was not (Q1 – avg. 3.95±0.8 / 5), that vibrotactile feedback did not distract them from performing the given balance task (Q2 – avg. 4.21±0.8 / 5), and that they felt more confident in their ability to maintain balance when vibrotactile feedback was available (Q3 – avg. 3.95±0.7 / 5). Furthermore, subjects agreed that they could use the device at home by themselves if it were provided to them as-is (Q4 – avg. 4.21±0.6 / 5) and most subjects understood how to use the vibrotactile feedback provided (Q5 – avg. 4.68±0.4 / 5). Finally, when subjects were asked to rate their preference for *not* using vibrotactile feedback during stance tasks, they disagreed with the statement (Q6 – avg. 2.42±1.2 / 5). The subjects with vestibular involvement consistently rated the utility of the feedback higher than the healthy subjects: Q1 – 4.5±0.6 vs. 3.80±0.9; Q2 – 4.50±0.6 vs. 4.13±0.8; Q3 – 4.75±0.5 vs. 3.73±0.6; Q4 – 4.25±0.5 vs. 4.20±0.7; Q5 – 5.00±0.0 vs. 4.60±0.5; Q6 – 1.25±1.2 vs. 2.73±1.1.

5.5. Discussion

The main finding of this work is that trunk tilt can be robustly captured by a cell phone equipped with a tri-axial accelerometer and used to assist with balance. This finding offers several advantages in terms of size, weight, cost, functionality, flexibility, and accessibility versus more complex laboratory and commercial systems dedicated to this purpose. Comparisons of trunk tracking performance between the cell phone system and

a sophisticated IMU technology often implemented in non-portable laboratory systems [25, 33, 35, 38-39] demonstrate that the cell phone system can provide resolution trunk tracking with less than 0.2° error. This result is comparable to the resolution of commercially available IMU-based trunk tracking systems (tracking errors less than 0.1°). Moreover, the EKF motion estimation algorithm implemented for the cell phone system largely eliminates inherent sensor noise and provides a robust estimate for trunk tilt without a significant time delay.

Since the cell phone based system studied here only incorporates a tri-axial accelerometer, trunk tilt estimation is inferior to IMU systems that incorporate both an accelerometer and a gyroscope. This limitation could be overcome by employing further sensors, such as a tri-axial gyroscope for orientation sensing or a tri-axial magnetometer for measuring the Earth's magnetic field. A second concern is that the system studied here requires the cell phone to be placed on the body segment being evaluated, since the sensor capturing body motion is embedded within the phone itself. Consequently, a second-generation tactor bud that incorporates a small IMU (containing both a tri-axial accelerometer and a gyroscope) is currently being developed. Finally, since the system was tested using only a small number of subjects, some of the true differences between conditions may not have been detected in the analysis.

The results of this proof-of-concept study show that healthy subjects exhibit significant improvements in the most challenging stance condition (tandem Romberg) when cell phone based vibrotactile feedback is provided. Indeed, the majority of healthy subjects remained inside the given dead zone for the stance tasks executed. In addition,

164

analysis of EA suggests that vibrotactile feedback reduces trunk tilt area while subjects were provided with vibrotactile feedback.

The MPF results suggest that more frequent corrections of trunk tilt contributed to an increase in mean power frequency in the presence of vibrotactile feedback (i.e., subjects actively moved their trunk in response to the cues as opposed to stiffening their bodies and remaining as still as possible in order to prevent movement outside of the dead zone). In the case of M/L MPF, however, results for tandem Romberg stance in the presence of vibrotactile feedback showed a non-significant change in comparison to the feedback-off trials. This can be explained by the challenging nature of this stance, especially when performed with the eyes closed; in these trials, subjects may have stiffened their bodies in order to remain still and did not search for and use the limits of stability coded by the vibrotactile feedback. As such, sway frequency differences between the feedback-on and feedback-off testing conditions were not significant.

Similar findings were observed in the vestibular involvement subject cohort, except for the EA metric, for which subjects showed similar EA in both the presence and absence of vibrotactile feedback during eyes-open trials. Furthermore, for this group the main effects of vibrotactile feedback were observed only in the direction in which vibrotactile feedback was provided. For example, neither A/P RMS nor A/P MPF showed significant changes in the presence or absence of vibrotactile feedback in either eyes-open or eyes-closed conditions when feedback was provided solely in the M/L direction.

The collected survey results indicate that the majority of subjects feel that the proposed cell phone balance training system could be used at home without difficulty. In addition, subjects felt they could use the system more effectively in distraction-free

settings. Specifically, subjects with vestibular involvement indicated a higher confidence level (avg. 4.75 / 5) than healthy subjects (avg. 3.4 / 5) in their ability to maintain balance with the aid of vibrotactile feedback. This reinforces the positive balance metric outcomes shown in the vestibular involvement subject group when feedback was present, suggesting that vestibulopathic subjects can adequately rely on the proprioceptive input provided via vibrotactile feedback to compensate for their vestibular loss.

References

[1]   J. A. Stevens, P. S. Corso, E. A. Finkelstein, and T. R. Mille, "The costs of fatal and non-fatal falls among older adults," *Injury Prevention,* vol. 12, no. 5, pp. 290-295, 2006.

[2]   E. E. Hansson, N. O. Mansson, K. A. Ringsberg, and A. Hakansson, "Falls among dizzy patients in primary healthcare: An intervention study with control group," *International Journal of Rehabilitation Research,* vol. 31, no. 1, pp. 51-57, Mar 2008.

[3]   J. Y. Jung, J. S. Kim, P. S. Chung, S. H. Woo, and C. K. Rhee, "Effect of vestibular rehabilitation on dizziness in the elderly," *American journal of otolaryngology,* vol. 20, no. 5, pp. 295-299, Feb 2009.

[4]   M. Pavlou, A. Shumway-Cook, F. Horak, L. Yardley, and A. Bronstein, "Rehabilitation of balance disorders in the patient with vestibular pathology," vol. Clinical disorders of balance and gait, A. Bronstein, Brandt, Thomas, Woollacott,

Marjorie H. and Nutt, JG. 1996, Ed., ed New York. : Oxford University Press, Inc., 2004, pp. 211-235 (Arnold Publications Series).

[5]   B. A. Alsalaheen, A. Mucha, L. O. Morris, S. L. Whitney, J. M. Furman, C. E. Camiolo-Reddy, M. W. Collins, M. R. Lovell, and P. J. Sparto, "Vestibular rehabilitation for dizziness and balance disorders after concussion," *Journal of Neurologic Physical Therapy,* vol. 34, no. 2, pp. 87-93, Jun. 2010.

[6]   T. C. Hain. 2010, *Vestibular Rehabilitation Therapy (VRT)*.

        Available: http://www.dizziness-and-balance.com/treatment/rehab.html#general

[7]   S. L. Whitney, R. G. Jacob, P. J. Sparto, E. F. Olshansky, G. Detweiler-Shostak, E. L. Brown, and J. M. Furman, "Acrophobia and pathological height vertigo: indications for vestibular physical therapy?," *Physical Therapy,* vol. 85, no. 5, pp. 443-458, May 2005.

[8]   C. L. Kao, L. K. Chen, C. M. Chern, L. C. Hsu, C. C. Chen, and S. J. Hwang, "Rehabilitation outcome in home-based versus supervised exercise programs for chronically dizzy patients," *Archives of Gerontology and Geriatrics,* vol. 51, no. 3, pp. 264-267, Nov/Dec. 2009.

[9]   O. Topuz, B. Topuz, F. N. Ardic, M. Sarhus, G. Ogmen, and F. Ardic, "Efficacy of vestibular rehabilitation on chronic unilateral vestibular dysfunction," *Clinical Rehabilitation,* vol. 18, no. 1, pp. 76-83, Feb. 2004.

[10]   H. Huang, S. L. Wolf, and J. He, "Recent developments in biofeedback for neuromotor rehabilitation," *Journal of Neuroengineering and Rehabilitation,* vol. 3, no. 1, pp. 11-22, Sep. 2006.

[11] O. Cakrt, M. Chovanec, T. Funda, P. Kalitova, J. Betka, E. Zverina, P. Kolar, and J. Jerabek, "Exercise with visual feedback improves postural stability after vestibular schwannoma surgery," *European archives of oto-rhino-laryngology* vol. 267, no. 9, pp. 1355-1360, Sep. 2010.

[12] D. Fitzgerald, N. Trakarnratanakul, L. Dunne, B. Smyth, and B. Caulfield, "Development and user evaluation of a virtual rehabilitation system for wobble board balance training," in *Annual International Conference of the IEEE Engineering in Medicine and Biology Society*, Vancouver, BC, Canada, Aug., 2008, pp. 4194 - 4198

[13] B. Lange, S. Flynn, R. Proffitt, C. Y. Chang, and A. S. Rizzo, "Development of an interactive game-based rehabilitation tool for dynamic balance training," *Topics in stroke rehabilitation,* vol. 17, no. 5, pp. 345-352, Sep. 2010.

[14] W. Young, S. Ferguson, S. Brault, and C. Craig, "Assessing and training standing balance in older adults: a novel approach using the 'Nintendo Wii' Balance Board," *Gait and Posture,* vol. 33, no. 2, pp. 303-305, Feb. 2011.

[15] L. C. Chin, T. Y. Huang, C. L. Yu, C. H. Wu, C. C. Hsu, and H. S. Yu, "Increased cutaneous blood flow but impaired post-ischemic response of nutritional flow in obese children," *Atherosclerosis,* vol. 146, no. 1, pp. 179-85, Sep. 1999.

[16] M. Dozza, L. Chiari, and F. B. Horak, "Audio-biofeedback improves balance in patients with bilateral vestibular loss," *Archives of physical medicine and rehabilitation,* vol. 86, no. 7, pp. 1401-1403, Jul. 2005.

[17]   M. Dozza, F. B. Horak, and L. Chiari, "Auditory biofeedback substitutes for loss of sensory information in maintaining stance," *Experimental Brain Research,* vol. 178, no. 1, pp. 37-48, Sep. 2007.

[18]   J. Hegeman, F. Honegger, M. Kupper, and J. H. Allum, "The balance control of bilateral peripheral vestibular loss subjects and its improvement with auditory prosthetic feedback," *Journal of Vestibular Research,* vol. 15, no. 2, pp. 109-117, Jan. 2005.

[19]   P. Bach-y-Rita, "Tactile sensory substitution studies," *Annals of the New York Academy of Sciences,* vol. 1013, pp. 83-91, May. 2004.

[20]   P. Bach-y-Rita and S. W. W Kercel, "Sensory substitution and the human-machine interface," *Trends in cognitive sciences,* vol. 7, no. 12, pp. 541-546, Dec. 2003

[21]   A. S. Cauquil and B. L. Day, "Galvanic vestibular stimulation modulates voluntary movement of the human upper body.," *Journal of physiology,* vol. 513, no. 2, pp. 611-619, Dec. 1998.

[22]   M. Dozza, C. Wall, 3rd, R. J. Peterka, L. Chiara, and F. B. Horak, "Effects of practicing tandem gait with and without vibrotactile biofeedback in subjects with unilateral vestibular loss," *Journal of Vestibular Research,* vol. 17, no. 4, pp. 195-204, Jan. 2007.

[23]   R. Johansson, M. Magnusson, and P. A. Fransson, "Galvanic vestibular stimulation for analysis of postural adaptation and stability," *IEEE Transactions on Biomedical Engineering* vol. 42, no. 3, pp. 282-292, Mar. 1995.

[24]   E. Kentala, J. Vivas, and C. Wall, "Reduction of postural sway by use of a vibrotactile balance prosthesis prototype in subjects with vestibular deficits," *The Annals of otology, rhinology, and laryngology,* vol. 112, no. 5, pp. 404-409, May. 2003.

[25]   K. H. Sienko, M. D. Balkwill, L. I. Oddsson, and C. Wall, "Effects of multi-directional vibrotactile feedback on vestibular-deficient postural performance during continuous multi-directional support surface perturbations," *Journal of Vestibular Research,* vol. 18, no. 5-6, pp. 273-285, Jan. 2008.

[26]   Y. K. Stolbkov and I. V. Orlov, "Artificial vestibular feedback in conditions of a modified body scheme," *Neuroscience and Behavioral Physiology,* vol. 39, no. 2, pp. 173-181, Feb. 2009.

[27]   N. Vuillerme, N. Pinsault, O. Chenu, M. Boisgontier, J. Demongeot, and Y. Payan, "How a plantar pressure-based, tongue-placed tactile biofeedback modifies postural control mechanisms during quiet standing," *Experimental Brain Research,* vol. 181, no. 4, pp. 547-554, Sep. 2007.

[28]   N. Vuillerme, N. Pinsault, A. Fleury, O. Chenu, J. Demongeot, Y. Payan, and P. Pavan, "Effectiveness of an electro-tactile vestibular substitution system in improving upright postural control in unilateral vestibular-defective patients," *Gait & Posture,* vol. 28, no. 4, pp. 711-715, Nov. 2008.

[29]   C. Wall and E. Kentala, "Control of sway using vibrotactile feedback of body tilt in patients with moderate and severe postural control deficits," *Journal of Vestibular Research,* vol. 15, no. 5-6, pp. 313-325, Apr. 2005.

[30] C. Wall, D. M. Merfeld, S. D. Rauch, and F. O. Black, "Vestibular prostheses: the engineering and biomedical issues," *Journal of Vestibular Research,* vol. 12, no. 2-3, pp. 95-113, Jan. 2002-2003.

[31] D. L. Wardman, J. L. Taylor, and R. C. Fitzpatrick, "Effects of galvanic vestibular stimulation on human posture and perception while standing," *Journal of physiology,* vol. 551, no. 3, pp. 1033-1042, Sep. 2003.

[32] L. Chiari, M. Dozza, A. Cappello, F. B. Horak, V. Macellari, and D. Giansanti, "Audio-biofeedback for balance improvement: an accelerometry-based system," *IEEE Transactions on Biomedical Engineering,* vol. 52, no. 12, pp. 2108-2111, Dec. 2005.

[33] C. Wall, L. E. Oddsson, F. B. Horak, D. W. Wrisley, and M. Dozza, "Applications of vibrotactile display of body tilt for rehabilitation," in *Conf. Proc. 26th IEEE Ann. Int. Conf. Engineering in Medicine and Biology Society (EMBS' 04)*, San Francisco, CA, USA, 2004, pp. 4763-4765.

[34] N. Vuillerme, N. Pinsault, O. Chenu, J. Demongeot, Y. Payan, and Y. Danilov, "Sensory supplementation system based on electrotactile tongue biofeedback of head position for balance control," *Neuroscience letters,* vol. 431, no. 3, pp. 206-210, Sep. 2008.

[35] M. S. Weinberg, C. Wall, J. Robertsson, E. O'Neil, K. Sienko, and R. Fields, "Tilt determination in MEMS inertial vestibular prosthesis," *Journal of Biomedical Engineering,* vol. 128, no. 6, pp. 943-956, Dec. 2006.

[36] B. C. Lee, S. Chen, and K. H. Sienko, "A wearable device for real-time motion error detection and vibrotactile instructional cuing," *IEEE Transactions on*

Neural Systems and Rehabilitation Engineering, vol. 19, no. 4, pp. 374-381, Aug. 2011.

[37]   F. A. Geldard, "Some Neglected Possibilities of Communication," *Science,* vol. 131, no. 3413, pp. 1583-1588, May. 1960.

[38]   S. Haggerty, L. T. Jiang, A. Galecki, and K. H. Sienko, "Effects of vibrotactile feedback on response time and postural stability in older adults," *Gait & Posture,* 2011 (In Press).

[39]   D. Ursu, L. T. Jiang, and K. H. Sienko, "Effect of vibrotactile trunk tilt feedback on postural stability in older adults," in *Annual American Society of Biomechanics Meeting*, Penn State University, Aug., 2009.

[40]   BalanceFreedom™. 2008, *Balance International Innovations*.
        Available: http://www.b2i.info

[41]   VertiGuard®RT. 2008, *VestiCure*.
        Available: http://www.vesticure.com/index.php?id=9&L=1

[42]   Marketwire. 2010, *Number of Smartphone Users to Quadruple, Exceeding 1 Billion Worldwide by 2014*. Available: http://www.marketwire.com/press-release/Number-of-Smartphone-Users-to-Quadruple-Exceeding-1-Billion-Worldwide-by-2014-1136308.htm

[43]   N. Serigioli, R. Reina Munoz, and E. C. Rodriguez, "Biomedical signals monitoring based in mobile computing," in *Engineering in Medicine and Biology Society (EMBC), 2010 Annual International Conference of the IEEE*, 2010, pp. 3868-3871.

[44]   J. M. Sanches, B. Pereira, and T. Paiva, "Headset Bluetooth and cell phone based continuous central body temperature measurement system," in *Engineering in Medicine and Biology Society (EMBC), 2010 Annual International Conference of the IEEE*, 2010, pp. 2975-2978.

[45]   M. Morris and F. Guilak, "Mobile Heart Health: Project Highlight," *IEEE Pervasive Computing,* vol. 8, no. 2, pp. 57-61, 2009.

[46]   M. Sung, C. Marci, and A. Pentland, "Wearable feedback systems for rehabilitation," *Journal of neuroengineering and rehabilitation,* vol. 2, no. 1, p. 17, Jun. 2005.

[47]   E. Dogbevi. (2010, *More in Africa use mobile phones than on any other continent*. Available: http://www.ghanabusinessnews.com/2010/01/04/more-in-africa-use-mobile-phones-than-on-any-other-continent/

[48]   K. H. Sienko, V. V. Vichare, M. D. Balkwill, and C. I. I. I. Wall, "Assessment of vibrotactile feedback on postural stability during pseudorandom multidirectional platform motion," *IEEE Transactions on Biomedical Engineering,* vol. 57, no. 4, pp. 944-952, Apr. 2010.

[49]   C. Wall and M. S. Weinberg, "Balance prostheses for postural control," *Engineering in Medicine and Biology Magazine,* vol. 22, no. 2, pp. 84-90, Mar. 2003.

[50]   IPhone. Available: http://developer.apple.com/iphone/

[51]   G. Welch and G. Bishop, "An Introduction to the Kalman Filter," in *Technical Report TR 95-041*, Chapel Hill, 2001.

[52]   C. Wall, M. S. Weinberg, P. B. Schmidt, and D. E. Krebs, "Balance prosthesis based on micromechanical sensors using vibrotactile feedback of tilt," *IEEE Transactions on Biomedical Engineering,* vol. 48, no. 10, pp. 1153-1161, Oct. 2001.

CHAPTER 6: Discussion

6.1. Vibrotactile biofeedback control signal

The majority of laboratory-based vibrotactile biofeedback systems used for balance-related [1-9] and kinesthetic-based motion guidance [10-16] applications have provided feedback based on a control signal that is proportional to the error between the target and the subject's position (P), the rate of change of the error (D), or a combination of the P and D signals (PD). In balance-related and kinesthetic-based motion guidance applications, information is coded in the form of vibrotactile stimuli applied over the skin to provide real-time knowledge of performance (KP). During motor learning exercises, KP enables the user (e.g., trainee or patient) to obtain information about his/her movements and develop internal models that map movement characteristics to performance outcomes [17]. The majority of previously published upper limb motion guidance studies involving vibrotactile biofeedback have used a P control signal [10-14]. However, performance of vibrotactile-based motion guidance may be further improved if the rate of change of position (velocity) or other predictive information is used to generate the feedback control signal due to a time delay associated with perceiving,

processing and responding to vibrotactile biofeedback. Wall and Kentala [18] and Goodworth et al. [1] showed that trunk sway was significantly improved during dynamic posturography with the addition of velocity information to the position information when compared to either position or velocity information alone.

The studies presented in Chapters 3 and 4 investigated the effects of varying the nature of the control signal during a simple motion replication task. Based on the experimental results, subjects had the smallest position errors and time delays, and the largest cross-correlation values when they replicated the motion using feedback based on a PD control signal. This result is in agreement with investigations by Wall and Kentala [2] and Goodworth et al. [1]. Therefore, incorporating velocity information with position information might help subjects to compensate for the time delay associated with using vibrotactile biofeedback that is introduced by sensory transduction, afferent transmission (conduction velocity), processing, and efferent muscle activation. Furthermore, the use of velocity information in the vibrotactile biofeedback control signal effectively reduces the tactor activation threshold so that subjects receive tactile stimulation prior to reaching the preprogrammed tactor activation threshold.

Recently, Wall and Kentala [2] showed that vibrotactile biofeedback based on a predictive control signal (e.g., predicted motion of trunk sway based on prior 100 msec trajectory) results in smaller RMS trunk sway values than a PD control signal during dynamic posturography. Loughlin et al. [19] proposed a "custom design" approach using system identification methods to identify subject-specific feedback parameters for achieving desired body sway frequency responses; subjects attempted to fit a certain frequency response profile. Their approach included a gain that was proportional to the

rate of change of velocity (acceleration) in addition to terms that were proportional to P and D signals. Through simulation, they found that the "subject-specific filtered feedback", incorporating position, velocity, and acceleration information of the body, needs to be provided in order to reduce trunk sway in the lower frequency range (less than 0.5 Hz) [19]. Therefore, it is likely that the incorporation of a higher order derivative (e.g., acceleration) or a predictive term into the tactor control signal, which was not investigated in this dissertation, may improve a subject's performance in motion replication and balance rehabilitation applications. Likewise, customized control signals that adaptively change the gain parameters for the PD control signal as a function of the speed of a subject's movements should be investigated in order to achieve a high fidelity control scheme for the provision of vibrotactile biofeedback control.

6.2. Vibrotactile biofeedback coding scheme

6.2.1. Directional coding

A two-column single-row display was used for the cell phone balance training system to provide directional information in either the A/P or M/L direction. This simple display, as opposed to a multiple-row by multiple-column array configuration of tactors, was pursued based on the results reported by Sienko et al. [5]; their data showed that when feedback was provided, subjects spent the majority of the experimental trial in the dead zone (tactors off) and in the zone corresponding to the first row (lowest level) of tactor activation (i.e., when the tilt exceeded the smallest dead zone threshold, 1.0° in A/P and M/L directions) during perturbed stance [5]. Furthermore, Sienko et al. [5] did not find

any significant differences in RMS trunk sway reductions when feedback was provided via a 4-column, 8-column, or 16-column display. They concluded that a display with a spatial resolution of 90° was as effective as a display with a spatial resolution of 22.5° for the particular task studied [5]. The subjects that participated in the cell phone balance training study (Chapter 5) were able to use the simple two-column display to perform three different stance conditions. Note, the two-column display was aligned along the axis of least stability; in the case of the Romberg and semi-tandem Romberg stances, feedback was provided along the A/P axis, while in the case of the tandem Romberg stance, feedback was provided along the M/L axis. The results suggest that the simple two-column binary display is adequate for simple standing tasks. However, the two-column display requires the user to actively reposition the tactors based on the exercise being performed. Thus, a future version of the cell phone training system should minimally support a 4-column display in order to reduce the time associated with reconfiguring the device during the training session.

6.2.2. Magnitude coding

The vibrotactile biofeedback coding scheme used throughout this work was binary in nature; the tactors were either off or on at any given point in time. Using the simple displays employed in this research, subjects could accurately mimic the simple task of slowly bending at the waist and could decrease their trunk sway during different three stance conditions. However, a binary display is unable to convey information about the magnitude of the error or magnitude of the body displacement. The error magnitude is

critical to motor learning [20-21]. Previous studies have demonstrated that knowledge of the error magnitude not only reinforces the preferred direction of motion, but also helps the user dynamically determine his/her body position during upper limb motion guidance [11, 13-16] and balance-related exercises [22]. Therefore, it is assumed that continuously displaying error magnitudes (where the location, pattern, or intensity of vibrotactile biofeedback is controlled by the execution of the movement in real-time) could decrease motion or range discrepancies in motion replication and balance rehabilitation applications.

One potential way to overcome the above-mentioned limitation is to use a position-based magnitude coding scheme. Wall et al. [23] and Sienko et al. [5] developed a position-based coding scheme to convey information about the magnitude of the body displacement with respect to the upright (vertical) position. The lowest row was activated when the tilt exceeded the dead zone threshold. Tactor activation progressed from the lowest to the highest row of tactors in a stepwise fashion with activation of the middle and highest tactor rows corresponding to a tilt in excess of, respectively, 33% and 67% of the measured limit of stability [5], which was defined by the subject's maximum possible erect postural tilt without loss of balance during quiet stance. However, a position-based coding scheme requires more instrumentation, which would increase hardware cost and complexity; it is desirable to have the simplest high-performing system for clinical and home-based use. In addition, perceptual resolution and sensitivity must be taken into consideration for the design of the torso-based vibrotactile biofeedback displays. Studies by Weinstein [24], van Erp [25], and Cholewiak et al. [26] have shown that two-point tactile discrimination thresholds (spatial acuity of the body with respect to two-point

tactile stimulation) on the torso are on the order of 3.2-4.1 cm. Therefore, the maximum number of tactors that can be placed within a single column or row of a torso-based array is constrained by the two-point discrimination capability.

An alternative option to position-based magnitude coding is either frequency- or intensity-based magnitude coding. Frequency-based coding affords the ability to use a single tactor to generate vibrations at various frequencies. In the context of a vibrotactile biofeedback display for balance-related applications, the beat frequency of the stimulation could be modified as a function of the magnitude of the error. Lyford [22] has recently demonstrated that frequency-based vibrotactile biofeedback of trunk tilt magnitude can be as effective in providing information about body sway as the position-based methodology described above [22]. Through a common clinical postural control task (maintaining an upright stance involving surface perturbations with eyes closed) in the anterior-posterior (A/P) direction, both frequency-based and position-based vibrotactile biofeedback performed equally well in reducing trunk sway and reducing the percentage of falls when compared to the no feedback condition [22]. Intensity-based coding for vibrotactile biofeedback is yet another viable option worth further exploration in balance rehabilitation applications. In the case of intensity-based coding, the intensity of the vibration could be increased or decreased as a function of the error. Brewster and Brown [27-28] showed that people are able to identify at least three different types of intensity changes: increases, decreases, and level stimuli. To date, the intensity-based coding scheme, which uses small shaftless actuators that vary their vibration intensity as a function of the DC voltage input, has been used for upper limb motion guidance applications and has been shown to reduce motion error between the desired and actual

limb trajectories [11, 13-16]. The abovementioned frequency- and intensity-based magnitude coding schemes require fewer tactors and could potentially reduce the complexity and cost of the biofeedback system.

6.3. Instructional cues

The work presented in Chapter 2 characterized the non-volitional response to vibrotactile stimulation applied around the torso; a location frequently used for vibrotactile feedback displays [3-6, 23]. Vibrational stimulation applied over the internal oblique and erector spinae muscles induced a postural shift in the direction of the stimulation, and the observed vibration-induced postural shift was on the order of approximately 1.0° based on the assumption that subjects followed the given stance instruction (e.g., behaving like an inverted pendulum). This finding suggests that the cutaneous receptors of the torso contribute to an internal representation of the upper body. To date, repulsive cues have been used for balance-related standing and locomotor tasks [4-5, 8, 23]. Although the repulsive cues used during the cell phone balance trainer study elicited significant reductions in body sway during standing tasks, it may be possible to achieve faster and/or larger corrections with attractive cues if one can leverage the natural postural response to the vibrotactile stimulation.

Attractive cues may require more training than repulsive cues, but may obtain equal if not better results. The effects of attractive versus repulsive vibrotactile instructional cues during a simple motion replication task were primarily investigated in Chapter 3. This proof-of-concept study showed that repulsive vibrotactile instructional cues resulted in the greatest cross-correlation values, the least amount of time delay, and the least amount

of average position error between expert and subject motions after a short training period comprising six practice trials followed by six consecutive testing trials. The study's outcomes suggest that repulsive cues may be preferable for short-term applications, such as in a rehabilitation setting where time with the patient is limited. However, analysis of learning effects suggests that additional training trials are required to reach asymptotic steady-state performance (such that subject's performance plateaus) for both attractive and repulsive cues. Furthermore, conclusions regarding whether one cuing strategy is better than the other during long-term use have yet to be drawn. Indeed, the investigation of the effectiveness of attractive versus repulsive vibrotactile instructional cues during long-term use may be of clinical importance, since one of the two cues may result in superior performance or may better leverage non-volitional responses.

6.4. Technology platforms

Accurate motion tracking plays a critical role in continuously monitoring patient movements. While extensive work has been performed for motion tracking for rehabilitation [29], IMU-based motion tracking has the advantages of being unobtrusive, wearable (i.e., small size, light weight, and low power consumption), and capable of real-time data processing. The above-mentioned characteristics of IMU-based motion tracking provided a clear motivation for the development of the MIMIC and cell-phone-based vibrotactile systems, presented in Chapters 3 and 5. The MIMIC and cell-phone-based vibrotactile systems demonstrated the potential for home-based balance rehabilitation training.

Both systems (MIMIC and cell-phone) accomplish real-time motion estimation using an embedded EKF algorithm (see Appendix B). With the evaluation of the EKF algorithm described in Chapters 3 and 5, the achieved rate of noise reduction in angular position was approximately 60% for the MIMIC system and 93% for the cell-phone system. The reduction in noise with the employment of the EKF algorithm accomplished a resolution equal to approximately 0.2° in both A/P and M/L directions for both the MIMIC and cell-phone system, which was comparable to the estimation performance of the commercially available high fidelity IMU (~ 0.2° resolution).

The proposed IMU-based vibrotactile biofeedback systems could be designed with previously recorded expert motions or instructions for various tasks. The MIMIC system was evaluated with pre-specified target trajectories of motion, which were previously recorded, representing ideal expert performance during anterior-posterior movements of the trunk. In the current configuration, the system is limited to providing feedback to a single body segment using pre-recorded motion trajectories. Thus, the current MIMIC system is not useful during complicated motion tasks involving more than one body segment. In the case of a cell-phone-based vibrotactile system, the user needs assistance with both donning and operating the cell phone system, since the phone is itself utilized as a sensing system. Thus, placement of the phone on the torso implies that it cannot be easily operated by the user. Furthermore, the accelerometers present in current smart phones produce an estimate of tilt that is less robust than that of an inertial measurement unit. The lack of information regarding angular velocities in space is a potential limitation on the use of the current cell phone system being applied to gait-based balance rehabilitation exercises. Furthermore, the device software is not intuitive, and the

vibrotactile activation thresholds for the various exercises of the work proposed here have not been determined.

6.5. Balance rehabilitation exercises

The balance rehabilitation exercises used in the studies were limited to normal or modified standing and simple trunk bending movements. However, a practical clinical or home-based feedback system would need to be able to provide meaningful information during a wide range of motions and activities including walking.

Among clinical balance rehabilitation exercises, weight-shifting exercises are commonly used [30-31]. These exercises involve shifting the body's center of weight (referred to as the body's center of mass, COM) smoothly and rhythmically in the A/P, M/L, or combined A/P and M/L directions. The position of the body's COM is usually estimated by measuring the body's center of pressure (COP), which is defined as a point under the feet of a standing person where the total sum of a pressure field acts [32]. During weight-shifting exercises, patients are asked to lock their knee and hip joints and move in a manner similar to an inverted pendulum (i.e., employ an ankle [33] versus a hip strategy [34]). The primary performance metrics are movement velocity and directional control of whole body motion [35-38]. The regular performance of weight-shifting balance exercises has been shown to improve motor function for maintaining balance and reduce the risk of falling in young healthy adults [39-40], older adults [36-37, 39-40], stroke patients [38], and patients with Parkinson's disease [41]. In previous studies, visual instructions were provided by showing subjects COP, and the exercise

focused on slow and low-impact movements that shifted the subject's COM in the A/P, M/L, or combined A/P and M/L directions. Although the current MIMIC and cell phone systems are unable to measure the body's COP, other studies have shown that reductions in trunk sway are coupled with decreases in COP when vibrotactile biofeedback is provided.

6.6. References

[1]   A. D. Goodworth, C. Wall, and R. J. Peterka, "Influence of Feedback Parameters on Performance of a Vibrotactile Balance Prosthesis," *IEEE Transactions on Neural Systems and Rehabilitation Engineering,* vol. 17, no. 4, pp. 397-408, Aug. 2009.

[2]   C. Wall and E. Kentala, "Effect of displacement, velocity, and combined vibrotactile tilt feedback on postural control of vestibulopathic subjects," *Journal of Vestibular Research,* vol. 20, no. 1, pp. 61-69, Jan. 2010.

[3]   S. Haggerty, L. T. Jiang, A. Galecki, and K. H. Sienko, "Effects of vibrotactile feedback on response time and postural stability in older adults," *Gait & Posture,* 2012 (In press).

[4]   E. Kentala, J. Vivas, and C. Wall, "Reduction of postural sway by use of a vibrotactile balance prosthesis prototype in subjects with vestibular deficits," *The Annals of otology, rhinology, and laryngology,* vol. 112, no. 5, pp. 404-409, May. 2003.

[5]   K. H. Sienko, M. D. Balkwill, L. I. Oddsson, and C. Wall, "Effects of multi-directional vibrotactile feedback on vestibular-deficient postural performance during continuous multi-directional support surface perturbations," *Journal of Vestibular Research,* vol. 18, no. 5-6, pp. 273-285, Jan. 2008.

[6]   K. H. Sienko, V. V. Vichare, M. D. Balkwill, and C. I. I. I. Wall, "Assessment of vibrotactile feedback on postural stability during pseudorandom multidirectional platform motion," *IEEE Transactions on Biomedical Engineering,* vol. 57, no. 4, pp. 944-952, Apr. 2010.

[7]   V. V. Vichare, C. Wall, M. D. Balkwill, and M. D. Sienko, "Assessing the effect of vibrotactile feedback during continuous multidirectional platform motion: a frequency domain approach," in *Conf Proc IEEE Engineering in Medicine and Biology Society*, Minneapolis, MN, USA, Sep., 2009, pp. 6910-6913.

[8]   C. Wall and E. Kentala, "Control of sway using vibrotactile feedback of body tilt in patients with moderate and severe postural control deficits," *Journal of Vestibular Research,* vol. 15, no. 5-6, pp. 313-325, Apr. 2005.

[9]   C. Wall and M. S. Weinberg, "Balance prostheses for postural control," *Engineering in Medicine and Biology Magazine,* vol. 22, no. 2, pp. 84-90, Mar. 2003.

[10]   E. R. Bachmann, Y. Xiaoping, D. McKinney, R. B. McGhee, and M. J. Zyda, "Design and implementation of MARG sensors for 3-DOF orientation measurement of rigid bodies," in *Conf. Proc. IEEE Int. Conf. Robotics and Automation (ICRA' 03)*, Taipei, Taiwan, Sep., 2003, pp. 1171-1178.

[11]   P. Kapur, M. Jensen, L. J. Buxbaum, S. A. Jax, and K. J. Kuchenbecker, "Spatially distributed tactile feedback for kinesthetic motion guidance," in *IEEE Haptics Symposium*, Waltham, MA, USA, 2010, pp. 519-526.

[12]   J. Lieberman and C. Breazeal, "Development of a wearable vibrotactile feedback suit for accelerated human motor learning," in *Conf. Proc. IEEE Int. Conf. Robotics and Automation (ICRA' 09)*, Kobe, Japan, Oct., 2007, pp. 4001-4006.

[13]   F. Sergi, D. Accoto, D. Campolo, and E. Guglielmelli, "Forearm orientation guidance with a vibrotactile feedback bracelet: On the directionality of tactile motor communication," in *Biomedical Robotics and Biomechatronics, 2008. BioRob 2008. 2nd IEEE RAS & EMBS International Conference on*, Scottsdale, AZ, USA, 2008, pp. 433-438.

[14]   J. van der Linden, E. Schoonderwaldt, and J. Bird, "Towards a real-time system for teaching novices correct violin bowing technique," in *Haptic Audio visual Environments and Games, 2009. HAVE 2009. IEEE International Workshop on*, Lecco, Italy, 2009, pp. 81-86.

[15]   K. Bark, P. Khanna, R. Irwin, P. Kapur, S. A. Jax, L. J. Buxbaum, and K. J. Kuchenbecker, "Lessons in using vibrotactile feedback to guide fast arm motions," in *IEEE World Haptics Conference (WHC)*, Philadelphia, PA, USA, Jun., 2011, pp. 355-360.

[16]   P. Kapur, S. Premakumar, S. A. Jax, L. J. Buxbaum, A. M. Dawson, and K. J. Kuchenbecker, "Vibrotactile feedback system for intuitive upper-limb rehabilitation," in *Conf. Proc. World Haptics 2009 - Third Joint EuroHaptics*

conf. and IEEE Inter. Symp. Haptic Interfaces for Virtual Environment and Teleoperator Systems, Salt Lake City, UT, USA, Mar., 2009, pp. 621-622.

[17]   R. A. Magill, *Motor learning and control: Concepts and applications*, 7th ed. New York: McGraw-Hill, 2003.

[18]   C. Wall, "Application of vibrotactile feedback of body motion to improve rehabilitation in individuals with imbalance," *Journal of Neurologic Physical Therapy,* vol. 34, no. 2, pp. 98-104, Jun. 2010.

[19]   P. Loughlin, A. Mahboobin, and J. Furman, "Designing vibrotactile balance feedback for desired body wway reductions," in *Ann. Int. Conf. of the IEEE Engineering in Medicine and Biology Society (EMBC '11)*, 2011, pp. 1310-1313.

[20]   D. E. Rumelhart, G. E. Hinton, and R. J. Williams, "Learning representations by back-propagating errors," *Nature,* vol. 323, no. 6088, pp. 533-536, Oct. 1986.

[21]   S. G. Lisberger, "The neural basis for learning of simple motor skills," *Science,* vol. 242, no. 4879, pp. 728-735, Nov. 1988.

[22]   N. Lyford, "Evaluating vibrotactile feedback for balance deficient subjects using waveform-based display coding," Master, Biomedical Engineering Boston University, Boston, 2008.

[23]   C. Wall, M. S. Weinberg, P. B. Schmidt, and D. E. Krebs, "Balance prosthesis based on micromechanical sensors using vibrotactile feedback of tilt," *IEEE Transactions on Biomedical Engineering,* vol. 48, no. 10, pp. 1153-1161, Oct. 2001.

[24] S. Weinstein, *Intensive and extensive aspects of tactile sensitivity as a function of body part, sex, and laterality*. In: Kenshalo, D.R. (Ed.), The Skin Senses. Thomas, Springfield, Ill, pp. 195-222, 1968.

[25] J. B. F. van Erp, "Tactile Navigation Display," in *First International Workshop on Haptic Human-Computer Interaction*, Glasgow, UK, Aug.-Sept., 2001, pp. 165-173.

[26] R. W. Cholewiak, C. J. Brill, and A. Schwab, "Vibrotactile localization on the abdomen: Effects of place and space," *Perception and Psychophysics,* vol. 66, no. 6, pp. 970-987, Aug. 2004.

[27] S. Brewster and L. M. Brown, "Tactons: Structured Tactile Messages for Non-Visual Information Display," in *Conf. Proc. Australasian User Interface Conference*, Dunedin, New Zealand, Jan., 2004, pp. 15-23.

[28] L. M. Brown, "Tactons: Structured Vibrotactile Messages for Non-Visual Information Display," University of Glasgow, Scotland, UK, 2007.

[29] H. Zhou and H. Hu, "Human motion tracking for rehabilitation—A survey," *Biomedical Signal Processing and Control,* vol. 3, no. 1, pp. 1-18, 2008.

[30] D. Avers and C. Lindsey, "What You Need to Know about Balance and Falls; a Physical Therapist's Perspective," in *American Physical Therapy Association patient education brochures*, ed, 1998.

[31] C. Sherrington, S. Lord, and J. Close, "Best Practice Recommendations for physical activity to prevent falls in older adults," in *NSW Department of Health*, ed, 2008.

[32]   NeuroCom, "Balance Master operator's manual," NeuroCom International Inc., Clackamas, OR, USA, 2001.

[33]   P. Gatev, S. Thomas, T. Kepple, and M. Hallett, "Feedforward ankle strategy of balance during quiet stance in adults," *Journal of Physiology,* vol. 514 (Pt 3), pp. 915-28, Feb. 1999.

[34]   M. Saffer, T. Kiemel, and J. Jeka, "Coherence analysis of muscle activity during quiet stance," *Experimental Brain Research,* vol. 185, no. 2, pp. 215-226, Feb. 2008.

[35]   P. T. Cheng, S. H. Wu, M. Y. Liaw, A. M. Wong, and F. T. Tang, "Symmetrical body-weight distribution training in stroke patients and its effect on fall prevention," *Archives of physical medicine and rehabilitation,* vol. 82, no. 12, pp. 1650-1654, Dec. 2001.

[36]   V. Gouglidis, T. Nikodelis, V. Hatzitaki, and I. G. Amiridis, "Changes in the limits of stability induced by weight-shifting training in elderly women," *Experimental Aging Research,* vol. 37, no. 1, pp. 46-62, Jan. 2011.

[37]   D. S. Marigold, J. J. Eng, A. S. Dawson, J. T. Inglis, J. E. Harris, and S. Gylfadóttir, "Exercise leads to faster postural reflexes, improved balance and mobility, and fewer falls in older persons with chronic stroke," *Journal of the American Geriatrics Society,* vol. 53, no. 3, pp. 416-423, Mar. 2005.

[38]   C. Walker, B. J. Brouwer, and E. G. Culham, "Use of visual feedback in retraining balance following acute stroke," *Physical Therapy,* vol. 80, no. 9, pp. 886-895, Sep. 2000.

[39]   V. Hatzitaki, I. G. Amiridis, T. Nikodelis, and S. Spiliopoulou, "Direction-induced effects of visually guided weight-shifting training on standing balance in the elderly," *Gerontology,* vol. 55, no. 2, pp. 145-152, Jul. 2009.

[40]   V. Hatzitaki and S. Konstadakos, "Visuo-postural adaptation during the acquisition of a visually guided weight-shifting task: age-related differences in global and local dynamics," *Experimental Brain Research,* vol. 182, no. 4, pp. 525-535, Oct. 2007.

[41]   C. Y. Yen, K. H. Lin, M. H. Hu, R. M. Wu, T. W. Lu, and C. H. Lin, "Effects of virtual reality-augmented balance training on sensory organization and attentional demand for postural control in people with Parkinson disease: a randomized controlled trial," *Physical Therapy,* vol. 91, no. 6, pp. 862-874, Jun. 2011.

CHAPTER 7: Future Work

7.1. Vibrotactile biofeedback

In order to determine the best vibrotactile instructional method, a comprehensive investigation of the natural postural response to vibrotactile stimulation that takes the effects of age and co-vibration (defined as a vibration stimulus applied simultaneously over two muscle groups) into account must be conducted. In general, it is evident that cutaneous vibratory sensation and proprioception deteriorates with age [1-2] and abdominal obesity, which progressively increases with age [3-5]. A significant change in cutaneous sensation is also associated with increasing age [6-9]. This may indicate that the non-volitional postural response to vibrotactile stimulation over the torso could be absent or reduced in the elderly. Furthermore, the effects of co-vibration on posture regulation must be assessed in order to determine whether such a stimulus combination contributes to a summation of postural responses as seen when applied to the sole-flexor muscles of the foot, soleus, ankle, and dorsal neck muscles [10]. Moreover, while the study of postural effects in response to uninstructed vibrotactile stimulation focuses on the postural response of the torso, the natural postural tendencies of other body segments

(e.g., the head or lower limbs) require further investigation in order to assess whether the relative contribution among different body segments exists (i.e., the reorganization of different body segments for postural coordination).

Future studies should include more complex and dynamic standing balance rehabilitation exercises. The exercises used in this research were relatively simple. The use of the MIMIC and cell phone system during locomotor-based activities will require additional software and hardware considerations. Furthermore, additional patient populations could be employed as potential subjects.

With regard to the magnitude coding for vibrotactile biofeedback, the developed wearable IMU-based vibrotactile biofeedback systems described in Chapters 3 and 5 utilize a microcontroller unit (MCU) to drive coin-style tactors. Since the coin-style tactor varies its rotation speed as a function of the DC voltage input, the implementation of frequency-based magnitude coding is not viable. However, it is possible to control the intensity of the vibrations with a varying PWM (Pulse Width Modulation) signal using different duty ratios [11-14]. In general, a microcontroller unit (MCU) has a limited number of PWM ports (e.g., two PWM ports in the ATMEL ATmega 128 and ATmega 8 MCUs). Thus, a PWM waveform generation algorithm using general digital I/O ports is necessary to support more than three tactors. A detailed PWM signal generation algorithm which employs MCU I/O (Input/output) channels is provided in Appendix C.1, and could be used for continuously displaying error magnitudes.

The simulation model of the MIMIC system, described in Chapter 4, assumes that lower limbs do not contribute to postural correction. This assumption allows the simple hip joint inverted pendulum to be implemented as a numerical model. However, multi-

body segments (e.g., hip, knee, and ankle joints) are usually involved in postural control, so it follows that multiple body segments would also contribute to postural corrections [15-17]. Winter [18] asserts that balance can be achieved by employing various combinations of ankle, hip, and knee movements while standing and walking. Thus, a high fidelity model incorporating multi-body segments may be required to predict the muscle torque generated in multi-body segments. With a high fidelity model, an investigation of the effects of control parameters (e.g., higher derivative terms and/or predictive information), vibrotactile biofeedback coding schemes, and vibrotactile instructional methods (i.e., attractive versus repulsive) could be performed in order to optimize vibrotactile cuing signals for motion replication and balance rehabilitation exercises.

7.2. Future system design

One long-term goal of this work is to develop a web-based MIMIC and a ubiquitous cell-phone-based balance rehabilitation tool. The MIMIC will be developed as a web-based motion and/or balance training tool that supports motion instruction for multiple body segments (e.g., head, trunk, and lower limb) and enables an expert (e.g., a physical therapist) to map his/her movements to a trainee (e.g., a patient) remotely. A web-based MIMIC system could be used to simultaneously instruct a classroom of trainees and individuals at home, allowing them to perform common balance rehabilitation exercises. The instructed movement could be based on either previously expert recorded motions or streamed live via the Internet.

In order to design a ubiquitous cell-phone-based balance rehabilitation tool, the user must be able to operate the system without the assistance of a health care provider or family member. One step toward achieving this goal is to use the cell phone for selecting exercises and displaying data. In this design scenario, the subject will not need to use the phone's built-in accelerometer to detect and estimate tilt, but will instead be able to use the phone as an interface to communicate with a customized wearable unit composed of a six-degree-of-freedom IMU, a microcontroller, and a four-tactor feedback assembly. In addition, since phones have the capability of providing text-based, auditory, and video instructions to demonstrate each exercise, the phone can deliver audio prompts to indicate the beginning and end of each trial, display KP, and communicate results to the physical therapist.

The ability to acquire motor skills can be improved by integrating information from multiple sensory inputs (e.g., visual, auditory, or tactile) [19]. Future versions of the MIMIC might include visual information in addition to vibrotactile cues. Previous studies have demonstrated that a visual biofeedback display synchronized with vibrotactile biofeedback can improve users' performance during motion learning [14, 20-22] and balance-related exercises [23].

References

[1]   H. B. Skinner, R. L. Barrack, and S. D. Cook, "Age-related decline in proprioception," *Clinical Orthopaedics and Related Research,* no. 184, pp. 208-211, Apr. 1984.

[2]   A. D. Whanger and H. S. Wang, "Clinical correlates of the vibratory sense in elderly psychiatric patients," *Journals of Gerontology,* vol. 29, no. 1, pp. 39-45, Jan. 1974.

[3]   I. S. Okosun, T. E. Forrester, C. N. Rotimi, B. O. Osotimehin, W. F. Muna, and R. S. Cooper, "Abdominal adiposity in six populations of West African descent: prevalence and population attributable fraction of hypertension," *Obessity Research,* vol. 7, no. 5, pp. 453-462, Sep. 1999.

[4]   I. S. Okosun, T. E. Prewitt, and R. S. Cooper, "Abdominal obesity in the United States: prevalence and attributable risk of hypertension," *Journal of Human Hypertension,* vol. 13, no. 7, pp. 425-430, Jul. 1999.

[5]   I. S. Okosun, T. E. Prewitt, Y. Liao, and R. S. Cooper, "Association of waist circumference with ApoB to ApoAI ratio in black and white Americans," *International Journal of Obesity,* vol. 23, no. 5, pp. 498-504, May. 1999.

[6]   R. T. de Jongh, E. H. Serne, I. J. RG, G. de Vries, and C. D. Stehouwer, "Impaired microvascular function in obesity: implications for obesity-associated microangiopathy, hypertension, and insulin resistance," *Circulation,* vol. 109, no. 21, pp. 2529-35, Jun. 2004.

[7]   H. Loffler, J. U. Aramaki, and I. Effendy, "The influence of body mass index on skin susceptibility to sodium lauryl sulphate," *Skin Research and Technology,* vol. 8, no. 1, pp. 19-22, Feb. 2002.

[8]   L. C. Chin, T. Y. Huang, C. L. Yu, C. H. Wu, C. C. Hsu, and H. S. Yu, "Increased cutaneous blood flow but impaired post-ischemic response of nutritional flow in obese children," *Atherosclerosis,* vol. 146, no. 1, pp. 179-85, Sep. 1999.

[9]   P. Valensi, O. Smagghue, J. Paries, P. Velayoudon, B. Lormeau, and J. R. Attali, "Impairment of skin vasoconstrictive response to sympathetic activation in obese patients: influence of rheological disorders," *Metabolism,* vol. 49, no. 5, pp. 600-606, May. 2000.

[10]   A. Kavounoudias, R. Roll, and J. P. Roll, "Foot sole and ankle muscle inputs contribute jointly to human erect posture regulation," *Journal of Physiology,* vol. 532, no. Pt 3, pp. 869-878, May. 2001.

[11]   B. C. Lee, J. Lee, J. Cha, C. Seo, and J. Ryu, "Immersive live sports experience with vibrotactile sensation," in *Conf. Proc. on Human-Computer Interaction*, Rome, Italy, 2005, pp. 1042-1045.

[12]   B. C. Lee, H. Park, J. Lee, and J. Ryu, "Tactile visualization with mobile AR on a handheld device," in *Conf. Proc. on the 2nd Int. Conf. on haptic and audio interaction design*, Seoul, South Korea, 2007, pp. 11-21.

[13]   F. Sergi, D. Accoto, D. Campolo, and E. Guglielmelli, "Forearm orientation guidance with a vibrotactile feedback bracelet: On the directionality of tactile motor communication," in *Biomedical Robotics and Biomechatronics, 2008. BioRob 2008. 2nd IEEE RAS & EMBS International Conference on*, Scottsdale, AZ, USA, 2008, pp. 433-438.

[14]   J. van der Linden, E. Schoonderwaldt, and J. Bird, "Towards a real-time system for teaching novices correct violin bowing technique," in *Haptic Audio visual Environments and Games, 2009. HAVE 2009. IEEE International Workshop on*, Lecco, Italy, 2009, pp. 81-86.

[15] A. D. Kuo, "An optimal control model of human balance: can it provide theoretical insight to neural control of movement?," in *Proc. of the American Control Conference, 1997.* , Albuquerque, NM, USA, Jun., 1997, pp. 2856-2860.

[16] K. Barin, "Evaluation of a generalized model of human postural dynamics and control in the sagittal plane," *Biological Cybernetics* vol. 61, no. 1, pp. 37-50, 1989.

[17] S. Park, F. B. Horak, and A. D. Kuo, "Postural feedback responses scale with biomechanical constraints in human standing," *Experimental Brain Research,* vol. 154, no. 4, pp. 417-427, Feb. 2004.

[18] D. A. Winter, "Human balance and posture control during standing and walking," *Gait & Posture,* vol. 3, no. 4, pp. 193-214, Dec. 1995.

[19] K. M. Newell, "Motor skill acquisition," *Annual Review of Psychology,* vol. 42, pp. 213-237, Jan. 1991.

[20] P. Kapur, M. Jensen, L. J. Buxbaum, S. A. Jax, and K. J. Kuchenbecker, "Spatially distributed tactile feedback for kinesthetic motion guidance," in *IEEE Haptics Symposium*, Waltham, MA, USA, 2010, pp. 519-526.

[21] J. Lieberman and C. Breazeal, "Development of a wearable vibrotactile feedback suit for accelerated human motor learning," in *Conf. Proc. IEEE Int. Conf. Robotics and Automation (ICRA' 09)*, Kobe, Japan, Oct., 2007, pp. 4001-4006.

[22] A. Nakamura, S. Tabata, T. Ueda, S. Kiyofuji, and Y. Kuno, "Multimodal presentation method for a dance training system," presented at the CHI '05 extended abstracts on Human factors in computing systems, Portland, OR, USA, 2005.

[23] A. U. Alahakone and S. M. N. A. Senanayake, "A Real-Time System With Assistive Feedback for Postural Control in Rehabilitation," *IEEE/ASME Transactions on Mechatronics,* vol. 15, no. 2, pp. 226-233, Apr. 2010.

APPENDICES

Appendix A: Publications

A.1. Peer-reviewed journal papers

▪ **Beom-Chan Lee**, Shu Chen, and Kathleen H. Sienko, "A wearable device for real-time motion error detection and vibrotactile instructional cuing", IEEE Transactions on Neural System and Rehabilitation Engineering, Vol. 19, No. 4, pp. 374-381, 2011.

▪ **Beom-Chan Lee**, Jeonghee Kim, Shu Chen, and Kathleen H. Sienko, "Cell phone based balance trainer", Journal of NeuroEngineering and Rehabilitation, in press.

A.2. Abstracts published in peer-reviewed journals

▪ **Beom-Chan Lee**, Kelli Bechly, and Kathleen H. Sienko, "Cell phone based vibrotactile feedback system for home-based vestibular rehabilitation balance training", Journal of Vestibular Research, Vol. 20, No. 3,4, pp. 234-235, 2010.

▪ **Beom-Chan Lee** and Kathleen H. Sienko, "Wireless Mimic Device for Rehabilitation and Training Applications", Journal of Medical Device, Vol. 3, No. 2, 027526, 2009.

▪ Vivek Vishwas Vichare, **Beom-Chan Lee**, Wendy Carender, Annamarie Asher, and Kathleen H. Sienko, "Vibrotactile Balance Rehabilitation Gait Assist Device", Journal of Medical Device, Vol. 3, No. 2, 027509, 2009.

A.3. Conference papers

▪ **Beom-Chan Lee**, Bernard J. Martin, and Kathleen Helen Sienko, "Postural Post-Effects in Response to Torso-based Vibrotactile Stimulation", 39th annual meeting of the Society for Neuroscience, 2009.

▪ **Beom-Chan Lee** and Kathleen H. Sienko, "Balance training via multimodal biofeedback", International Conference on Fall Prevention and Protection (ICFPP'10), pp. 77-80, 2010.

▪ **Beom-Chan Lee** and Kathleen H. Sienko, "Effects of attractive versus. repulsive vibrotactile instructional cues on motion replication tasks", *33rd Annual International Conference of the IEEE Engineering in Medicine and Biology Society (EMBS)*, pp. 3533-3536, 2011.

▪ **Beom-Chan Lee**, Jeonghee Kim, Wendy Carender and Kathleen H. Sienko, "Cell phone based sensory augmentation for balance training", Annual Meeting of the Gait & Clinical Movement Analysis Society (GCMAS), 2012.

▪ **Beom-Chan Lee**, Bernard J. Martin, and Kathleen H. Sienko, "Comparison of non-volitional postural responses induced by two types of torso based vibrotactile stimulations", Haptics Symposium, 2012.

A.4. Conference or symposium presentations

▪ **Beom-Chan Lee** and Kathleen H. Sienko, "Wireless Mimic Device for Rehabilitation and Training Applications", Design of Medical Devices Conference, Minneapolis, MN, April 14-16, 2009.

▪ **Beom-Chan Lee**, Bernard J. Martin, and Kathleen Helen Sienko, "Postural Post-Effects in Response to Torso-based Vibrotactile Stimulation", 39th annual meeting of the Society for Neuroscience, Chicago, IL, October 17-21, 2009.

▪ **Beom-Chan Lee** and Kathleen H. Sienko, "Balance training via multimodal biofeedback", International Conference on Fall Prevention and Protection (ICFPP'10), Morgantown, WV May 18-20, 2010.

Appendix B: MIMIC Software Architecture and Estimation Algorithm

B.1. Software architecture

To maximize the embedded MCU performance, a component-based software architecture as shown in Figure B.1 was designed to carefully manage computational resources, prioritize real-time motion capture and estimation, enable data transmission, and incorporate saving capabilities. The core software architecture implemented in the MCU is the same in both the EM and TM. The only difference between the two modules is the number of data packets communicated to/from peripheral interfaces; the TM acquires raw linear accelerations and angular velocities from the trainee IMU as well as estimated tilt data from the EM.

At its center lies the task manager that supervises the remainder of the computational components. It has a crucial role in stripping away all the functionality deemed unnecessary for running the application on the MCU. Furthermore, the TM takes charge of time scheduling so that each sub-computational component has access to sufficient computational resources. For example, the motion estimation is updated at a rate of 100 Hz from the IMU data set.
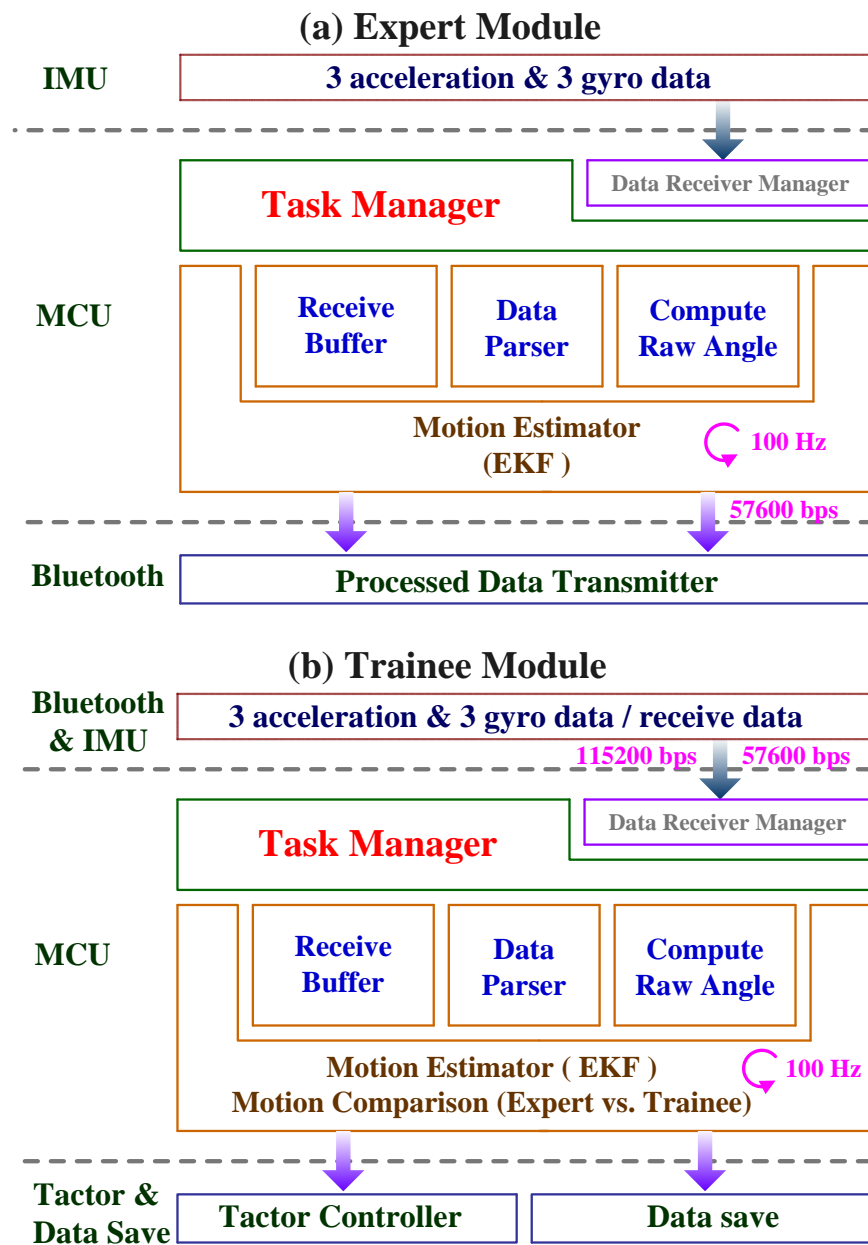
Figure B.1. Component-based software architecture imbedded in the EM and TM.

The data receiver manager allows the MCU to receive acceleration/angular rate data or information from another module. Since serial data communication through either a

205

wired or wireless connection is accomplished with an 8-bit data transceiver process, the

transceiver process between the MCU and the IMU or another module is achieved by

packet communication. Figure B.2 shows the communication packet with data capacities

between the MCU and the IMU (Figure B.2 (a)) and between the MCU of the EM and the

MCU of the TM (Figure B.2 (b)).

(a)

	AccX (16 bits)		AccY (16 bits)		AccZ (16 bits)		GyroX (16 bits)		GyroY (16 bits)		GyroZ (16 bits)		
Header	AccX H	AccX L	AccY H	AccY L	AccZ H	AccZ L	GyroX H	GyroX L	GyroY H	GyroY L	GyroZ H	GyroZ L	Tail
8 bits	8 bits	8 bits	8 bits	8 bits	8 bits	8 bits	8 bits	8 bits	8 bits	8 bits	8 bits	8 bits	8 bits

(b)

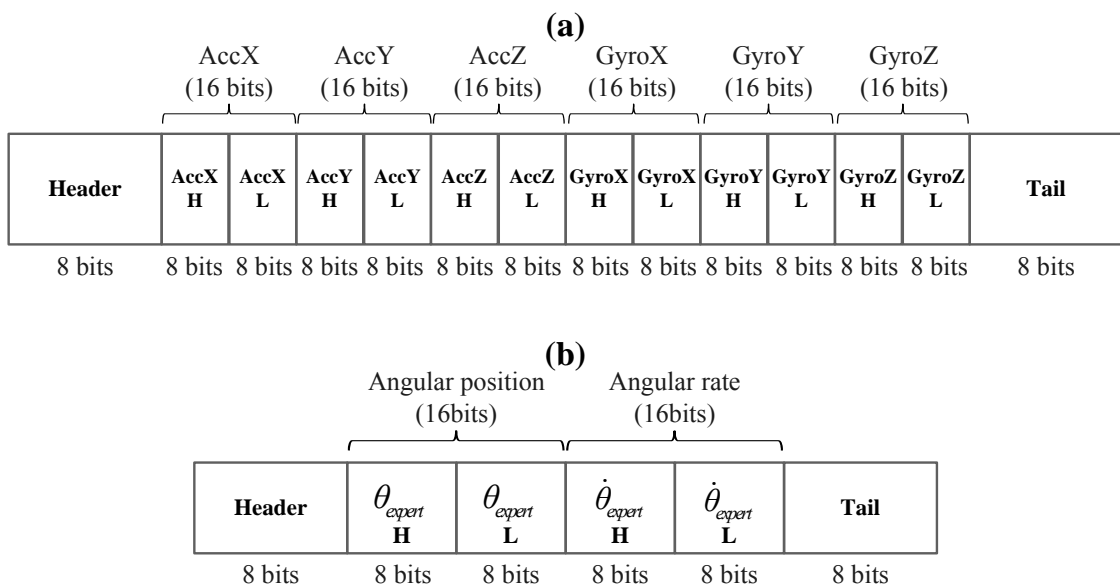|	Angular position (16bits)		Angular rate (16bits)		
Header	θ_{expert} H	θ_{expert} L	$\dot{\theta}_{expert}$ H	$\dot{\theta}_{expert}$ L	Tail
8 bits	8 bits	8 bits	8 bits	8 bits	8 bits

Figure B.12. Communication data packet. (a) Packet between between the MCU and the
IMU. (b) Packet between between the EM and the TM.

The received data packets are transferred to the receiver buffer and

parsed/decomposed with respect to data types (e.g., 16 bits) in the data parser. Then the

parsed data is converted into actual accelerations and angular velocities based on the

sensitivity of each sensor and resolution of the analog-to-digital (ADC) converter. Actual

acceleration and angular rate data about each axis are determined by Equations B.1 and B.2.

$$a = \frac{\text{Output (V) of accelerometer}}{\text{Max range (V)} \div \text{Sensitivity (g)} \times \text{Resolution}_{ADC}} \quad (B.1)$$

$$\dot{\theta} = \frac{\text{Output (V) of gyroscopes}}{\text{Max range (V)} \div \text{Sensitivity(deg/sec)} \times \text{Resolution}_{ADC}} \quad (B.2)$$

where both outputs represent the voltage output of each sensor, sensitivity indicates how the sensor's output changes when the measured quantity changes, and resolution indicates the number of discrete values the ADC can produce over the range of analog values. The maximum voltage ranges for each sensor are 5 V, the sensitivity of both the tri-axial accelerometer and gyroscopes are ±4 g and ±500°/s, respectively. In addition, the resolution of the analog-to-digital (ADC) converter is 12 bits. Raw acceleration and angular rate information is processed using the motion estimation algorithm to produce an estimate of body tilt.

B.2. Implementation of Extended Kalman Filter (EKF)

The EKF is commonly referred to as a statistical estimation process using a deterministic model of a system as shown in Figure B.3, which can filter measurement data with noise through a successive estimation and correction process [1].
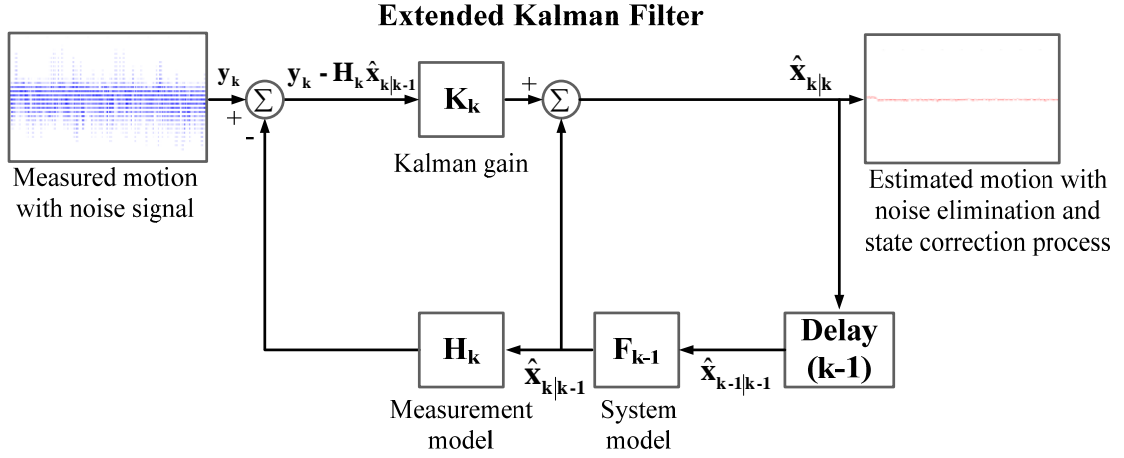
Extended Kalman Filter

Figure B.23. Schematic block diagram of the Extended Kalman Filter embedded in the vibrotactile based balance rehabilitation system.

Tilt estimates in this dissertation are computed using an Euler-angle-based extended Kalman filter (EKF) [2] with four state variables. Two of the state variables (pitch (θ_{pitch}) and roll (θ_{roll}) angular positions) are calculated from the output of the tri-axial accelerometer [3]:

$$\theta_{pitch} = -\sin^{-1}\left(\frac{g_x}{\|g\|_2}\right)$$

$$\theta_{roll} = \sin^{-1}\left(\frac{g_y}{\|g\|_2 \cos(\theta_{pitch})}\right)$$

(B.3)

where $\|g\|_2$ is the magnitude of gravity ($g = [g_x \ g_y \ g_z]$) and the subscripts indicate the Euclidean norms. The remaining two state variables (roll and pitch angular velocities) are directly acquired from the gyroscopes. The system and measurement models used within the EKF are expressed by

208

$$\begin{cases} \mathbf{x}_{k+1} = \mathbf{F}_k \mathbf{x}_k + \mathbf{w}_k \\ \mathbf{y}_k = \mathbf{H}_k \mathbf{x}_k + \mathbf{v}_k \end{cases} \tag{B.4}$$

where $\mathbf{x}_{k+1}$ and $\mathbf{x}_k$ denote the state vector at times $\mathbf{k+1}$ and $\mathbf{k}$ and $\mathbf{y}_k$ denotes the measurement vector at time $\mathbf{k}$. $\mathbf{F}_k$ and $\mathbf{H}_k$ denote the coefficients at time $\mathbf{k}$ which determine the characteristics of the system model and measurement model respectively. System noise and measurement noise are respectively denoted by $\mathbf{w}_k$ and $\mathbf{v}_k$ at time $\mathbf{k}$. Based on a first-order linear state transition model and a non-linear measurement model, the system model can be expressed as follows in order to determine trunk motion:

$$\begin{bmatrix} \mathbf{x}_{k+1} \\ \dot{\mathbf{x}}_{k+1} \end{bmatrix} = \begin{bmatrix} 1 & \Delta t \\ 0 & 1 \end{bmatrix} \begin{bmatrix} \mathbf{x}_k \\ \dot{\mathbf{x}}_k \end{bmatrix} + \begin{bmatrix} \mathbf{w}_1(\mathbf{k}) \\ \mathbf{w}_2(\mathbf{k}) \end{bmatrix} \tag{B.5}$$

where $\mathbf{w}_{k,1}$ and $\mathbf{w}_{k,2}$ are the angular position noise and angular velocity noise, respectively, at time $\mathbf{k}$. The noise is assumed to be a zero mean, uncorrelated random sequence ($\mathbf{w}_k \sim \mathbf{N(0, Q_k)}$, $\mathbf{Q}_k$ represents the process noise covariance).

The measurement model of the system can be represented by

$$\mathbf{y}_k = \mathbf{H}_k \mathbf{x}_k + \mathbf{v}_k = [1 \quad 1]\mathbf{x}_k + \mathbf{v}_k \tag{B.6}$$

where $\mathbf{v_k}$ is noise that is generated due to uncertainties in the measured angular position and angular velocity. The noise is assumed to be a zero mean, uncorrelated random sequence ($\mathbf{v_k} \sim \mathbf{N(0, R_k)}$, $\mathbf{R_k}$ represents the measurement noise covariance). Note that both $\mathbf{Q_k}$ and $\mathbf{R_k}$ are assumed to be constant and part of the recursive updating procedure of EKF [1]. The detailed computational processes are explained in [1].

References

[1]   G. Welch and G. Bishop, "An introduction to the kalman filter," Technical Report TR 95-041, Dept. Com. Sci., University of North Carolina, Chapel Hill, USA, Apr. 2005.

[2]   D. E. Leader, "Kalman filter estimation of underwater vehicle position and attitude using a doppler velocity aided inertial motion unit," Ph. D., Joint Program in Oceanographic Engineering, Massachusetts Institute of Technology, Boston, Massachusetts, 1994.

[3]   J. Vaganay, M. J. Aldon, and A. Fournier, "Mobile robot attitude estimation by fusion of inertial data," in *Robotics and Automation, 1993. Proceedings., 1993 IEEE International Conference on*, 1993, pp. 277-282.

Appendix C: Software and Hardware Considerations for Future MIMIC and Cell Phone System Configurations

C.1. PWM waveform generation

$$D = \frac{W}{T} \times 100\% \qquad T = \frac{1}{F}$$

D : Duty cycle   T : Waveform period
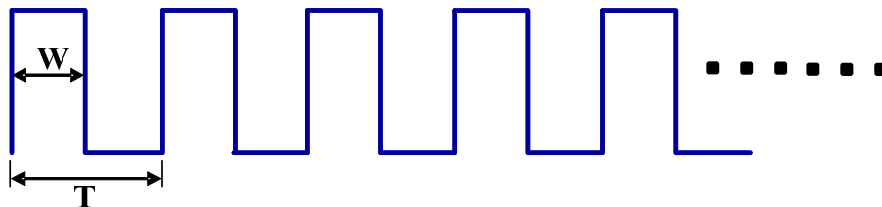W : Pulse width   F : Frequncy

Figure C.1. PWM signal.

In general, a microcontroller unit (MCU) has a limited number of (Pulse Width Modulation) PWM ports, e.g., two PWM ports in the ATMEL ATmega 128. Thus, a PWM (pulse width modulation) waveform generation algorithm using general digital I/O ports is necessary to support more than three vibrotactile units (i.e., tactors). This

appendix describes the PWM waveform generation algorithm to enable tactors to generate variable intensities.

The PWM waveform is used for generating magnitude and frequency similar to the control of a DC motor, as shown in Figure A.1. The term 'duty cycle' describes the proportion of 'on' time to the regular interval or 'period' of time; a low duty cycle corresponds to low power, because the power is off for more than 50% of the time. Duty cycle is expressed in percent, 100% being fully on. The MCU, ATmega 128 for example, supports two of the 16-bit timer/counter units that allow accurate program execution timing, wave generation, and signal timing measurement. There are different types of PWM generating modes such as fast, phase correct as well as phase and frequency correct PWM modes. Among the three modes, fast PWM mode was used, because it provides a high frequency PWM waveform generation option. The fast PWM differs from the other PWM options by its single-slope operation. The TCNTn has 16-bit registers and its value can determine the PWM frequency. The PWM waveform is generated in the timer interrupt routine, the PWM frequency, $f_{desired}$, for the output can be calculated by

$$f_{desired} = \frac{f_{system}}{N \times Count}$$

(C.1)

Where the f_{sysem} represents the system frequency up to 16 MHz (i.e., clock frequency supported by the ATmega 128) and the N stands for the prescaler divider (1, 8, 64, 256, or 1024). $Count$ represents the count number.

The actual calculated timer/count bottom value (2^{16}- **Count**) is calculated by equation C.1 and written to the TCNTn register. The counter counts from the bottom value to top value (2^{16}) then restarts from bottom value. Enablement of timer interrupt routine is set by overflow of the counter. For example, if the prescaler divider, the system frequency, and desired frequency are 64, 16 MHz, and 200 Hz (e.g., 5ms, W from Figure C.1), respectively, then the resulting count number is 1250. According to count number, the bottom value (2^{16}-1250) is written to the TCNTn register. Consequently, a 100 Hz (i.e., 1ms) with 50% duty cycle waveform output (T from Figure C.1) can be achieved.

The duty ratio of the PWM waveform is decided by changing the bottom value of the timer/count resister. The bottom value can be calculated by

$$V_{bottom} = 2^{16} - (\frac{f_{system}}{f_{desire}} \times \frac{Duty}{100}) \tag{C.2}$$

By setting the bottom value, the PWM waveform is generated with the desired frequency (i.e., F=1/T) in the digital I/O ports, which can be used for the generation of vibration using the coin-style tactor, which is actuated as a function of the DC voltage input. In addition, the strength of the tactor's vibration can be changed by the duty cycle (the proportion of 'on' time) since the tactor's rotation speed is determined by the proportion of 'on' time.

C.2. MCU Benchmarks

	ATmega128	LPC2141	PIC24H64GP206	Arm7TDMI
Image				
CPU	8bit ATmega128L	16bit ARM7TDMI	8bit PIC24H	32bit HMS39C7092
Performance	8MIPS at 8Mhz	17MIPS at 25MHz	40MIPS at 32kHz	1.1MIPS at 1MHz
Flash Rom	128kB	32kB	64kB	192kB
RAM	4kB	8kB	8kB	4kB
I/O port	48Ports	44Ports	53Ports	11Ports
Serial Port	2UARTS	2UARTS	2UARTS	2UARTS
PWM	2 channels	2 channels	2 channels	2 channels
Input Voltage	2.7V~5.5V	5V	3.3V	3V
Compiler	AVR studio, WinAVR	IAR, LPC compiler	CCSC	QUICK WRITER
Size (mm)	36x38	47x47	14x14	85x85

C.3.IMU Benchmarks

	Vn-100	CHR-UM6	CHR-6d	Gyro Cube3	6DOF v4
Image					
Angular resolution (deg)	0.05	0.01	0.01	N/A	N/A
Acceleration range (g)	±6	±2	±3	±10	±6
Gyro range (deg/sec)	±500	±2000	±400	±200	±500
Magnetometer range (Gauss)	±6	±4	N/A	±6	±6
Output mode	Yaw, Pitch, Roll Acceleration, angular rate, magnetic field	Yaw, Pitch, Roll Acceleration, angular rate, magnetic field	Pitch, Roll Acceleration, angular rate	Acceleration, angular rate, temperature	Acceleration, angular rate, magnetic field
Output interface	TTL UART	TTL UART	TTL UART	Analog output	TTL UART, Bluetooth
Acquisition rate	200 Hz	500 Hz	300 Hz	40 Hz	300 Hz
Size (mm)	22x24x3	27.9x35.6x12.7	20.3x17.8x2.5	30.5x31.8x15.2	480x400x130
Power consumption (mW)	325 (65mA@5V)	260 (52mA@5V)	180 (50mA@3.6V)	135 (27mA@5V)	350 (70mA@5V)
Price ($)	500	299	125	570	350